

https://dspace.org/

Assessing the spatiotemporal variability of urban heat island and thermal comfort in Greater Francistown City

Kudoma, Bongayi

2024-08

University of the Witwatersrand, Johannesburg

https://hdl.handle.net/10539/46691

Kudoma, Bongayi. (2024). Assessing the spatiotemporal variability of urban heat island and thermal comfort in Greater Francistown City. [Master's dissertation, University of the Witwatersrand, Johannesburg]. WIReDSpace. https://hdl.handle.net/10539/46691

Downloaded from a DSpace repository. https://dspace.org/

ASSESSING THE SPATIOTEMPORAL VARIABILITY OF URBAN HEAT ISLAND AND THERMAL COMFORT IN GREATER FRANCISTOWN CITY

by

Bongayi Kudoma

2782669

Research Report

Submitted in fulfilment of the requirements for the degree

Master of Science

in

Geographical Information Systems and Remote Sensing

In the Faculty of Science, University of the Witwatersrand, Johannesburg, South Africa

Supervisor

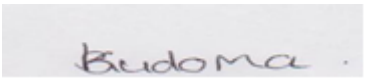
Prof Elhadi Adam

5 August 2024

DECLARATION

I, Bongayi Kudoma, declare that this research report is my unaided work. It is being submitted for the Degree of Master of Science in Geographical Information Systems and Remote Sensing at the University of the Witwatersrand, Johannesburg. It has not been submitted before for any degree or examination at any other University.

Signature of candidate



5th day of August 2024 at Francistown, Botswana.

ABSTRACT

Climate change and global warming have increased land surface temperature (LST) in urban areas, causing urban heat islands (UHI), affecting residents' thermal comfort. The UHI effect in Greater Francistown City is causing temperatures to rise, potentially affecting residents' thermal comfort. The study combined remote sensing and statistical techniques to collect Landsat-8 OLI/TIRS-1 data and analyses spatiotemporal variability of LST, vegetation, built-up areas, UHI phenomenon and thermal comfort levels in the city from 2014-2023. Results revealed that built-up areas covered 59.02% of the City in 2023, reducing vegetation to 33.26% and affecting thermal comfort. UHI effects have grown due to LST variations near bare-land and built-up areas. Urban hotspots increased, peaking at 3.12% in 2023, with thermal comfort levels varying between 2016 and 2023. Expanding the built-up regions, reduced vegetation, land-cover changes contributed to the UHI effects and changes in thermal comfort patterns. Recommending sustainable urban planning to improve urban liveability.

Keywords: Urban Thermal Field Variance Index, Thermal Comfort, Land surface temperature, Urban Heat Island, Landsat 8 OLI/TIRS, Francistown City, Botswana

DEDICATION

This dissertation is dedicated with profound gratitude and love to the pillars of strength and inspiration: my beloved mother, Jane Makova, and cherished daughters, Tapiwanashe and Tadiwanashe Kudoma. Your unwavering support, encouragement, and understanding have been instrumental in my academic journey, and this achievement is equally yours. Thank you for constantly motivating me and instilling the determination to reach new heights. May this dedication serve as a small gesture of gratitude for your unwavering love and faith in me.

ACKNOWLEDGMENTS

I express my deepest gratitude to Prof Elhadi Adam, my supervisor, whose guidance, expertise, and unwavering support have been invaluable throughout this research journey. His mentorship has been instrumental in shaping this research report's direction and standard.

Special thanks to Mr Honest Madamombe for his practical and technical support in GIS and remote sensing. His expertise has significantly enriched the data analysis aspects of this study, contributing to its depth and accuracy.

I am profoundly grateful to the Murape family (Clever, Thirling, Ashley, Anotidaishe, Ian, and Jabu Naruvinga) for their generosity in providing accommodation during the study period. Their kindness has created a conducive and supportive environment, allowing me to focus on my research accomplishments with peace of mind.

My heartfelt thanks go to Francistown BA ISAGO University staff and my employer for their understanding and encouragement, which have facilitated a harmonious balance between work and academic pursuits. Your love and understanding have been my constant motivation. I am also grateful to Prophet Walter Magaya and YADAH TV for their unwavering spiritual support during this scholarly pursuit. The declaration of “the year of upgrade” has come to reality.

This research report is a testament to these individuals and entities' collaborative efforts and support. I am sincerely thankful for each's impact on this academic achievement.

TABLE OF CONTENTS

DECLARATION ii

ABSTRACT iii

DEDICATION iv

ACKNOWLEDGMENTS v

LIST OF FIGURES ix

LIST OF TABLES x

LIST OF EQUATIONS xi

LIST OF ACRONYMS xii

1. CHAPTER 1: INTRODUCTION 1

1.1 Background 1

1.2 Research Problem Statement 3

1.3 Significance of the Study 4

1.4 Aim and Objectives 5

1.4.1 Aim 5

1.4.2 Objectives of the Research 5

1.5 Scope of the Study 5

1.6 Limitations 5

1.7 Definition of Terms 7

1.8 Conclusion 7

2. CHAPTER 2: LITERATURE REVIEW 8

2.1 Introduction 8

2.2 Theoretical and Conceptual Framework 8

2.3 An Overview of Urban Heat Island and Thermal Comfort 9

2.4 Importance of Assessing UHI and Thermal Comfort 11

2.5 Chronological Trends of UHI and Thermal Comfort 12

2.5.1 Historical Context of UHI and Thermal Comfort 12

2.5.2 Recent Advances in UHI and Thermal Comfort 16

2.6 Spatiotemporal Assessment Urban Heat Island 17

2.7 Studies on Urban Heat Island in Similar Urban Environments 19

2.8 Spatial Distribution of Urban Heat Island 20

2.9 Impact of Urban Heat Island on Thermal Comfort 22

2.10 Thermal Comfort in Urban Environments 23

2.10.1 Assessment and Measurements of Thermal Comfort 23
2.10.2 Factors Influencing Thermal Comfort Levels 25
2.11 Techniques for Enhancing Thermal Comfort and Mitigating UHI in Cities 27
3. CHAPTER 3: METHODOLOGY 29
3.1 Introduction 29
3.2 Study Area 29
3.3 Research Design 30
3.4 Data Acquisition 31
3.5 Pre-Processing 33
3.6 Calculations of spatiotemporal parameters of UHI and Thermal Comfort 34
3.6.1 Classification and accuracy assessment of land cover 34
3.6.2 Estimation of Normalised Difference Built-up Index 36
3.6.3 Vegetation Indices Calculations 36
3.6.4 Land Surface Temperature Calculations 38
3.6.5 Estimation of the UHI, non-UHI, and Urban Hot Spot Areas 39
3.6.6 Estimation of Thermal Comfort Using the Urban Thermal Field Variance Index 40
3.7 Meteorological data 42
3.8 Statistical Evaluations 42
4. CHAPTER 4: RESULTS 44
4.1 Introduction 44
4.2 Spatiotemporal Assessment of Greater Francistown City Land Cover 44
4.3 Spatiotemporal Analysis of Normalized Difference Built-up Index 46
4.4 Analysis of Vegetation Indices 48
4.4.1 Spatiotemporal Distribution of NDVI 48
4.4.2 Spatiotemporal Distribution Fraction of Vegetation Cover 50
4.4.3 Spatiotemporal Distribution of the Land Surface Emissivity 52
4.5 Spatiotemporal Distribution of LST and Air Temperature Patterns 52
4.5.1 Spatiotemporal Distribution of Land Surface Temperature 52
4.5.2 Land Surface Temperature and Air Temperature Validation 54
4.6 Spatiotemporal Variations of UHI, non-UHI, and Urban Hotspot Areas 56
4.6.1 Spatiotemporal Distribution of UHI and non-UHI 56
4.6.2 Spatiotemporal Distribution of Urban Hotspots 58

4.7 Spatiotemporal Analysis of Thermal Comfort Based on UTFVI 59
5. CHAPTER 5: DISCUSSIONS 65
5.1 Introduction 65
5.2 Spatiotemporal Distribution of LULC, Vegetation and Built-up Areas 65
5.3 LST and Its Spatiotemporal Distribution in Greater Francistown City 68
5.4 Spatial Distribution and Intensity of UHI, Non-UHI, and Urban Hotspot Effect 71
5.5 Spatiotemporal Distribution of Thermal Comfort Levels 73
5.6 Socio-Economic Implications of UHI's Effects on Urban Residents 75
6 CHAPTER 6: CONCLUSION AND RECOMMENDATIONS 77
6.1 Introduction 77
6.2 Conclusion 77
6.3 Recommendations 79
7 LIST OF REFERENCES 82

LIST OF FIGURES

Figure 2.1 Conceptual Framework showing the relationship between LST, UHI, and Thermal Comfort 9
Figure 3.1. Study Area - Greater Francistown City 30
Figure 3.2. Study design schematic. 31
Figure 4.1. Maps of Greater Francistown LULC Classification for 2014, 2019, and 2023 45
Figure 4.2. Greater Francistown LULC Spatiotemporal Variability (2014-2023) 46
Figure 4.3. NDBI maps of Greater Francistown City for 2014, 2016, 2019, 2021, and 2023. 47
Figure 4.4. Computed NDBI Statistics for Greater Francistown for 2014-2023 48
Figure 4.5. Spatiotemporal Distribution of NDVI for 2014, 2016, 2019, 2021, and 2023 49
Figure 4.6. NDVI Computed Descriptive Statistics for 2014-2023 50
Figure 4.7. Spatiotemporal Distribution of Fraction of Vegetation over Greater Francistown 51
Figure 4.8. Spatiotemporal Distribution of the Land Surface Emissivity Over Francistown City 52
Figure 4.9. Spatiotemporal Distribution of Land Surface Temperature Over Francistown City 53
Figure 4.10. Correlation between LST and Air Temperature 55
Figure 4.11. Greater Francistown City Identified UHI and Non-UHI 57
Figure 4.12. Greater Francistown City Identified Urban Hotspot 59
Figure 4.13. The Spatiotemporal Distribution of UTFVI Across Greater Francistown 60

LIST OF TABLES

Table 3.1. An overview of the Landsat 8 sensor's attributes and the data acquisition dates. 33
Table 3.2. Description of Landsat 8 dataset utilised in the study area. 33
Table 3.3. Greater Francistown LULC Classification and Description 35
Table 3.4. Thresholds of UTFVI Employed in Greater Francistown 42

Table 4.1. Generated Classified LULC Maps' Accuracy 44
Table 4.2. Greater Francistown City LULC Area Analysis From 2014 to 2023 46
Table 4.3. Analysis of Fraction of Vegetation and Land Surface Emissivity 51
Table 4.4. The Summary of Comparison of LST and Air Temperature for 2014-2023 54
Table 4.5. Spatiotemporal Variations of UHI, non-UHI, and Urban Hotspot Areas 56
Table 4.6. Evaluations of UTFVI Thresholds and Area Covered for Each Class 61
Table 4.7. UTFVI Calculated Descriptive Statistics for the Period 2014 to 2023 62
Table 4.8. Pearson Correlation Coefficients for LST, NDBI, NDVI, FV UTFVI, and SUHI 63

LIST OF EQUATIONS

Equation 3.1. Normalised Difference Built-up Index 36
Equation 3.2. Normalised Difference Vegetation Index 37
Equation 3.3. Proportion of Vegetation 37
Equation 3.4. Land Surface Emissivity 37
Equation 3.5. Top of Atmospheric Spectral Radiance 38
Equation 3.6. TOA Brightness Temperature 39
Equation 3.7. Land Surface Temperature 39
Equation 3.8. Urban Heat Island 40
Equation 3.9. Non-Urban Heat Island 40
Equation 3.10. Urban Hot Spots 40
Equation 3.11. Urban Thermal Field Variance Index 40
Equation 3.12. Pearson Correlation Coefficient 43

LIST OF ACRONYMS

ASV	Actual Sensation Vote
AT	Apparent Temperature
BGI	Blue-green infrastructure
BT	Brightness Temperature
CIA	Central Intelligence Agency
CFD	Computational Fluid Dynamics
CV	Coefficient of Variation
DN	Digital Numbers
EEI	Ecological Evaluation Index
EM	Emissivity
FV	Fractional vegetation
GEE	Google Earth Engine
GIS	Geographical Information System
IoT	Internet of Things
LSE	Land Surface Emissivity
LST	Land Surface Temperature
LULC	Land Use and Land Cover
MODIS	Moderate Resolution Imaging Spectroradiometer\
MSE	Mean Square Error
NASA	National Aeronautics and Space Administration
NDBI	Normalised Difference Built-up Index
NDVI	Normalised Difference Vegetation Index
NET	Normal Effective Temperature
NIR	Near InfraRed
OA	Overall Accuracy
PET	Physiological Equivalent Temperature
PMV	Predicted Mean Vote
POWER	Prediction Of Worldwide Energy Resources
PV	Proportion of Vegetation
PPD	Predicted Percentage of Dissatisfied
RF	Random Forest
SAS	Statistical Analysis Software

SET	Standard Effective Temperature
SUHI	Surface Urban Heat Island
SUHII	Surface Urban Heat Island Intensity
TIRS	Thermal Infrared Sensor
THI	Temperature-Humidity Index
TOA	Top of Atmospheric
UHI	Urban Heat Island
UHS	Urban Hot Spots
UTFVI	Urban Thermal Field Variance Index
UTM	Universal Transverse Mercator
USGS	United States Geological Survey
WBGT	wet bulb-globe temperature index
WCI	Wind Chill Index
WGS	World Geodetic System

CHAPTER 1: INTRODUCTION

1.1 Background

Climate change and concomitant global warming have adversely impacted urban surroundings, leading to an increase in land surface temperature (LST) (Morabito et al., 2016; Dutta et al., 2021; Hashim et al., 2022), which has an adverse influence on the external thermal comfort condition of urban residents (Faragallah and Ragheb, 2022; Amir Siddique et al., 2023). Increased urban temperatures (Sharma et al., 2021) have resulted in thermal energy accrual, causing urban areas to become warmer than their adjacent suburbs and rural regions (Mijani et al., 2020; Barrao et al., 2022; Ullah et al., 2022). This occurrence is referred to as the “Urban Heat Island (UHI) Effect” (Chun and Guldmann, 2018; Zhao et al., 2023), a consequence of urbanisation (Ibrahim et al., 2018).

Urbanisation has transformed cities into complex and dynamic environments, profoundly impacting the local climate and the well-being of urban residents. Rapid urbanisation aggravates urban temperatures by expanding the number of concrete surfaces, decreasing open spaces and vegetation, and emitting heat from waste and buildings (Kabano et al., 2021; Mohammad Harmay and Choi, 2022; Zhou et al., 2023). The built-up structures absorb the sunlight's radiation during the day and slowly emit the accrued heat energy throughout the night-time, reducing the cooling impact in cities. UHI concentration contrasts from night to early morning (Sharma et al., 2021). Such urbanisation modification elevates the ambient temperature across the environment surrounding it (Qaid et al., 2016; Uddin et al., 2022) and causes land use cover changes (LULC) in urban places, altering the ground surface's radiative balance, layout, and composition, resulting in identifiable urban climatic conditions or microclimate (Addas et al., 2020; Khiladi and Karimimoshaver, 2023). Moreover, the impact of UHI extends beyond mere temperature rise; it influences humans’ thermal comfort, resulting in higher demand for cooling loads, energy consumption, and overall urban sustainability (Athmani et al., 2022).

Thermal comfort is a critical aspect of urban living, influencing daily activities, productivity, and overall well-being. It relates to satisfaction with the immediate surroundings of the thermal environment (Lee et al., 2017; Amani-Beni et al., 2021) and its influence on urban life, with negative consequences on the well-being and

productivity of humans (Mijani et al., 2020; He et al., 2022). Anthropogenic activities in urban locations lead to an increase in thermal discomfort and have harmful effects on humans (Qaid et al., 2016). Urban temperature and humidity and their seasonal changes are essential aspects of thermal comfort and are linked to health risks, living environment, human behaviour, and urban design (Omonijo, 2017). The lack of thermal comfort can lead to health issues, reduced productivity, and decreased overall satisfaction with the urban living environment. Individuals, particularly the elderly and new-borns, may endure thermal discomfort and acquire heat-related diseases when subjected to extreme temperatures for extended periods in urban areas (Chun and Guldmann, 2018; Isioye and Akomolafe, 2020; Sharma et al., 2021).

As urban development expands, the cities face escalating challenges related to the UHI effect and thermal comfort. The spatiotemporal variability of UHI and thermal comfort concepts are crucial for effective urban planning, adaptation to climate change, and enhancing residents' quality of life. The growing capacity of remote sensing to identify spatial attributes and natural events gives an ideal chance to comprehend the urban heating environment on an excellent spatiotemporal measurement (Feng et al., 2020). The utilisation of remote sensing in the UHI and thermal comfort studies has significantly advanced (Goldblatt et al., 2021), enabling the analysis of SUHI across global cities (Peng et al., 2012; Leal Filho et al., 2018), assessment of rapid urbanisation impacts, and land cover (Khamchiangta and Dhakal, 2020; Arshad et al., 2022), and the synergy between external thermal comfort and thermal infrared remote sensing (Fiorillo et al., 2023). Additionally, the assessment of the UHI using Landsat 8 data has been conducted, demonstrating the broad utilisation of remote sensing imagery to evaluate the UHI effect on increasingly urbanised areas (Ullah et al., 2023). These studies demonstrate remote sensing technology's increasing importance and applicability in understanding the spatiotemporal variability of UHI and thermal comfort in different cities. Studies have also shown an upsurge in urban heat intensity, causing regional temperature differences and resulting in UHI accumulation in big metropolises (Zullo et al., 2019; Tariq et al., 2021). The consequences of landscaping design on UHI impacts have received much attention (Li et al., 2021), with built-up areas and dry landscapes prone to exacerbating UHI effects (Nguyen et al., 2019). In contrast, water bodies

and wide-open areas offer a soothing effect (Sari, 2021). LST was found to be substantially affected by the land's structure, nature, and characteristics. (Adulkongkaew et al., 2020). Additionally, research has demonstrated that the UHI intensity measured in several metropolises is increasing, ranging from 2.01^{o}C to over 2.4^{o}C (Richard et al., 2021).

Botswana cities are not an exception, they are rapidly warming and are expected to have one of Africa's highest temperature increases (Betts et al., 2018; Ouma et al., 2021). This implies that immediate action is required to accelerate Botswana's reactions to the requirement for adaptation efforts. Even though much attention from scientists and others in decision-making positions has been focused on modeling heat waves in the cities where UHI is experienced, the problem is still difficult and complicated. Due to global warming and growing urbanisation, the likelihood of UHI and thermal discomfort occurrences will increase in the years to come, hence the need to carry out this study in Botswana.

1.2 Research Problem Statement

Botswana has a remarkably high level and rate of urban population (70.9%) and rate of urbanisation (2.87%) compared to the rest of Sub-Saharan Africa (Chiguvi, 2022). This is due to the country's cautious economic management, which has attracted significant investors, creating opportunities for rapid economic growth (Gwebu, 2012). As a result, Botswana cities and towns are seeing increasing urbanisation, which adds significantly to UHI intensity and thermal discomfort.

Botswana's second city, Francistown, serves as a regional economic hub for various reasons, experienced a significant rate of population increase (1.4%) and urbanisation (2.07%) in recent years (Central Intelligence Agency (CIA); 2020' Statistics Botswana, 2022). The city's rapid urbanisation, characterised by increased population density and extensive infrastructure development, has led to significant changes in LULC (Chiguvi and Kgathi-Thite, 2022).

Increased population and urbanisation combined with climate change and semi-arid weather have created a microclimate change, resulting in changes in the function and structure of the city's ecosystems (Ouma et al., 2021; Chiguvi, 2022). Specifically, the UHI effect is becoming more pronounced, leading to an upsurge in temperature in the city's built-up locations, particularly during the spring and

Summer. Such modification contributes to the intensification of the UHI effect and potentially reduces the thermal comfort condition of Francistown residents, which in turn leads to thermal discomfort.

The city temperatures are projected to exceed the previous highest temperature of 41.4^{o}C recorded in 2011 (Botswana Climate, 2011; New and Bosworth, 2018), which will result in increased warming and drying compared to the rest of the world (Nkemelang et al., 2018). This will defeat the Paris Agreement's objective of reducing global warming to less than 2°C, perhaps 1.5°C in the next decade, and create environmental challenges (Betts et al., 2018).

However, despite the growing concerns about the UHI effect, Greater Francistown City lacks comprehensive research and data on the spatiotemporal patterns of UHIs and thermal comfort at the microclimate level. The knowledge and impact of UHIs and thermal comfort have not been considered in the city's development projections in Francistown City. Available studies are on heat waves (Moses, 2017; van der Linden et al., 2019) and UHI (Jonsson, 2004; Ouma et al., 2021) studied in Gaborone, the capital city of Botswana. The identified knowledge and research gaps suggest the need to assess the spatiotemporal variability of UHI and thermal comfort in Greater Francistown City. With the adverse impacts of climate change and global warming, information on the UHI effect and thermal comfort spatiotemporal patterns is necessary to develop modern cities.

1.3 Significance of the Study

The significance of this study lies in the need for urgent microclimate scale monitoring to evaluate the UHI outcome and thermal comfort spatiotemporal patterns in the city. This study provides policymakers and urban planners with valuable insights (urban planning and design approaches) into the UHI phenomenon and its impacts on human well-being. The novel research aids in alleviating the adverse effects of extreme UHI and thermal discomfort. It also strengthens Greater Francistown City's resilience to the effects of UHI, which ultimately helps combat climate change. There has also been an upsurge in new information and discoveries concerning UHI and thermal discomfort mitigation practices.

1.4 Aim and Objectives

1.4.1 Aim

This research report aims to assess the spatiotemporal variability of the Urban Heat Island effect and thermal comfort levels in Greater Francistown City from 2014 to 2023.

1.4.2 Objectives of the Research

The specific research objectives are:

- To investigate the spatiotemporal distribution and extent of land use, vegetation cover, and built-up areas in Greater Francistown City using Landsat 8 OLI data.
- To estimate the spatiotemporal dynamic of land surface temperature in the city using Landsat-8 TIRS-1 data.
- To quantify and map the spatial distribution and intensity of the UHI, non-UHI, and Urban Hotspot effect within the city.
- To determine the spatiotemporal distribution of thermal comfort levels experienced by residents in the city.

1.5 Scope of the Study

The study specifically concentrated on the Greater Francistown City area, assessed the UHI phenomenon, and examined the thermal comfort levels in the urban environment. The scope includes spatial (different locations within Greater Francistown City) and temporal (variations over time, from 2014 to 2023) dimensions to capture the dynamic nature of UHI and thermal comfort.

1.6 Limitations

Although this study provides valuable insights into the spatiotemporal variability of UHIs and thermal comfort in Greater Francistown City, certain limitations may have influenced the results and interpretations. The study's findings are primarily based on remote sensing data sources, with limited ground-truthing and field measurements. This may affect the validation and accuracy of the remote sensing-based UHI and thermal comfort assessments. The findings of this study are specific to Greater Francistown City and may not be directly generalised to other urban areas with different climatic, geographic, or socio-economic contexts. While this study provides

recommendations for UHI mitigation and enhancing thermal comfort, the actual implementation of these strategies may face practical, financial, and political constraints beyond the research scope.

1.7 Definition of Terms

Land Use/Land Cover (LULC): The physical and functional characteristics of the land surface, including its usage (residential, commercial, industrial) and cover types (vegetation, water bodies, built-up areas) (Karimimoshaver, 2023).

Spatiotemporal Variability: The variation in data or phenomena across both space (geographical locations) and time (temporal periods) (Aghamolaei et al., 2021).

Thermal comfort: An emotional state of cognisance that indicates contentment with the thermal surroundings (Kalogeropoulos et al., 2022)

Urban Heat Island: A phenomenon that refers to the significant rural-urban temperature disparity (Barrao et al., 2022).

Urban Thermal Field Variance Index: A thermal comfort metric which explores the influence of high urban temperatures on urban people's standard of living (Hishe et al., 2023).

1.8 Conclusion

Chapter One has laid the groundwork for understanding the critical issues related to UHI and thermal comfort in the context of Greater Francistown City. Several emerging issues have been highlighted, which were essential addressed in the subsequent chapters of this study. Addressing these issues through the objectives outlined study contributed to developing sustainable urban environments that prioritise residents' well-being and resilience against climate change.

CHAPTER 2: LITERATURE REVIEW

2.1 Introduction

This chapter comprehensively reviews the existing literature on UHI and thermal comfort. It establishes a solid theoretical foundation and contextual framework for the study by exploring key concepts, methodologies, and findings from previous research. The literature review is organised into several sections, each addressing a critical aspect of UHI and thermal comfort

2.2 Theoretical and Conceptual Framework

The UHI effect essentially represents the LST differential between built-up areas covered by man-made structures and the peri-urban or rural surroundings predominantly covered by vegetation. Man-made structures covering urban surfaces are characterised by low albedo and high thermal inertia (Taha, 1997). These have solar absorption and retention capacities, elevating temperatures in urban regions. On the other hand, vegetation, which is preponderant in peri-urban or rural areas, has a cooling effect on the environment through shading, evapotranspiration, and solar radiation reflection. The result is lower LST in peri-urban or rural areas than in urban areas. In urban areas, these three mechanisms act as a counterbalance to the warming influence of built-up areas.

The specific spatiotemporal variations in temperature in urban and rural areas are a function of a complex interaction of factors, which amount to human activities that alter the nature of land cover and surface properties. These factors include the composition, arrangement, and density of built-up areas, the imperviousness of surfaces, and the extent and density of vegetation cover.

In turn, the overall LST affects the degree of physical and mental satisfaction experienced by urban dwellers with the temperatures in the environment. This satisfaction is called urban thermal comfort (Lee et al., 2017; Zhang et al., 2022). The relationships among these variables are depicted in the conceptual framework (Figure 2.1).

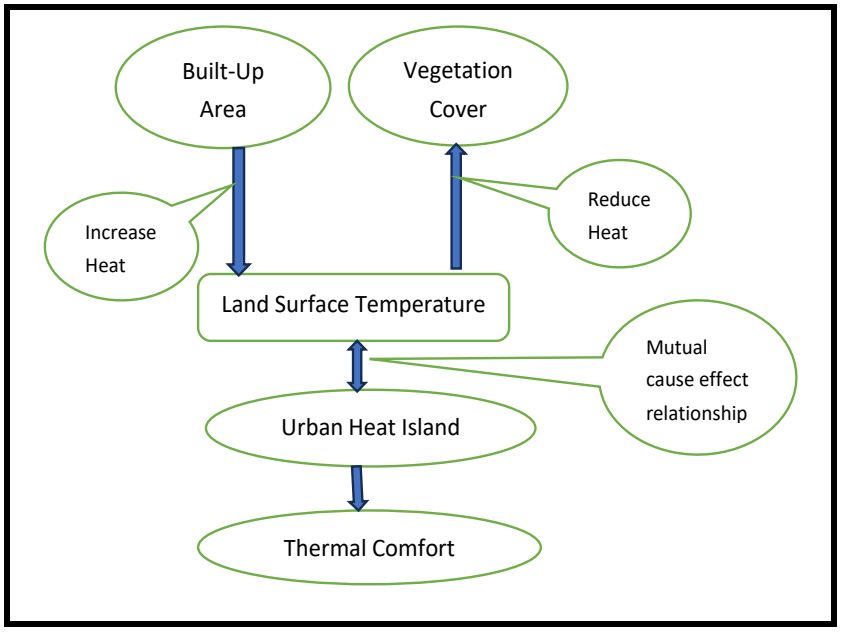


Figure 2.1 Conceptual Framework showing the relationship between LST, UHI, and Thermal Comfort

From Figure 2.1, the core variable of interest is LST, which is a function of the nature of the surface, with two essential categories. The built-up areas tend to increase LST (hence the arrow pointing LST-wards), and the rural regions exert a cooling influence on the surface (hence the arrow pointing away from the LST variable). The actual heating or cooling effect differential across space and time of urban and rural areas is moderated by the specific nature of the respective surfaces. LST differences between urban and rural regions define the UHI effect, and there is a reciprocal relationship between LST and UHI, hence the bi-directional arrow between the two variables. In turn, the overall UHI effect determines the thermal comfort of dwellers in a specific geographical location.

2.3 An Overview of Urban Heat Island and Thermal Comfort

The UHI phenomenon refers to the significant rural-urban temperature disparity. Human activities, higher urbanisation, and modifications to the natural environment primarily cause this temperature difference (Barrao et al., 2022). These factors contribute to the absorption and retention of heat, resulting in elevated urban temperatures compared to their non-urban counterparts (Ibrahim et al., 2018; Kabano et al., 2021).

The concept of UHI was first recognised and defined in early studies as the region of warmth associated with cities (Chandler, 1962; Oke, 1969, 1973; Martin-Vide et al.,

2015). UHI is not limited to large cities but can also occur in smaller urban areas (Peng et al., 2012; Zhou et al., 2017). The magnitude of the UHI effect is a function of, among others, city size, geographical location, climate, and local meteorological conditions (Corburn, 2009; Zhou et al., 2017; Nguyen et al., 2019; Mohammad et al., 2022).

On the other hand, thermal comfort is the mental satisfaction one experiences in the thermal environment (Lee et al., 2017; Amani-Beni et al., 2021). It is a critical aspect of human well-being, particularly in urban areas affected by the UHI effect. The UHI phenomenon significantly impacts thermal comfort (Mijani et al., 2020). The UHI effect exacerbates heat stress and heat-related disorders, causing reduced thermal comfort and increased health risks during heat waves (Omonijo, 2017). The urban-rural temperature difference disparity, a key feature of UHI, hinders the body's recovery from daytime high-heat exposure, further affecting thermal comfort (Lai et al., 2019; van der Linden et al., 2019). Achieving thermal comfort is essential for maintaining well-being and productivity, particularly in urban areas where high temperatures and UHI effects can pose challenges. Both concepts are interconnected and significantly shape the quality of urban life.

Studies have shown that UHI can significantly impact outdoor thermal comfort (Lai et al., 2019; Mutani and Todeschi, 2020; Fiorillo et al., 2023; Prasad and Satyanarayana, 2023). Mutani and Todeschi (2020) confirm the impact of UHI on outdoor thermal comfort conditions and energy utilisation. In addition, the impact of UHI on mortality rates during heat waves has been linked to the exponential increase in mortality with rising temperatures, highlighting the adverse effects of UHI on human health and well-being (Heaviside et al., 2016; Lee et al., 2017). Evaluating comfort conditions has revealed a strong relationship between microclimatic factors, such as solar radiation and air temperature, and thermal comfort (Yin et al., 2012; Zhang et al., 2022).

Spatiotemporal analysis of UHI and thermal comfort involves the examination of temperature patterns across different locations and over time. Studies have utilised various methodologies to understand the spatiotemporal dynamics of UHI and thermal comfort (Yin et al., 2012; Aslan & Koc-San, 2016; Mushore et al., 2018; Huang et al., 2019; Khallef et al., 2020; Mijani et al., 2020; Kasniza Jumari et al.,

2023; Zhao et al., 2023). These studies demonstrate the diverse approaches and methods employed in the spatiotemporal analysis of UHI and thermal comfort, enhancing our understanding of the complex variations of urban temperature patterns over space and time.

2.4 Importance of Assessing UHI and Thermal Comfort

Assessing the UHI and thermal comfort is essential for comprehending the influence of urbanisation on local climate and people's well-being. The UHI effect is a major concern for public health, especially during summer (Scott et al., 2018). Urban areas, with their high concentration of buildings, pavement, and human activities, tend to absorb and retain more heat, leading to elevated temperatures (Ibrahim et al., 2018; He et al., 2022; Imran et al., 2022). This increase in temperature can have numerous harmful effects on the environment and human health.

Assessing UHI is vital for the sustainability of cities. Urban areas experience higher temperatures which increase energy consumption for cooling purposes (van der Linden et al., 2019; Mutani and Todeschi, 2020). Knowing the extent of UHI and its effects on energy demand can help town planners develop energy-efficient approaches to reduce the urban heat load. This can include optimising building designs, promoting renewable energy sources, and implementing urban greening initiatives (Oke, 1973; Chun and Guldmann, 2018; Scott et al., 2018). By mitigating UHI, cities can reduce their carbon footprint and contribute to a more sustainable future (He, 2019; Chen and You, 2020; Karimi et al., 2023).

Thermal comfort is a critical aspect of urban living as it directly impacts the well-being and productivity of the urban population (Amir Siddique et al., 2023). Its assessment is equally important, especially in indoor and outdoor spaces (He et al., 2022; Ren et al., 2023). Human beings spend significant time in urban environments, and their comfort levels are crucial for their overall quality of life. By assessing thermal comfort, urban planners can identify areas of discomfort and implement strategies to improve the microclimate (Mushore et al., 2018; Xu et al., 2017). This can include providing shaded areas, optimising natural ventilation, and incorporating green infrastructure (He, 2019). Enhancing thermal comfort can improve mental and physical health, increase outdoor activity, and strengthen community social cohesion.

Moreover, assessing thermal comfort is essential for equitable urban planning. Vulnerable groups, including children, the elderly, and low-income communities, are often disproportionately affected by extreme temperatures (Lanza et al., 2023; Ngcamu, 2023). Assessing the thermal comfort needs of different population groups, urban planners can ensure that their design interventions prioritise the well-being of those most susceptible to thermal stresses. This can help promote social equity and reduce the negative impacts of urban heat on disadvantaged communities.

The inclusion of solar radiation effects when assessing thermal comfort near glazed walls and the ability of shading devices to improve thermal comfort conditions demonstrate the significance of considering environmental factors in thermal comfort evaluations (Oliveira and Corvacho, 2021). Moreover, assessing thermal comfort in different climatic conditions and building types is essential for understanding the parameters influencing thermal comfort and illumination, emphasising the subjective nature of thermal comfort and the existence of indices for its evaluation (Kumar and Sharma, 2020; Schweiker et al., 2020). Lotfabadi and Hançer, (2019) highlighted the influence of building envelope design on the thermal environment and the significance of architectural elements in achieving thermal comfort within inhabited spaces.

Evaluating UHI and thermal comfort requires a comprehensive assessment of environmental factors, anthropogenic heat, and building design to develop effective strategies for mitigating heat-related challenges and ensuring comfortable living and working environments. Greater Francistown City in Botswana faces unique challenges due to rapid urbanisation and climate change (Ouma et al., 2021; Chiguvi, 2022). Understanding the UHI effect and thermal comfort dynamics is crucial for addressing concerns, creating sustainable urban spaces, and enhancing residents' quality of life.

2.5 Chronological Trends of UHI and Thermal Comfort

2.5.1 Historical Context of UHI and Thermal Comfort

The historical context of UHI and thermal comfort research reveals a progression from early observations to the establishment of foundational concepts, reflecting a growing awareness of the impact of urbanisation on microclimates and human well-being. The study of UHI can be traced back to the early 19th century when Luke

Howard, a British meteorologist, observed urban-rural temperature differences in London (Stewart, 2011). However, it wasn't until the mid-20th century that systematic studies on UHI emerged, and the term "Urban Heat Island" gained prominence (Zhang et al., 2018). One of the pioneering studies was also conducted by Gordon Manley in the 1950s, which observed and quantified the temperature differences between urban and rural regions in the UK (Oke, 1969). In the 1960s (Landsberg, 1970), pioneering studies introduced the concept systematically, emphasising the temperature differentials between urban and rural territories. Oke's seminal paper in 1973 addressed the influence of city size on UHI, setting the stage for subsequent research into the factors contributing to temperature variations in urban environments (Oke, 1973; Taha, 1997). The understanding of surface cover types, anthropogenic heat, and urban morphology emerged as critical components in the development of UHI models (Taha, 1997). Early seminal works by (Chandler, 1962; Oke, 1969) and (Oke, 1969) contributed to recognising and documenting the UHI phenomenon. These foundational studies laid the groundwork for subsequent research on UHI and highlighted the role of urbanisation in modifying local climates.

In the 1960s and 1970s, studies on UHI expanded globally, with researchers investigating UHI phenomena in different cities worldwide (Chandler, 1962; Mcelroy, 1973). These studies focused on understanding the factors contributing to UHI, such as land use changes, building materials, and anthropogenic heat emissions. Notable research during this period includes the work of (Tyson et al., 1972) who discussed the development of heat islands over South African cities, reviewed literature on vertical temperature structures, and illustrated the complexity of Johannesburg's structure.

Subsequent studies have explored the spatial variability of UHI in different urban settings, such as the investigation of the UHI in Uppsala, Sweden, which laid the groundwork for much of the work that followed (Imamura, 1993; Taha, 1997). Furthermore, the effect of urban gardens on external thermal comfort has been evaluated, emphasising the mitigating role of green spaces on UHI effects (Oke, 1969; Landsberg, 1970).

These early investigations have been instrumental in shaping the field of urban climatology and have set the stage for subsequent research on UHI. The recognition

and characterisation of UHI have paved the way for further studies aimed at understanding its spatial and temporal dynamics, its impacts on human health, and strategies for mitigating its effects.

Parallel to this, thermal comfort research developed significantly during the 20th century. Fanger's 1960s and 1970s work, particularly the Predicted Mean Vote (PMV) and the Predicted Percentage of Dissatisfied (PPD) indices model, established a framework for assessing and designing indoor environments for human comfort, considering factors like radiant temperature, air temperature, clothing insulation, and humidity (Fanger and Toftum, 2002; Fanger 1970). The 1970s also saw the emergence of adaptive thermal comfort models (Wu et al., 2017; Zhao et al., 2021). Gagge et al. (1986) introduced the Standard Effective Temperature (SET) model, shifting towards a more personalised and context-specific approach to thermal comfort assessment. The thermal comfort concept has spawned a growing interest in understanding human adaptation to unique climatic conditions, such as high-altitude areas and subtropical highland climates (Natarajan et al., 2015).

Since then, research on thermal comfort has expanded to include outdoor environments and the effect of urban settings. Urban influences on thermal comfort, such as the presence of green spaces, shading, and wind patterns, have been explored (Matzarakis and Mayer, 2000; Gómez et al., 2004; Lee et al., 2017). Studies have also assessed the impact of building design and retrofitting on indoor thermal comfort, particularly in historical and heritage buildings, dating back to the 19th century (Bakhtiari et al., 2020; Piasecki et al., 2020; Moghaddam et al., 2021). The assessment of thermal comfort in different climatic conditions, such as cold regions, tropical savanna climates, and African desert climates, has facilitated a thorough comprehension of thermal comfort parameters (Chen and You, 2020; Thapa, 2020; Bassoud et al., 2021; Jia et al., 2022; Mustapha et al., 2022). The development of new measurement techniques, such as thermal comfort indices specific to outdoor environments, has allowed for more accurate assessments of thermal comfort in urban contexts (Blazejczyk et al., 2012; Petralli et al., 2014; Kabano et al., 2021; Hishe et al., 2024).

The late 20th century and early 21st century witnessed a growing recognition of the interconnectedness between UHI and thermal comfort. Pioneering Works (Taha, 1997) underscored the importance of considering urban climatic conditions in building and city design to improve and enhance the city's thermal comfort. Studies have also investigated how UHI affects and vice versa (He et al., 2022) and have shown that UHI can lead to higher discomfort levels, reduced outdoor activity, and increased energy consumption for cooling (Lee et al., 2018; Mushore et al., 2018; Gonzalez-Trevizo et al., 2021). Recent studies, such as those exploring the effect of green infrastructure on UHI and comfort, represent a continuation of efforts to integrate ecological solutions into urban design (Tiwari et al., 2021; He et al., 2022). This understanding has led to the development of integrated strategies that address UHI and thermal comfort such as the integration of green infrastructure and cool material technologies.

Advancements have also influenced the evolution of research on UHI and thermal comfort in building environmental control systems and the development of standards, such as ASHRAE Standard 55, which has undergone revisions to address thermal comfort in buildings that rely on natural ventilation (Kaushal et al., 2024). Furthermore, computational fluid dynamics (CFD) has enabled the simulation of indoor dynamic thermal comfort, reflecting the integration of advanced modeling techniques in thermal comfort research (Setaih et al., 2014; Huo et al., 2021).

However, the challenges in understanding UHI and thermal comfort include the complex, dynamic nature of urban environments, the influence of climate change, and the need for interdisciplinary collaboration (Gonzalez-Trevizo et al., 2021). Future research will likely focus on comfort handling approaches, considering the socio-economic dimensions of thermal comfort and creating efficient strategies to mitigate the UHI phenomenon.

Overall, the historical context of UHI and thermal comfort research reflects a progression from foundational studies on external thermal comfort to a comprehensive understanding of UHI effects, external thermal comfort, and the influence of environmental factors and building design. As research advanced, the relationship between UHI and thermal comfort became evident, leading to integrated approaches considering both aspects. The historical development of these fields can

help build the existing knowledge and continue to develop effective policies for creating sustainable and comfortable urban environments.

2.5.2 Recent Advances in UHI and Thermal Comfort

Recent studies have increasingly utilised sophisticated remote sensing and GIS technologies to map and analyse UHI and thermal comfort (Kasniza Jumari et al., 2023). High-resolution satellite imagery and drone-based thermal imaging contribute to a more nuanced understanding of spatial variations in surface temperatures within urban areas (Duffy et al., 2021). These technologies enable researchers to identify UHI hotspots and assess their dynamics over time (Wang et al., 2019). Studies on microclimate modeling and simulation have also been recently explored (Huo et al., 2021; Oliveira & Corvacho, 2021; Fiorillo et al., 2023; Khalvandi and Karimimoshaver, 2023). Computational modeling and simulation advances have become valuable tools in studying UHI and thermal comfort. These tools allow for a more detailed analysis of microclimates within urban environments. The models consider building morphology, green spaces, and anthropogenic heat sources (He, 2019). Thereby identifying effective strategies for reducing UHI and improving thermal comfort in specific urban areas. For instance, Computational Fluid Dynamics (CFD) simulations enhance comprehension of airflow patterns and their influence on thermal comfort (Setaih et al., 2014; Aghamolaei et al., 2021).

Smart cities have brought innovations in monitoring and managing urban environments (Bibri, 2018). Internet of Things (IoT) devices and sensor networks are increasingly employed to gather real-time data on temperature, humidity, and other environmental parameters (Das et al., 2018). This real-time data aids in dynamic urban planning decision-making and enhances thermal comfort. For example, Ravnikar et al. (2023) explored integrating smart city technologies and big data to address thermal comfort challenges, proposing a framework for future urban microclimate planning.

Recent research has focused on understanding thermal comfort from a more human-centric perspective, considering factors beyond traditional environmental parameters (Lotfabadi and Hançer, 2019). Studies explore the influence of personal preferences, cultural differences, and behavioural adaptations on perceived comfort, contributing to developing more inclusive and adaptive thermal comfort models (Thapa, 2020;

Lanza et al., 2023). Ratajczak et al. (2023) explored the challenges of traditional thermal comfort models by highlighting the gender-specific differences in thermal demand, emphasizing the importance of individualized approaches.

Urban climate informatics is an emerging research field that uses data-driven approaches to understand urban climate dynamics (Amani et al., 2020; de Almeida et al., 2021). Researchers can identify patterns and trends related to UHI and thermal comfort by analysing large datasets. This field combines techniques from data science, machine learning, and urban climatology to acquire a deeper understanding of the intricate interplay between cities and their atmospheric environment (Zhang et al., 2018; Li et al., 2020; Vergara et al., 2023; Waleed et al., 2023).

Integrated assessment approaches have been used to evaluate the impacts of UHI on human health and well-being. These approaches consider multiple factors, such as temperature measurements, air pollution, and human vulnerability, to assess the overall impacts of UHI on urban populations (Zupancic and Bulthuis, 2015; Gonzalez-Trevizo et al., 2021; Ngcamu, 2023). With the complex interactions between UHI and human health, policymakers and urban planners can develop effective mitigation strategies. These recent advances in UHI and thermal comfort research leverage cutting-edge technologies and innovations that contribute to a more holistic understanding of urban climates and provide practical insights for sustainable urban development.

2.6 Spatiotemporal Assessment Urban Heat Island

UHI assessment is crucial for understanding their spatial and temporal distribution, impacts, and dynamics. Studies employ various techniques and data sources to analyse UHI dynamics over large areas. These data sources provide valuable information on land surface temperature and can be used to assess spatial and temporal variations in UHI (Xu et al., 2017; Addas et al., 2020; Goldblatt et al., 2021). Zhou et al. (2019) have highlighted the merits of remote sensing and satellite data as effectual and reliable methods for evaluating and understanding the spatial properties and dynamic shifts in urban thermal environments. These methods have been instrumental in quantifying UHI intensity and identifying land cover changes associated with UHIs (Cristóbal et al., 2018; Dutta et al., 2021). Li and Stein (2020)

noted that remote sensing may not accurately capture microscale variations due to spatial resolution issues and cloud cover and may not provide detailed information on the underlying causes of UHI. The GIS technology has also enabled the integration and analysis of spatial data, allowing researchers to examine temperature patterns in relation to land use, vegetation cover, and other urban characteristics (Guha et al., 2020; Kasniza Jumari et al., 2023). Sidiqui et al. (2022) used GIS-based approaches to identify UHI hotspots, assess the dynamic relationship between land use and temperature, and develop UHI vulnerability maps.

Studies (Cristóbal et al., 2018; García-Santos et al., 2018; Onačillová et al., 2022) have emphasised the use of remote sensing technology for retrieving LST as a commonly used method for assessing UHIs. These studies have shown the effectiveness of remote sensing technology in capturing the spatial spread and temporal variability of UHIs. The LST method may not accurately represent air temperatures due to inaccuracies in wind cooling effects, surface emissivity, and atmospheric conditions (García-Santos et al., 2018). There is a lack of comprehensive studies that analyse the temporal dynamics of LST in Greater Francistown City, especially over an extended period (Sharma et al., 2021; Ullah et al., 2022). This study addresses this gap by examining LST variations from 2014 to 2023, providing insights into how LST has changed over time in response to urbanisation and climate change.

Setaih et al. (2014) and Aghamol et al. (2021) demonstrated using CFD simulation and mesoscale models for assessing UHIs. The urban climate modeling and simulation methods have contributed to accurately estimating urban heat islands and the simulation of urban microclimates. Spatiotemporal modeling approaches, such as cellular automata and agent-based models, have simulated and predicted temperature patterns in urban areas. The models consider urban morphology, land use changes, and climate conditions to understand how UHI and thermal comfort may evolve (Aburas et al., 2016). Deep learning models have been developed to forecast the magnitude and characteristics of UHI in urban areas, considering UHI's high temporal variability and spatial heterogeneity (Xia et al., 2022; Ma et al., 2023).

Memon et al. (2009) have examined UHI intensity as an indicator of urban heating, highlighting the importance of UHI intensity assessment in understanding urban heat

islands. These studies have provided valuable insights into the quantification of UHII and its implications for urban heating.

The Normalised Difference Built-up Index (NDBI) and Normalised Difference Vegetation Index (NDVI) are widely used for assessing UHIs. A study by Guha et al. (2018) analysed LST with NDVI and NDBI employing Landsat 8 OLI and TIRS data, demonstrating the relationship of estimated LST with NDVI and NDBI. Furthermore, (Zhang et al., 2022) highlighted the importance of NDBI and NDVI as reliable predictors of LST, emphasising their effectiveness in UHI assessment.

The methods for assessing urban heat islands encompass a range of approaches and have been instrumental in understanding the spatial and temporal variations of UHIs and their impacts on urban environments.

2.7 Studies on Urban Heat Island in Similar Urban Environments

Studies on UHIs in similar urban environments, including comparative studies in other cities or regions, provide valuable insights into their spatial distribution, intensity, and impacts. Comparative studies have been conducted across various cities and regions, shedding light on the factors influencing UHI patterns and the lessons learned from these studies.

Peng et al. (2012) conducted a comprehensive study across 419 global big cities, revealing that the average annual daytime surface UHI intensity (SUHII) is higher than the annual night-time SUHII. This study provides a global perspective on UHI patterns and highlights the significance of temporal variations in UHI intensity.

Tan et al. (2010) examined the causal association between UHI and heat waves and human health in Shanghai, emphasising the greater heat sensitivity of the urban population vis-à-vis their rural counterparts. This study underscores the health implications of UHIs and the need for targeted interventions to mitigate heat-related health risks in urban areas.

Garuma (2023) focused on tropical surface UHIs in East Africa, highlighting the limited city-scale studies in tropical sub-Saharan Africa. This study underscores the need for more research in tropical regions to understand the unique characteristics and impacts of UHIs in these areas. Zhang et al. (2021) examined the spatiotemporal evolution of the urban thermal environment in Nanjing, China,

providing insights into the driving factors of UHIs. The research findings offer valuable scientific and technological support for formulating urban development plans and improving the ecological environment in similar cities worldwide.

Studies (Jonsson, 2004; Ouma et al., 2021) on UHI and thermal comfort have focused on major cities globally, with limited research specific to smaller or less-studied urban areas like Francistown. This study provides valuable insights specific to Greater Francistown City, addressing the need for localised research that considers regional climatic and urbanisation contexts.

Lessons learned from these studies include the need for tailored interventions to address UHI impacts in specific urban contexts. Comparative studies, such as those conducted by Li et al. (2018) and Tang (2022), have enabled direct comparisons of UHI intensities in different regions, offering significant insights into the influence of urbanisation, land use, and ecological factors on UHI patterns. Alahmad et al. (2020) and (Garuma, 2023) have highlighted the global rise of UHIs and their potential intensification of droughts in tropical regions. These findings underscore the interconnectedness of UHIs with broader environmental challenges and the need for holistic approaches to address urban climate issues.

Ngie (2020) Utilised the mono-window algorithm to estimate LST for Johannesburg and Cape Town metros, illuminating our understanding of the spatial distribution of UHIs in these urban areas.

Studies on UHIs in similar urban environments and comparative studies in other cities or regions have contributed to a deeper understanding of UHI patterns, driving factors, and their implications for human health and the environment. These studies have provided valuable lessons for urban planners, policymakers, and researchers, emphasising the importance of context-specific interventions and the need for further research in diverse urban and climatic settings.

2.8 Spatial Distribution of Urban Heat Island

The spatial distribution of UHIs refers to the patterns and variations of UHI intensity within urban areas (Xu et al., 2010; Alahmad et al., 2020). These spatial patterns and the factors influencing the localised UHI intensity are crucial for addressing thermal comfort and implementing effective mitigation strategies.

The spatial patterns of UHIs in urban areas are UHIs are a function of various factors, including land cover, land use, and urbanisation (Xu et al., 2010). Studies (Wu et al., 2018; Fatemi and Narangifard, 2019; Zullo et al., 2019; Jombo et al., 2022) have shown that UHIs exhibit distinct spatial patterns, with higher temperatures concentrated in densely built-up areas, industrial zones, and areas with reduced vegetation cover. These areas experience reduced vegetation cover, limited shading, and increased heat absorption, leading to higher temperatures (Jombo et al., 2022). UHI intensity may also vary depending on the size and shape of urban areas, with well-defined urban islands exhibiting distinct UHI patterns (Martin-Vide et al., 2015).

The link between land use and UHI intensity affects UHI spatial distribution, with the spatial variability of UHI expansion being explained by the spatial patterns of economic progress, population expansion, and thickness of vegetation cover (Jonsson, 2004; Zhang et al., 2013; Ngcamu, 2023). The distribution of UHIs has been closely linked to industrial land and impervious surfaces, which contribute to increased heat absorption and reduced evaporative cooling (Wu et al., 2018; Li et al., 2021).

Factors influencing localised UHI intensity include land cover types, impervious surfaces, vegetation cover, and urban infrastructure such as highways and built-up areas (Zhang et al., 2018; Tang, 2022; Xiong et al., 2022). The spatial and temporal dynamics of UHIs have been studied employing remote sensing and geospatial analysis, revealing the influence of land cover changes and urbanisation processes on UHI patterns (Xu et al., 2010; Sharma et al., 2021). Also, the relationship between UHIs and surface biophysical characteristics, such as the NDVI, has been investigated to understand the impact of vegetation on UHI intensity and spatial distribution (Guha et al., 2018; Ouma et al., 2021).

The spatial distribution of UHIs presents challenges for urban planners and designers, particularly in developing strategies to mitigate UHI effects and improve thermal comfort in urban areas. Identifying spatial distribution patterns and their impact on the emergence of UHIs has become a primary concern for urban planners, necessitating the formulation of technical policies and solutions to reduce UHIs (Duhita Puspita et al., 2022). Assessing how land-use types affect surface UHIs is

crucial for developing comfortable living environments and sustainable urban development (Hoan et al., 2018). The spatial transfer features and patterns of UHIs influence thermal comfort and urban ecological services, highlighting the need for spatial analysis techniques to address UHI impacts (Huang and Ye, 2015).

Previous studies, (Chun and Guldmann, 2018; Ibrahim et al., 2018) have often focused on general UHI effects without detailed spatial mapping of UHI intensity and distribution within the city. This study aims to fill this gap by providing a detailed spatial analysis of UHI intensity and identifying specific urban hotspots, which is crucial for targeted mitigation strategies.

A complex interplay of LULC and urbanisation influences the spatial distribution of UHIs in urban areas. The spatial patterns of UHIs and their relationship with environmental factors are crucial for formulating efficient urban planning strategies, mitigating UHI effects, and making sustainable and comfortable cities. Previous studies on LULC in Greater Francistown City have often relied on low-resolution data, limiting the accuracy of findings (Kabano et al., 2021; Zhou et al., 2023). This study aims to fill this gap by using high-resolution Landsat 8 OLI data to provide a more detailed and accurate analysis of LULC changes over time.

2.9 Impact of Urban Heat Island on Thermal Comfort

The UHI effect has multifaceted impacts on thermal comfort, with significant implications for urban residents' health and social and economic well-being (Isioye and Akomolafe, 2020; Mohammad Harmay and Choi, 2022). The UHI effect exacerbates heat waves, leading to adverse health effects such as heat stress, dehydration, and illnesses related to heat. The absence of surface moisture and minimal wind velocities accompanying heat waves in urban areas further intensify the impact on human health (Tan et al., 2010). Additionally, the UHI effect contributes to increased heat stress disorders and poses a risk to the health and welfare of urban residents, especially in highly populated urban areas (Tang, 2022). These health implications underscore the urgent need for effective UHI mitigation strategies to safeguard public health and well-being.

Socially, the UHI effect can exacerbate social disparities and inequalities, as vulnerable people, like the elderly and low-income groups, are disproportionately affected by heat-related health risks (Lanza et al., 2023; Ngcamu, 2023). The

economic consequences of the UHI effect are also substantial, as it leads to increased energy consumption, heightened demand for cooling systems, and associated costs for individuals and businesses. Moreover, the UHI effect can impact labour productivity, outdoor activities, and overall quality of life, thereby influencing the economic vitality of urban areas (Ren et al., 2023). The economic and social challenges posed by the UHI effect necessitate comprehensive urban planning and design involvements to alleviate its impact and promote equitable access to thermal comfort and well-being.

Urban planners and designers face several challenges in addressing the UHI effect and its influence on thermal comfort. The rapid urbanisation and unregulated land use changes contribute to the intensification of the UHI effect, posing challenges for sustainable urban development (Karimi et al., 2023). The complex interactions between urban morphology, land use, and climate conditions also present challenges in implementing effective UHI mitigation strategies (Mohammad Harmay and Choi, 2022; Zhang et al., 2022). Furthermore, the trade-offs between urban development, green space preservation, and UHI mitigation require interdisciplinary approaches and innovative solutions to balance competing urban priorities. The negative impacts of the UHI effect on the thermal environment, energy consumption, and public health necessitate a holistic and integrated approach to urban planning and design to address these challenges effectively.

The UHI effect significantly impacts thermal comfort, with far-reaching health, social equity, and economic well-being implications. Addressing the UHI effect requires concerted efforts from urban planners and designers to implement sustainable and resilient strategies prioritising public health, social equity, and economic vitality in urban environments.

2.10 Thermal Comfort in Urban Environments

2.10.1 Assessment and Measurements of Thermal Comfort

Thermal comfort is an emotional state of cognisance that indicates contentment with the thermal surroundings (Qaid et al., 2016; Amani-Beni et al., 2021; Kalogeropoulos et al., 2022). Recognising thermal comfort trends is crucial to health, human thermal comfort, global warming, and energy waste in city microclimates (Mushore et al.,

2018). Thermal comfort is essential for sustainable cities as populations rise and cities expand Mijani et al., 2020; Kalogeropoulos et al., 2022). It also monitors and predicts urban environment spatial and temporal thermal comfort patterns.

Several remote sensing and meteorological studies have assessed urban thermal comfort. Landsat, MODIS, and meteorological datasets modelled outdoor thermal comfort (Mijani et al., 2020). Bare land had shown a higher mean discomfort index than other land covers. Xu et al. (2017) created external thermal comfort maps for Fuzhou, China, using in situ meteorological data and satellite images. Results indicate thermal comfort correlated with the built-up parameters and contrariwise associated with plant canopy and aquatic indicators.

Mushore et al. (2018) investigated external thermal comfort in Zimbabwe during various seasons and land cover types using ground-station ambient temperature data, relative humidity, and Landsat imagery. Results demonstrated that Landsat 8 satellite images could accurately model thermal comfort in various seasonal situations. Lai et al. (2019) examined heat-resistance techniques to enhance outdoor thermal conditions. According to the findings, city geometry exhibits the most significant impact on thermal comfort in the summertime, followed by aquatic bodies and plant cover.

Few studies have effectively integrated remote sensing data with thermal comfort assessments to understand their interrelationship (Fiorillo et al., 2023). This study bridges this gap by utilising remote sensing technology to analyse thermal comfort, offering a novel approach to studying how UHI impacts thermal comfort in urban areas.

Thermal comfort has been measured using several bioclimatic indices, questionnaires, and interviews. Bioclimatic indicators are classified into direct, rational, and empirical indices. Empirical indices (wet bulb-globe temperature index (WBGT), actual sensation vote (ASV), and temperature-humidity index (THI)) are linear equations that assess thermal comfort for a specific climate area (Haghshenas et al., 2021; Ren et al., 2023).

The direct indicators of Apparent Temperature (AT), Normal Effective Temperature (NET), and the Wind Chill Index (WCI) (Blazejczyk et al., 2012) are built on linear models that evaluate thermal comfort which consider meteorological characteristics

such as relative humidity, ambient temperature, and wind speed (Haghshenas et al., 2021). Rational indicators (Physiological Equivalent Temperature (PET), Standard Effective Temperature, Heat Index, Universal Thermal Climate Index, and Predicted Mean Vote) (Petralli et al., 2014; Kabano et al., 2021) are primarily dependent on the human energy equilibrium, considering the interplay among metabolic work rate, garment isolation, and climatic conditions, as well as the pedestrian's thermal perception (Qaid et al., 2016).

Another thermal comfort metric is the Urban Thermal Field Variance Index (UTFVI), which was established to explore the influence of high urban temperatures on urban people's standard of living (Hishe et al., 2023). The UTFVI is a widely used and verified index for measuring the thermal well-being of metropolitan settings. The UTFVI was utilised to calculate Abuja's intensity of thermal comfort, quantifying the effects of UHI on the character of urban living. According to the UTFVI map related to UHI, the city's outskirts are more environmentally friendly than its inner segment (Isioye and Akomolafe, 2020).

Satellite imagery has also been effective for external thermal comfort models. Remote sensing data can be applied to model ecological and surface biophysical variables at different temporal and spatial resolutions (Xu et al., 2017)While the importance of thermal comfort is recognised (Omonijo, 2017; He et al., 2022), limited research has been conducted on its spatiotemporal variability within Greater Francistown City. This study addresses this gap by evaluating thermal comfort levels across different parts of the city and at different times of the year, providing a comprehensive understanding of how thermal comfort varies spatially and temporally.

2.10.2 Factors Influencing Thermal Comfort Levels

Several factors significantly influence thermal comfort levels. The most obvious environmental factor affecting thermal comfort is the environment's temperature. Different individuals have different preferences when it comes to temperature. However, Yin et al, (2012) suggest that most people generally consider a temperature range between 20-24°C comfortable. Extreme deviations from this range can lead to discomfort and decreased productivity. Airspeed can influence perceived comfort (Zhang et al., 2021). Radiant temperature affects comfort by

transferring heat from the body to surrounding surfaces. Humidity reduces body evaporation, while airspeed influences comfort by providing a gentle breeze in warm environments (Xu et al., 2017).

Personal factors also play a pivotal role in thermal comfort, Khatoon and Kim (2020) stress that thermal comfort is a relative notion influenced by various environmental and personal factors. Thapa (2019) further supports this by highlighting the influence of physiological factors such as age, gender, and body mass index on adaptive thermal comfort. For example, older adults may be less able to regulate body temperature, making them more sensitive to extreme temperatures (Khatoon and Kim, 2020). Similarly, individuals with certain medical conditions may require specific temperature and humidity conditions for comfort and well-being. Additionally, (Mustapa et al (2016) emphasise the impact of occupants' behaviour and the indoor environment on thermal comfort, further underscoring the multifaceted nature of this phenomenon.

Gwak et al. (2019) point out that factors such as ambient temperature, mean air radiant temperature, indoor air velocity, and metabolic activity significantly underscore the intricate relationship between physiological responses and environmental conditions in determining thermal comfort. Psychological factors including individual preferences, perception, and psychological stress, can influence thermal comfort. People's expectations, past experiences, and cultural backgrounds can shape their perception of comfort levels. Additionally, high levels of stress or anxiety can affect thermal comfort, leading to a feeling of discomfort even at optimal temperature conditions (Wang and Liu, 2020; Qureshi and Rachid, 2021).

Building design and systems, occupancy, and spatial arrangements also influence thermal comfort levels (Yu et al., 2017; Ratajczak et al., 2023). Proper ventilation and insulation are crucial for maintaining air quality and regulating indoor temperatures (Thapa, 2019). Occupancy density and furniture arrangement also impact thermal comfort, with crowded areas feeling warmer due to combined heat. The design of a space also influences air circulation and radiant heat exchange (Yu et al., 2017; Oliveira and Corvacho, 2021; Jia et al., 2022). These multifaceted influences are crucial for designing environments that promote optimal thermal comfort for occupants.

2.11 Techniques for Enhancing Thermal Comfort and Mitigating UHI in Cities

Techniques for improving urban thermal comfort encompass a range of approaches, including urban vegetation, green infrastructure, and passive design strategies (Wong et al., 2010; Chun & Guldmann, 2018; Balany et al., 2020; Ferrini et al., 2020; Jombo et al., 2022). Taleghani. (2018) emphasises the effectiveness of vegetation, such as street trees, parks, green roofs, and walls, as common strategies for enhancing city thermal conditions. Similarly, Gatto et al. (2020) highlight the positive effect of urban vegetation on outdoor thermal comfort, particularly in Mediterranean and Northern European cities. Furthermore, (Li et al (2021); Zou and Zhang (2021) underscore the importance of landscape design methods in mitigating UHI effects and enhancing thermal comfort for urban citizens.

In addition to vegetation, green infrastructure plays a crucial role in improving thermal comfort. Ruiz-Aviles et al. (2020) advocate for integrating constructed wetlands and neighbourhood development to reduce UHI impacts and improve human comfort. Similarly, Dutta et al. (2021) and Jombo et al. (2022) emphasise the significance of increasing urban vegetation cover to reduce heat-induced stress and enhance outdoor thermal comfort for city dwellers.

Passive design strategies also contribute significantly to improving thermal comfort in cities. Athmani et al. (2022) highlight the effectiveness of passive solar heating and high thermal mass in enhancing thermal comfort, especially in winter. The aspect ratio of urban spaces is also identified as a key strategy for improving outdoor thermal comfort (Lai et al., 2019).

Moreover, using geospatial assessment and modeling tools is crucial for representing the spatial distribution of thermal comfort circumstances in cities, thereby aiding in prioritising strategies and effective urban planning (Mutani and Beltramino, 2022). Additionally, the function of green roofs in reducing ambient temperature and mitigating the heat island effect is underscored as an essential strategy for enhancing the thermal environment in cities (Li et al., 2021).

Mitigating the UHI effect is critical to urban planning and environmental management. Various approaches, including urban planning strategies, green infrastructure, sustainable design, and policy interventions, have been proposed to address UHI impacts. Li et al. (2014) investigated the efficacy of cool and green

roofs to alleviate the UHI effect, highlighting the potential of these approaches to reduce UHI effects. Similarly, Borzino et al. (2020) explored the willingness to pay for UHI mitigation strategies, emphasising the importance of public engagement and urban planning in implementing effective UHI interventions. Li et al. (2022) suggested that comprehensively analysing blue and green infrastructure would add value to UHI mitigation strategies targeting East African cities, with the likelihood of enhancing human comfort in high UHI-impact areas.

Antoszewski et al. (2020) emphasised the significance of blue-green infrastructure (BGI) in reducing the UHI effect, highlighting the need for nature-based solutions to reduce urban temperatures. In addition, Balany et al. (2020) reviewed green infrastructure's potential as a UHI mitigation strategy, underlining the significance of microclimate modifications through green spaces. Furthermore, Li et al (2014) studied the potential of green roofs as a UHI mitigation strategy, demonstrating the cooling effects of green infrastructure in urban areas.

The studies reviewed demonstrate that combining strategies, including cool and green roofs, BGI, and reflective materials, can effectively mitigate UHI effects. Public engagement and willingness to pay for UHI interventions are crucial for successfully implementing mitigation strategies. Evidence-based decision support tools and policy interventions are vital in formulating effective UHI mitigation policies. The potential of green infrastructure and sustainable design in reducing UHI effects highlights the importance of urban planning solutions based on nature.

CHAPTER 3: METHODOLOGY

3.1 Introduction

This chapter provides a detailed description of the study area and outlines the research methodology. It covers research design, data acquisition, pre-processing techniques, and calculations of spatiotemporal parameters related to UHI and thermal comfort.

3.2 Study Area

Francistown (21° 10' 24.9996" S, 27° 30' 45.0036‘’ E) is Botswana’s second city located in the Northeast district (Figure 3.1). The city has a population of approximately 103 417 (Statistics Botswana, 2022). The city has a total area of about 79 km^2, which is approximately 1.54% of the total area of the Northeast District (Figure 3.1). Greater Francistown City is characterised by a dynamic interplay of environmental variables significantly influencing its urban climate and morphology. Rapid urbanisation and evolving land use patterns transform the cityscape (Chiguvi, 2022). The city is dominated by commercial and industrial zones and residential areas characterised by irregular structures and experiences spatial heterogeneity exacerbated by differentiated urban functions (Ouma et al., 2021). The Greater Francistown City consists of peri-urban areas with tribal land tenure systems, with land continually being transformed from its natural status to developed built-up urban areas (Chiguvi and Kgathi-Thite, 2022). These changes alter surface properties, influencing heat absorption and retention, thereby impacting the city's microclimate.

Greater Francistown City experiences a hot desert climate with hot summers and cold winters. A hot semi-arid climate prevails, with mild winters and hot summers. The annual average temperature in city areas ranges from -6.5 °C to 41.1 °C (Climate Botswana, 2022). Precipitation in Greater Francistown City is scarce and unpredictable, with an average precipitation of 460mm per annum and less than 60 days of rain falling between October and April (Matenge et al., 2023). The scarcity of precipitation intensifies heat stress vulnerability, amplifying UHI effects and affecting daytime and night-time temperatures throughout the year.

Greater Francistown City will keep expanding rapidly in the coming years due to increased population growth and growing urbanisation, causing an alteration in

LULC and leading to the city sprawling (Chiguvi and Kgathi-Thite, 2022). The burgeoning population drives infrastructural development, escalating energy consumption and emissions, contributing significantly to the escalating UHI phenomenon. As a result of this modification, more vegetation is being turned into urban infrastructure, which changes the microclimate, increases the UHI effect, and decreases the thermal comfort levels of residents.

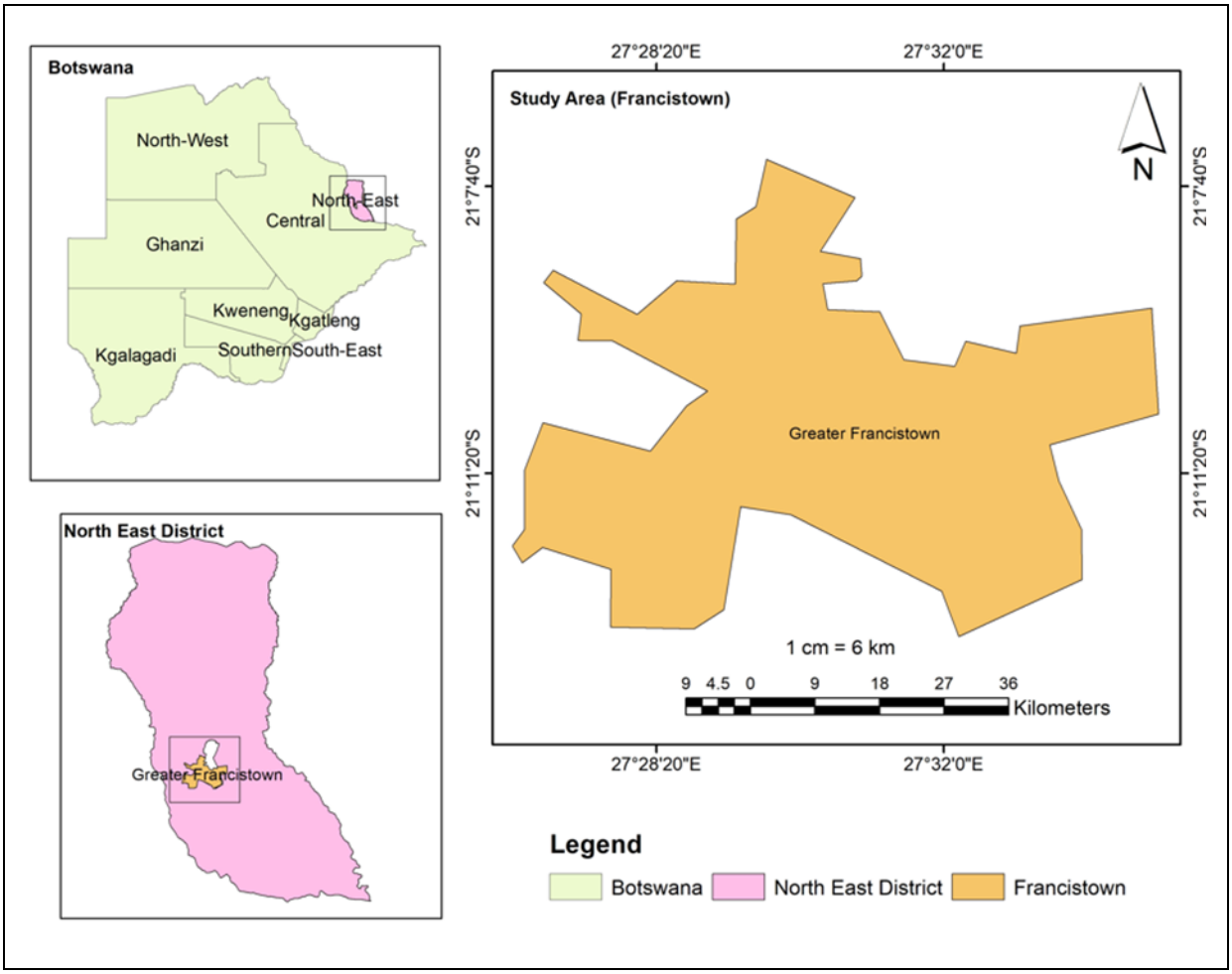


Figure 3.1. Study Area - Greater Francistown City

3.3 Research Design

This study employed the experimental research design following the methodology presented in the Flowchart (Figure 3.2). Experimental research design is a methodology that seeks to uncover causal relationships between variables through carefully controlled experimentation (Leatherdale, 2019). It involves the manipulation of an independent variable to observe the effects on a dependent variable while controlling for extraneous variables (Sufrianto and Candra, 2022). The experimental research design assessed the spatiotemporal variability of UHI and thermal comfort,

emphasising the importance of understanding the relationships between LULC, LST, built-up index, vegetation index, and UTFVI.

The total workflow has been divided into distinct tasks (Figure 3.2), which include the retrieval of LULC, LST, NDVI, UTFVI, and NDBI to identify UHI, non-UHI, and thermal comfort areas within the Greater Francistown City. A detailed explanation of each step in the workflow is presented in sections 3.4 - 3.6. The data sets for these tasks were analysed using Google Earth Engine (GEE), a cloud-based computing platform (Amani et al., 2020; Zhao et al., 2021). The other task entails the utilisation of GIS tools (QGIS and ArcMap Software) in conjunction with statistical techniques (statistical analysis software (SAS)) to conduct spatial-temporal quantifications.

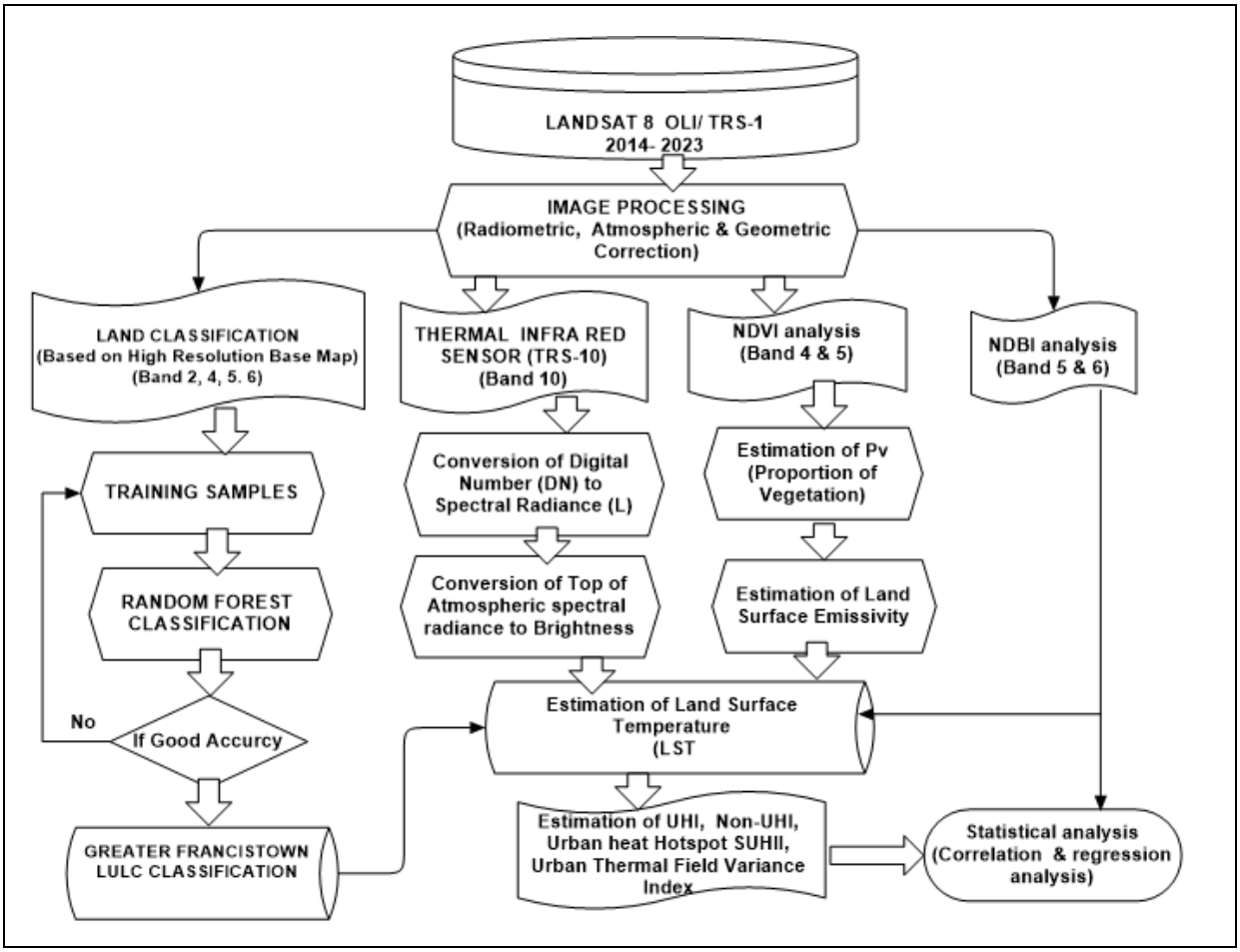


Figure 3.2. Study design schematic.

3.4 Data Acquisition

The study utilized Landsat 8 Operational Land Imager (OLI) and the Thermal Infrared Sensor (TIRS-1) data to assess the spatial-temporal variability of the UHI phenomenon and thermal comfort levels within the Greater Francistown City over a

decade-long period (2014 to 2023). The following five time point periods were considered: 2014, 2016, 2019, 2021 and 2023. The specified years provide a timeline encompassing the study period's baseline, lower quartile, midpoint, upper quartile, and endpoint (2014-2023). Cloud-free Landsat OLI/TIRS imagery was obtained at no cost from the United States Geological Survey (USGS) (http://earthexplorer.usgs.gov/) for the period 2014-2023 using data from the 1st of January to the 31st of December for each study year. The Landsat 8 data was readily accessible and has been incorporated into the GEE data catalogue.

The Landsat 8 earth observation satellite was deployed into orbit on February 11, 2013. It follows a sun-synchronous polar orbit and has a temporal resolution that allows for a global coverage revisit time of 16 days. This allows for the monitoring of changes over time. The satellite's OLI instrument collects data in nine multiple spectral bands and two TIRS thermal bands (Wulder et al., 2016).

The spatial resolutions of Landsat 8's spectral bands range from 15-30 meters per pixel, with the potential for downscaling to a finer spatial resolution of 10 meters when fused with Sentinel-2 data (Onačillová et al., 2022). The thermal infrared bands (10 and 11) have a 100-meter spatial resolution. The 11 spectral bands vary in wavelength from 0.433 µm to 12.51 µm (Table 3.1).

Landsat 8 data was utilised for this study owing to its unrestricted availability. This accessibility enhances the feasibility of the study and allows for the continuation of research over an extended period. The image selection procedure prioritised high-quality images with minimal cloud cover while also considering the specific date, month, and year of acquisition. The images provided by the USGS are georeferenced to the ellipsoid, Universal Transverse Mercator (UTM) coordinate system, map projection (Zone 34S), and World Geodetic System WGS84 datum. Landsat 8 has proven its capability to provide essential data for estimating LST, mapping UHIs, analysing the impact of LULC changes, and assessing external thermal comfort (Wang et al., 2015; Aslan and Koc-San, 2016; Yang et al., 2017; Huang et al., 2019; Khallef et al., 2020; Yang et al., 2022; Prasad and Satyanarayana, 2023). Leveraging Landsat 8 data ensures compatibility with existing literature, allowing comparisons with other urban areas and contributing to the broader body of knowledge on UHI dynamics.

Landsat 8 data also provides moderate spatial resolution imagery (30 meters) (Table 3.1), which is well-suited for urban studies. This resolution allows for the detailed examination of LULC patterns and urban morphology in Greater Francistown City, enabling a more accurate assessment of the factors contributing to UHI. The data also aids in precise land cover classification (Bands 2,3,4,5,6, and 7), distinguishing surface types like impervious surfaces, vegetation, and water bodies, which are crucial for assessing UHI and thermal comfort impact. Landsat 8's multispectral bands, including the thermal infrared band (Band 10), offer valuable information for studying surface temperature variations and directly assessing UHI, a critical factor in understanding heat island effects (Table 3.2).

Table 3.1. An overview of the Landsat 8 sensor's attributes and the data acquisition dates.

Dates Acquired	**Temporal Resolution**	**Spectral Band**	**Spectral Range (micrometers)**	**Spatial resolution (meters)**
2014-2023	16 days	Band_1 Coastal Aerosol	0.433 - 0.453	30 m
		Band_2 Blue	0.450 - 0.510	30 m
		Band_3 Green	0.530 - 0.590	30 m
		Band_4 Red	0.640 - 0.670	30 m
		Band_5 Near-Infrared	0.850 - 0.880	30 m
		Band_6 SWIR-1	1.570 - 1.650	30 m
		Band_7 SWIR-2	2.110 - 2.290	30 m
		Band_8 Panchromatic	0.500 - 0.680	15 m
		Band_9 Cirrus	1.360 - 1.380	30 m
		Band_10 TIRS-1	10.60 - 11.190	30/100 m
		Band_11TIRS-2	11.50 - 12.510	30/100 m

Source (http://earthexplorer.usgs.gov/)

The Landsat 8 images were attained from 01 January 2014 to 31 December 2023.

Table 3.2. Description of Landsat 8 dataset utilised in the study area.

Sensor	***Description***	***Band***	***Resolution***
Landsat 8 OLI	LULC	2, 3, 4, 5, 6, and 7	30m
Landsat 8 Tier-1	LST	10	30m
Landsat 8 OLI	NDVI	4 and 5	30m
Landsat 8 OLI	NDBI	5 and 6	30m

3.5 Pre-Processing

Using the GEE platform, a pre-processing procedure was applied to eliminate atmospheric impacts, geometric and radiometric errors from Landsat imagery, and image enhancement. The initial step in the data preparation phase was the filtration of Landsat-8 OLI and TIRS-1 data from the GEE catalogues obtained in the format of

a compilation of images. The application of pre-processing stages was performed on a per-image basis. The initial pre-processing stage involved masking techniques to remove clouds, dense aerosols, and cloud shadows from each image (Liu et al., 2022). The Landsat 8 data was cloud-screened and filtered to the Greater Francistown City region. The influence of cloud cover was minimised by masking the clouds. The water pixels were selectively masked to prioritise the analysis of land pixels, to mitigate the influence of water's high specific heat capacity on LST. Subsequently, the resultant images were clipped to conform to the boundaries defined in the Greater Francistown City shapefile.

3.6 Calculations of spatiotemporal parameters of UHI and Thermal Comfort

3.6.1 Classification and accuracy assessment of land cover

LULC was carried out for 2014, 2019, and 2023 using the Random Forest (RF) algorithm. The study used 2014 as the baseline, 2019 as an intermediate, and 2023 as the end year to analyse land cover changes over 10 years. Selecting these three specific years provides a foundation for correlating land cover changes with the corresponding LST, NDBI, NDVI, and UTFVI variations over the same timeframe. LULC classification is critical for evaluating the spatiotemporal variability of the UHI and thermal comfort in Greater Francistown City. The classification allows for identifying and categorising different land cover types within the study area. Each land cover type has distinct thermal properties, affecting the local microclimate and contributing to UHI (Zhao et al., 2020).

3.6.1.1 The Image Classification

RF is a robust and adaptable supervised machine-learning technique known for its high accuracy, robustness, and capability to handle complex relationships in data (Waleed and Sajjad, 2022). The algorithm was first introduced by Leo Breiman in 2001. The RF classification is based on building a forest of classification trees, in which every tree is grown on a bootstrap sample of the data (Breiman, 2001). The characteristic in each tree node is chosen from a randomly selected subset of all variables. Class classification is established by aggregating the votes of all the individual trees in the forest (Loola Bokonda et al., 2023).

In the context of land cover classification for Greater Francistown City, RF's ability to handle the complexity of the landscape and its accuracy in handling diverse land cover classes make it a suitable and effective choice for creating a reliable LULC map. A RF analysis was performed on the OLI Landsat 8 bands (2, 3, 4, 5, 6, and 7) (Table 3.2) to classify the study area. The Greater Francistown City LULC was classified into four major land cover classes: vegetation cover, built-up area, water bodies, and bare land (Table 3.3).

Table 3.3. Greater Francistown LULC Classification and Description

Class	Description
Built-up area	Residential, commercial, and industrial areas, roads, parking lots, runways, pavements, and other urban infrastructure
Vegetation	Trees, grass, forest, crop fields, land, shrubs, and other vegetation types.
Water bodies	Dams, rivers, streams, ponds
Bare land	Unused land, open space, fallow land, exposed soil.

Source (Nguyen et al., 2019).

3.6.1.2 Reference Data Collection

The reference data for historic Landsat 8 were attained visually by interpreting 2014, 2019, and 2023 images observed from GEE. A high-resolution base map digitised areas that visually represent each land cover class. These areas were marked as potential training sites. A total of 100 training samples were chosen for each selected year for the entire study area. The reference data was then randomly split into the training 70% and 30% validation samples. The supervised RF classifier was trained using training data, and a confusion matrix table was generated using validation data (Li et al., 2020). The confusion matrix technique was used to assess the LULC precision (Wang et al., 2019; Xia et al., 2022) maps generated. From the confusion matrix generated, the classifier's producer accuracy, total accuracy, user accuracy, and kappa were tabulated. These are important metrics in assessing the quality and reliability of remote sensing classifications (Wang et al., 2019; Xia et al., 2022). Additionally, the kappa coefficient is employed to evaluate the concordance between the classification outcomes and the reference data, considering the potential occurrence of chance agreement (Wang et al., 2019; Li and Stein, 2020; Ma et al., 2023).

3.6.2 Estimation of Normalised Difference Built-up Index

The NDBI is a spectral index utilised to identify and extract built-up areas from urban land in Greater Francistown City. The NDBI is a valuable tool for the identification and analysis of developed land inside metropolitan regions, assessing UHI effects, and monitoring land LULC changes (Azizah et al., 2022; Vergara et al., 2023). NDBI is also directly linked to LST and can be used to quantify the intensity of the UHI. By analysing the spatial distribution of NDBI values, areas with higher impervious surface coverage, which generally contributes to increased surface temperatures, can be identified (Guha et al., 2018; Ouma et al., 2021). The NDBI was computed from Landsat 8 reflectance bands using Equation 3.1

Equation 3.1. Normalised Difference Built-up Index

$$NDBI = \frac{\text{Band 6} - \text{Band 5}}{\text{Band 6} + \text{Band 5}}$$

The NDBI values range from -1 to +1, where negative values signify the existence of water bodies and positive values indicate the presence of developed areas. Vegetation exhibits a low NDBI value (Ullah et al., 2022).

A five-year time point period of 2014, 2016, 2019, 2021, and 2023 were selected for NDBI map creation. The selected specific years create a timeline that covers the baseline, lower quartile, midpoint, upper quartile, and endpoint of the study period (2014-2023), capturing both short- and long-term changes in NDBI. It enables the analysis of how built-up areas respond to urban heat over the specified time frame. Additionally, these intervals balance data collection frequency and the need for comprehensive insights, not vegetation dynamics.

3.6.3 Vegetation Indices Calculations

3.6.3.1 Normalised Difference Vegetation Index Calculations

The study utilised NDVI calculations to serve two tasks: interpreting vegetation distribution and determining the emissivity values, indicating vegetation cover, which reduces surface temperatures and aids in UHI mitigation strategies (Hishe et al., 2023). Landsat 8 satellite imagery was utilised to assess the influence of vegetation cover on LST and thermal comfort, using multispectral data, including bands 4 and 5 (Table 3.2). The NIR band 4 (0.85-0.88μm), highly sensitive to chlorophyll absorption

in healthy plants with a 30 m spatial resolution, was used for vegetation analysis (Imran et al., 2021). The (0.64-0.67μm) red band 5 was used to stipulate a measure of vegetation cover (Jombo et al., 2022). The NDVI was utilized to compute the amount of flora cover density and variations in the study area using Equation 3.2.

Equation 3.2. Normalised Difference Vegetation Index

$$\mathrm{NDVI} = \frac{NIR - RED}{\mathrm{NIR} + \mathrm{RED}}$$

It was computed by dividing the red band's top-of-atmospheric (TOA) reflectance by the NIR band reflectance (Equation 3.2). This index is valuable for evaluating surface reflectance (Hishe et al., 2023). Waleed and Sajjad (2022) reported a substantial association between the NDVI values for soil and vegetation and the PV. The PV was computed utilising Equation 3.3.

Equation 3.3. Proportion of Vegetation

$$P_v = \left(\frac{NDVI_i - NDVI_{\min}}{NDVI_{\max} - NDVI_{\min}}\right)^2$$

The variables in this context are Pv, NDVI, NDVImin, and NDVImax, representing the PV, NDVI values obtained from the image, and NDVImin (minimum) and NDVImax (maximum) respectively.

The Land Surface Emissivity (LSE) refers to the mean emissivity of a specific element on the earth's surface, which is determined by computing NDVI values. Hishe et al., (2023) defined LSE as the “ratio of energy emitted from a natural material to that of a perfect emitter (blackbody) at the same temperature”. The LSE (ε_λ) was calculated in GEE based on the computed Pv value using Equation 3.4. The LSE ε_λ ranges from 0.97 to 0.99 (Zhang et al., 2022).

Equation 3.4. Land Surface Emissivity

$$\varepsilon_\lambda = 0.004 * P_v + 0.986$$

3.6.4 Land Surface Temperature Calculations

3.6.4.1 *Digital Numbers Conversion and TOA Spectral Radiance Estimation*

The Landsat 8 data underwent an initial radiometric correction process to obtain the LST, wherein each band's digital numbers (DN) were transformed to spectral radiance by Equation 3.5. Radiation correction has been shown to increase the accuracy of LST and other index calculations (Waleed and Sajjad, 2022).

Equation 3.5. Top of Atmospheric Spectral Radiance

$$L_\lambda = M_L \times Q\mathrm{Cal} + A_L$$

Where: variable L_λ represents the TOA spectral radiance while M_L is the band-specific multiplicative rescaling factor obtained from the metadata. $Q\mathrm{Cal}$ represents the quantised and standardised product pixel value (DN), $\mathrm{and}\ L_\lambda$ refers to the band-specific additive rescaling factor obtained from the metadata.

Equation 3.5 was used to get the TOA radiance L_λ for the Landsat 8 OLI thermal band 10 (10.60µm – 11.19µm). The TOA spectral radiance measures radiant energy per unit area, unit solid angle, and unit wavelength at the outer boundary of Earth's atmosphere (Waleed et al., 2023). This measurement is expressed in watts per square meter per steradian per nanometer (W/(m²·sr·nm)).

The TOA Tie1 data of Landsat 8 were filtered for the following years: 2014, 2016, 2019, 2021, and 2023, and the medians of all values were calculated. The resulting images were clipped with the Greater Francistown City shapefile, and the resultant Landsat 8 TOA image was utilised to derive LST.

3.6.4.2 Spectrum Radiance Conversion to TOA Brightness Temperature

The spectral radiance calculated from the pixel DN values in section 3.5.4.1 was used to calculate the TOA brightness temperature (TB) using (Equation 3.6), which is the effective temperature sensed by the satellite assuming unit emissivity in Kelvin.

Equation 3.6. TOA Brightness Temperature

$$T_B = \frac{K_2}{\ln\left(\frac{K_1}{L_\lambda} + 1\right)}$$

The thermal conversion constants K_1 and K_2 represent band-specific values. The spectral radiance conversion factors for Landsat 8 OLI are K_1 = 774.89mW/cm^2 /sr/μm and K_2 = 1321.08 Kelvin.

3.6.4.3 Land Surface Temperature Retrieval

The LST was retrieved from Landsat 8 imagery satellite for 10 years (2014 to 2023) using thermal infrared data and atmospheric correction algorithms. The Landsat 8 TIRS-1 bands 10 (10.60 - 11.19μm) with 30m resolution was utilised. The TIRS-1 is exceptionally sensitive to urban temperature variations because of its shorter wavelength and ability to distinguish between temperature gradients in urban locations, where UHI effects are very noticeable (Hashim et al., 2022). Landsat 8 provides spatial and temporal information, making it an excellent choice for LST estimates due to its simplicity and precise retrieval (Cristóbal et al., 2018; Wang et al., 2019). Equation 3.7 was employed to convert satellite temperature to LST in Celsius.

Equation 3.7. Land Surface Temperature

$$\mathrm{LST}(^o\mathrm{C}) = \frac{T_B}{\left[1 + \left(\lambda \times \frac{T_B}{\rho}\right)\ln(e)\right]} - 273.15$$

Where λ is the wavelength of the radiated radiance, = h(c/s) = 1.4388 102m K = 14388 m K, h is the plank's constant = 6.626 1034Js, s is the Boltzmann constant = 1.38 1023J/K, and c is the velocity of light = 2.998 108m/s. The radiant temperature is corrected to achieve the findings in Celsius by adding the absolute zero (approximately -273.15^{o}C).

3.6.5 Estimation of the UHI, non-UHI, and Urban Hot Spot Areas

The UHI distribution and development vary by city, influenced by factors like LST (Peng et al., 2012). Intensity is determined by comparing UHI and non-urban areas using Equations 3.8 and 3.9. The study employed the usage of urban UHI and non-UHI classifications to delineate areas with elevated temperatures and areas without

such temperature anomalies, respectively. The Urban Hot Spots (UHS) areas for Greater Francistown City were computed using Equation 3.10. The UHS refers to areas within urban environments that exhibit significant spatial clustering of high LSTs (Ranagalage et al., 2018).

Equation 3.8. Urban Heat Island

$$\mathrm{UHI} = \mathrm{LST} > \mu + 0.5 * \delta$$

Equation 3.9. Non-Urban Heat Island

$$\text{Non- UHI } = 0 < \text{ LST } \leq \mu + 0.5 * \delta$$

Equation 3.10. Urban Hot Spots

$$\mathrm{UHS} = \mathrm{LST} > \mu + 2 * \sigma$$

Where μ and δ are the study area's LST's mean and standard deviation, respectively. UHI distribution as determined by this method, can be influenced by other factors. Therefore, to enhance precision, a technique that combines the LULC and LST maps was implemented to ascertain the heat island region. The heat island region is characterised in this analysis by the presence of both subsequent components, the UHI area and the LULC type.

3.6.6 Estimation of Thermal Comfort Using the Urban Thermal Field Variance Index

An effective method for evaluating UHI's influence on a city's overall well-being is through thermal comfort indices (Isioye and Akomolafe, 2020). The UTFVI value is an Ecological Evaluation Index (EEI) calculated to determine the impact of UHI and eternal thermal comfort (Kasniza Jumari et al., 2023) on the Greater Francistown urban environment and residents. The UTFVI assessed the urban environmental standard of living in the context of external thermal comfort pertaining to the UHI phenomena. It evaluated the general quality of urban living regarding the degree of external thermal comfort and well-being related to the UHI impact (Zhang et al., 2013). Equation 3.11 was used to compute the UTFVI.

Equation 3.11. Urban Thermal Field Variance Index

$$\mathrm{UTFVI} = \frac{Ts - Tmean}{Ts}$$

Ts represents the LST, and Tmean represents the mean LST of the study area. The values of UTFVI were categorised into six distinct groups, each associated with specific ecological interpretations and the UHI phenomenon (Table 3.4) (Waleed and Sajjad, 2022; Kasniza Jumari et al., 2023).

Table 3.4. Thresholds of UTFVI Employed in Greater Francistown

UTFVI	UHI Occurrence	EEI
<0.000	None	Excellent
0.000-0.005	Weak	Good
0.005-0.010	Middle	Normal
0.010-0.015	Strong	Bad
0.015-0.020	Stronger	Worse
>0.020	Strongest	Worst

3.7 Meteorological data

Historical in-situ air temperature measurements were utilised to validate the derived Landsat 8 LST data. The air temperature data for the study period (2014-2023) was retrieved from the National Aeronautics and Space Administration (NASA) Prediction of Worldwide Energy Resources (POWER) https://power.larc.nasa.gov/data-access-viewer/. NASA POWER is an agency of the United States government, tasked with collecting and providing meteorological data through ground-based measurements, re-analysis of data, satellite observations, and extensive data processing and quality control. The highest, lowest, and average air temperature measurements were utilised to verify the maximum, minimum, and average LST over the same period the Landsat 8 images were retrieved. The study utilised a combination of Pearson's correlation and linear regression analysis to evaluate the link between average LST values and the air temperature values obtained from NASA POWER.

3.8 Statistical Evaluations

Measures of central tendency and dispersion (mean, maximum, minimum, standard deviation and Coefficient of Variation (CV) were employed for the indices (NDBI, NDVI, PV, LSE, LST, UHI, SUHII and UTFVI) in the study areas. The descriptive statistics provided an overview of each index's distribution and central tendency. Regression and correlation analysis were computed to identify the association between the different indices.

Pearson correlation analysis identified the degree of association between indices strongly related to each other and those not using Equation 3.12.

Equation 3.12. Pearson Correlation Coefficient

$$r = \frac{n(\sum xy) - (\sum x)(\sum y)}{\sqrt{\left[n\sum x^2 - (\sum x)^2\right]\left[n\sum y^2 - (\sum y)^2\right]}}$$

Where r is the Pearson Correlation Coefficient

Pearson's correlation examination was implemented between LST and the indices (NDBI, NDVI, PV, UHI, SUHII, and UTFVI) to determine their influence on LST in Greater Francistown City.

CHAPTER 4: RESULTS

4.1 Introduction

This chapter comprehensively presents and analyses results aligned with the overarching research objectives, explicitly focusing on the spatiotemporal variability of UHI and thermal comfort in Greater Francistown City.

4.2 Spatiotemporal Assessment of Greater Francistown City Land Cover

Figure 4.1 displays the RF algorithm-based LULC classification findings between 2014 and 2023 with a 5-year class interval using 2014 as a base year. The four thematic land cover classes, built-up, vegetation, bare-land, and water bodies, were utilised to study spatiotemporal variability of UHIs and thermal comfort. The LULC has been significantly impacted by urbanisation growth which entails UHIs and thermal discomfort. As a result, LST, UTFVI, NDBI, and NDVI are highly correlated with changes in land cover in the sub-Sahara climate zones like Greater Francistown City.

Table 4.1 shows the results of an accuracy evaluation used to validate the resulting LULC classification. The results show that overall accuracy (OA) is more than 0.91 for 2014, 2019, and 2023, with a Kappa value exceeding 0.84, indicating a high degree of concordance between the classified and actual pixels. This demonstrates the precision of the classification predictions and the dependability of the RF method employed in this research. The generated classification is dependable and was utilised for subsequent analysis.

Table 4.1. Generated Classified LULC Maps' Accuracy

Year	Overall Accuracy	Kappa
2014	1.0	1.0
2019	0.91	0.84
2023	1.0	0.87

There is a clear observation that the built-up area and bare land have increased over the past ten years, while there has been a decline in water bodies and plant cover (Figure 4.1).

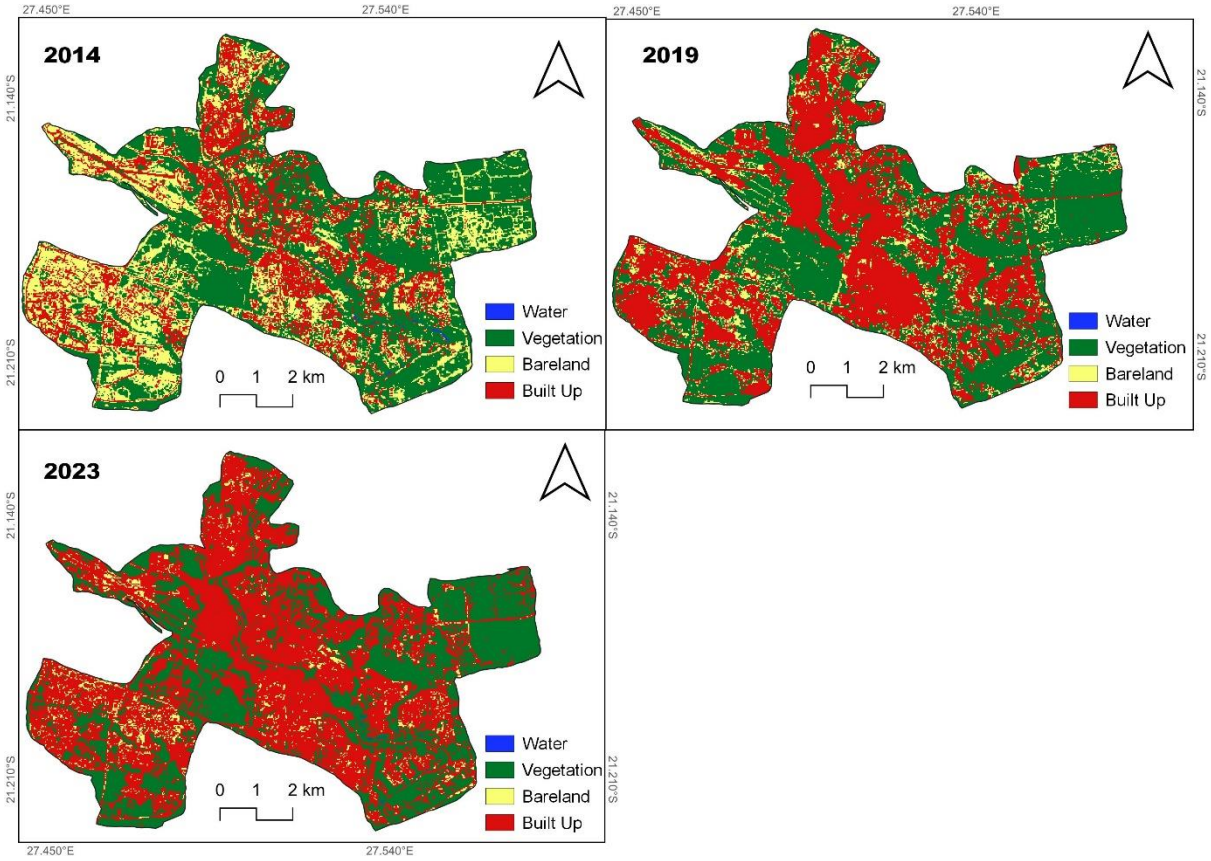


Figure 4.1. Maps of Greater Francistown LULC Classification for 2014, 2019, and 2023

Table 4.2 displays the LULC classes' area-wise distribution. It has been noticed that the built-up and vegetation classes dominate Greater Francistown city, with larger areas than the water and bare ground classes. An increasing trend is observed in the built-up area, doubling from 28.05% in 2014 to 59.02% in 2023. Conversely, the vegetation areas decreased from 45% (37.87km^2) in 2014 to 33.26% (28.00km^2) in 2023 (Figure 4.2). Water bodies constituted the smallest land cover over the study period, occupying an area of 0.12Km^2 in 2014, corresponding to 0.15% and 0.04.1Km^2 in 2019 (0.05%) of the total. From a more comprehensive viewpoint, it is evident that a significant portion of the vegetation land has been transformed into built-up areas, and water bodies dried up due to excessive heat and were transitioned primarily into bare land.

Table 4.2. Greater Francistown City LULC Area Analysis From 2014 to 2023

LULC Class	2014		2019		2023	
	Area (km^2)	Area (%)	Area (km^2)	Area (%)	Area (km^2)	Area (%)
Water	0.12	0.15	0.04	0.05	0	0
Vegetation	37.9	45	32.61	38.73	28.01	33.26
Bare land	22.56	26.80	3.41	4.04	6.50	7.72
Built-up	23.63	28.05	48.14	57.18	49.68	59.02

The expansion in bare land from 3.40km^2 in 2019 to 6.50km^2 resulted from a significant decrease in water bodies from 0.05% in 2019 to 0% in 2023 due to excessive heat and low rainfall received. Most water bodies dried up and were classified as bare land. Concisely, the outcomes of the LULC analysis indicate that significant land-use alterations are mainly attributed to a decrease in vegetation and a notable rise in built-up land, constituting 59% of the entire area in 2023.

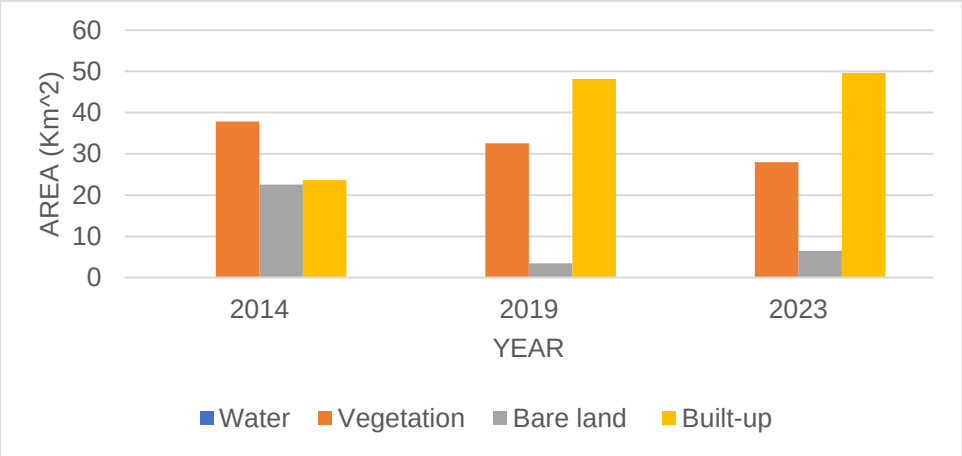


Figure 4.2. Greater Francistown LULC Spatiotemporal Variability (2014-2023)

Expanding the urban built-up area can raise the LST and impact the growth of UHIs in Greater Francistown City.

4.3 Spatiotemporal Analysis of Normalized Difference Built-up Index

Figure 4.3 depicts maps of the spatiotemporal distribution of NDBI for Greater Francistown City from 2014 to 2023, covering the five time points, 2014, 2016, 2019, 2021, and 2023 derived from Landsat 8 imagery. In all the five time points, places with high NDBI values were particularly observed in areas with built-up land. The vegetated areas have minimum values (Figure 4.3). By 2023, high NDBI areas spread throughout the city.

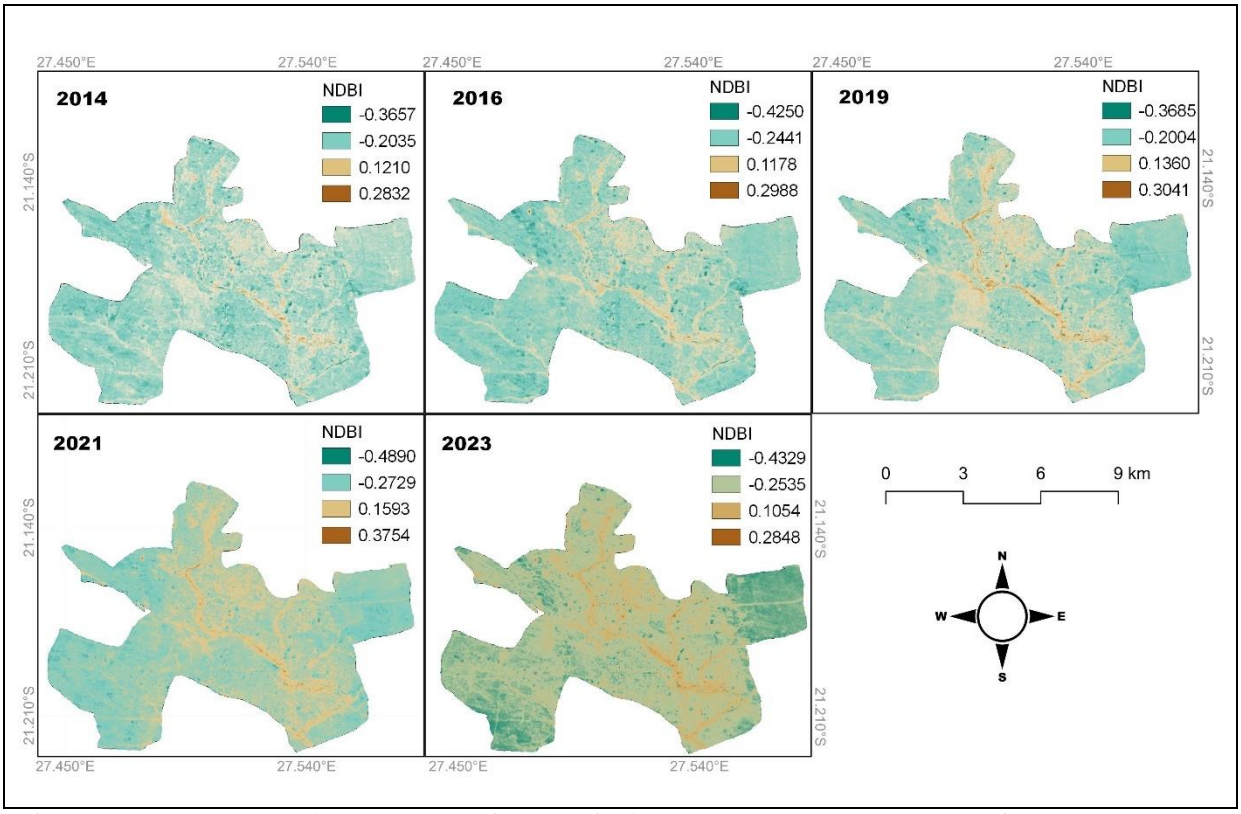


Figure 4.3. NDBI maps of Greater Francistown City for 2014, 2016, 2019, 2021, and 2023.

The built-up areas of the five-time points were computed, and the results are as follows: 15.85km^2 (20.03%) in 2014, 18.95km^2 (23.92%) in 2016, 20.20km^2 (25.51%) in 2019, 30.17km^2 (38.09%) in 2021 and 37.56km^2 (47.42%) in 2023. The built-up area has steadily increased throughout the study, from 15.85km² in 2014 to 37.56km² in 2023, implying a significant impact of urbanisation or built-up development on the landscape. The shift from 20.03% to 47.42% of the total area being built up in a decade indicates substantial changes in land use. As indicated by the increase in built-up areas observed throughout the study, the expansion of urban areas has implications for the effects on LST and UHI.

The mean NDBI statistics values were also computed, and the results are presented in Figure 4.4. The NDBI means show an increasing trend throughout the study, indicating a rise in built-up structures or impervious surfaces.

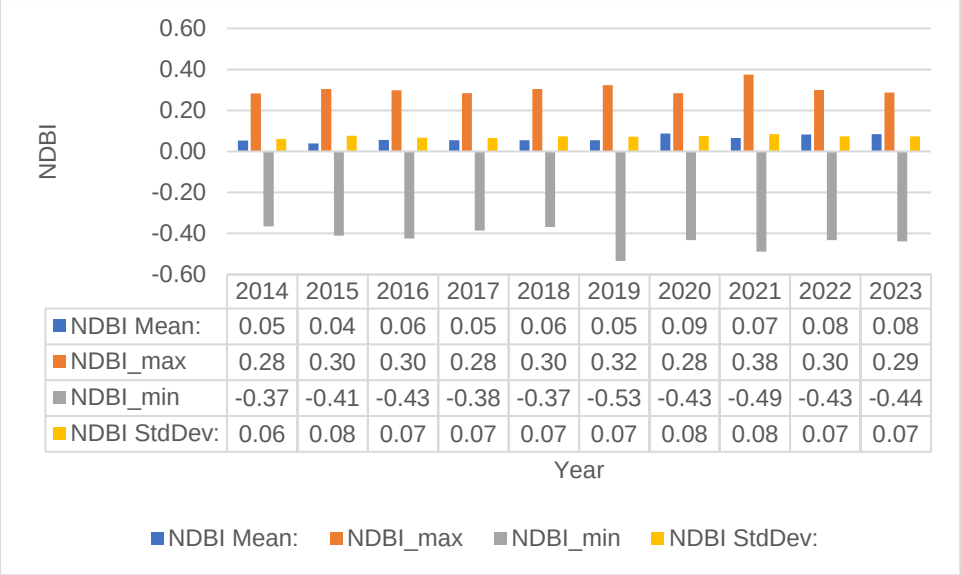


Figure 4.4. Computed NDBI Statistics for Greater Francistown for 2014-2023

The maximum NDBI values have varied over the years, with a notable peak in 2021. This could indicate areas with higher concentrations of built-up structures. The minimum NDBI values also show fluctuations, with a lower negative minimum in 2023 than in 2019. The low standard deviation values for NDBI (0.06, 0.07.and 0.08) across the study period (2014-2023) indicate a consistent and stable pattern in the built-up index, suggesting that the NDBI is a reliable indicator for monitoring built-up areas over time.

4.4 Analysis of Vegetation Indices

4.4.1 Spatiotemporal Distribution of NDVI

Figure 4.5 presents the spatiotemporal distribution of NDVI for Greater Francistown City for the five time points, 2014, 2016, 2019, 2021, and 2023. In all the five time points, places with High NDVI values were found in vegetated areas. The built-up and bare land sections have minimum NDVI values (Figure 4.5).

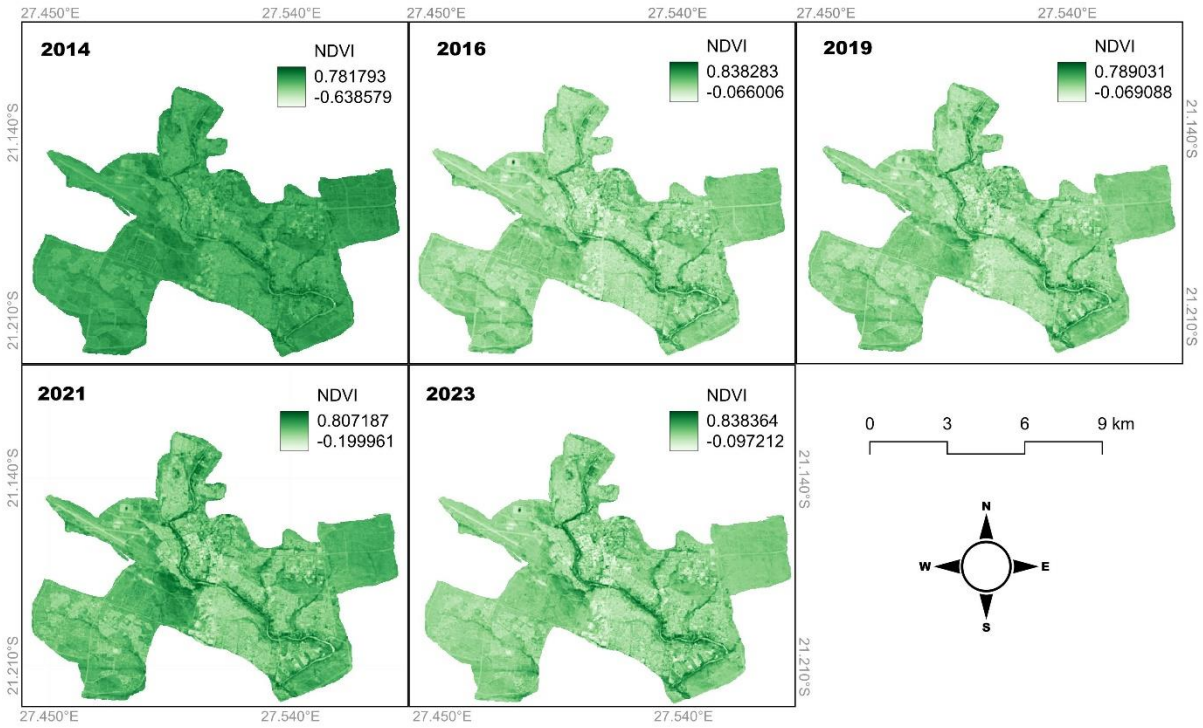


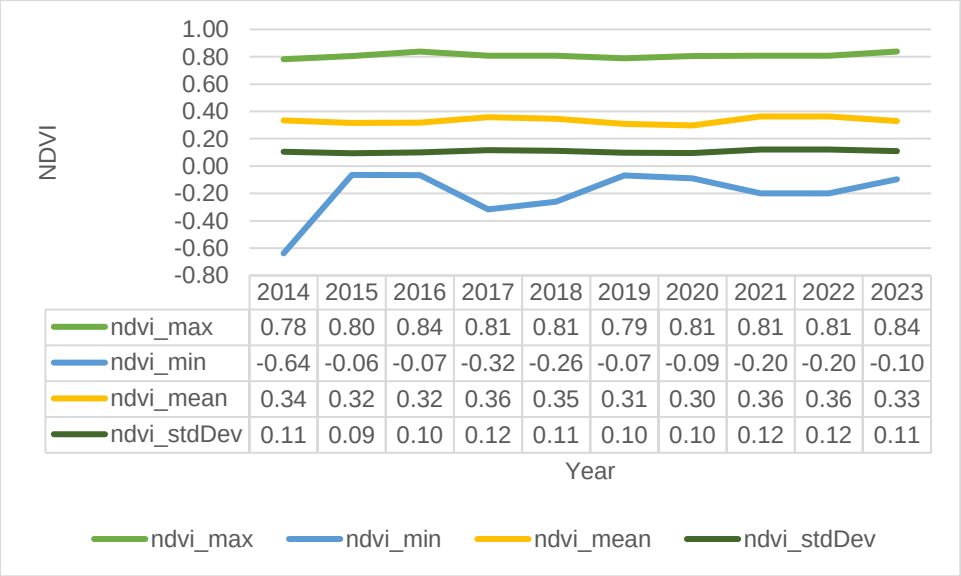
Figure 4.5. Spatiotemporal Distribution of NDVI for 2014, 2016, 2019, 2021, and 2023

In 2014, a substantial portion of land was covered by vegetation, covering 37.9 km^2 (Table 4.2) and resulting in high NDVI values. From 2016 to 2023, regions with minimum NDVI values were detected in the built-up area of Greater Francistown City, which is a result of the influence of the building.

At all five time points, 2014, 2016, 2019, 2021, and 2023, regions with minimum NDVI values were mostly observed in built-up areas. The central part of Greater Francistown City was characterised by a high concentration of buildings, which occupied most of the land area and had minimal or non-existent vegetation on their premises (Figure 4.5). The data presented in Figure 4.6 indicates that the highest NDVI values for the study period 2014 (0.7818), 2016 (0.8383), 2019 (0.7890), 2021 (0.8072), and 2023 (0.8384) were primarily concentrated along the Tati River banks within the city. This is a result of the existence of water from the river that nourishes the vegetation around it.

Descriptive statistics were computed to display the NDVI values for each year of the study period (2014-2023). Figure 4.6 displays the city's minimum, maximum, mean, and standard deviation NDVI values. Maximum NDVI values were found in 2016 (0.8383), 2022 (0.8322) and 2023 (0.838) and the lowest NDVI value of –0.639 was

recorded in 2014. The coefficient of variation (CV) exhibited variation among the different study periods, with 2023 having the highest CV value (33.53%) and the lowest CV value of 29.77% in 2015.



	2014	2015	2016	2017	2018	2019	2020	2021	2022	2023
ndvi_max	0.78	0.80	0.84	0.81	0.81	0.79	0.81	0.81	0.81	0.84
ndvi_min	-0.64	-0.06	-0.07	-0.32	-0.26	-0.07	-0.09	-0.20	-0.20	-0.10
ndvi_mean	0.34	0.32	0.32	0.36	0.35	0.31	0.30	0.36	0.36	0.33
ndvi_stdDev	0.11	0.09	0.10	0.12	0.11	0.10	0.10	0.12	0.12	0.11

Figure 4.6. NDVI Computed Descriptive Statistics for 2014-2023

The mean NDVI estimates illustrated a progressively slightly declining trend from 2014 to 2023 across Greater Francistown City, except in 2017 and 2021. The overall trend shows that the values of the NDVI standard deviation seem to fluctuate over the study period years, with some slight variations. There is some variability in the standard deviation values from year to year. The values in 2017 (0.1166) and 2021 (0.1214) are notably higher than the other years, indicating a higher degree of variability in NDVI during those years.

4.4.2 Spatiotemporal Distribution Fraction of Vegetation Cover

Figure 4.7 presents the spatiotemporal distribution of the fraction of vegetation cover (FV). The maximum (1) and the minimum (0) are constant for the course of the study, indicating that in all years, the maximum fraction of vegetation observed is 1. The FV Minimum is 0, suggesting no instances where the fraction of vegetation drops below 0 (Figure 4.7).

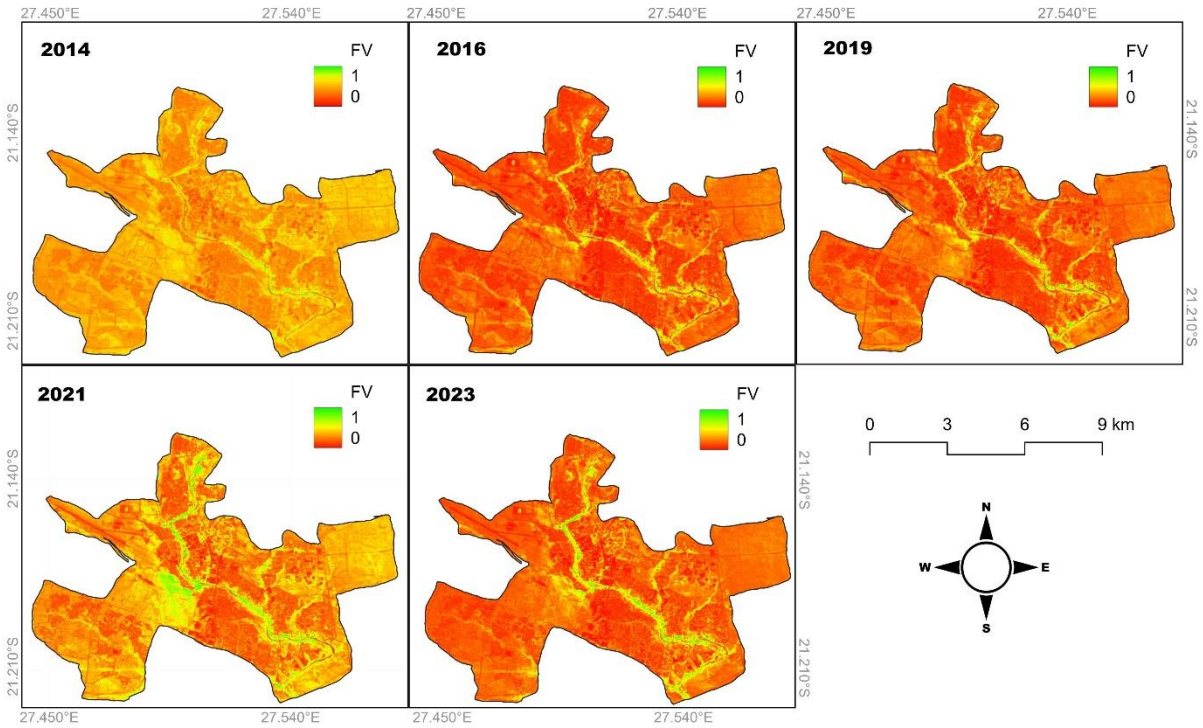


Figure 4.7. Spatiotemporal Distribution of Fraction of Vegetation over Greater Francistown

The mean FV varies across the study period (2014-2023), showing a decreasing trend from 2014 to 2016, peaking in 2017 (0.369), then decreasing sharply to 0.198 in 2020. This suggests a fluctuating pattern in the vegetation cover over the study period, with the lowest mean Pv (0.193) recorded in 2016.

The standard deviation measures the amount of variation in the fraction of vegetation values. The standard deviation values increased and peaked in 2017 (0.126), suggesting higher variability in vegetation fraction during that year (Table 4.3). The explanation is comparable to Greater Francistown City's variation in NDVI values.

Table 4.3. Analysis of Fraction of Vegetation and Land Surface Emissivity

	2014	2015	2016	2017	2018	2019	2020	2021	2022	2023
FV Mean:	0.475	0.204	0.19	0.369	0.334	0.208	0.198	0.327	0.327	0.222
FV stdDev	0.102	0.104	0.103	0.126	0.122	0.109	0.104	0.138	0.138	0.121
FV CV	21.51	50.84	53.22	34.15	36.46	52.37	52.45	42.233	42.23	54.33
EM Mean	0.988	0.986	0.987	0.987	0.987	0.986	0.987	0.987	0.987	0.987
EMstdDev	0.0004	0.0004	0.0004	0.0005	0.0005	0.0004	0.0004	0.0005	0.0005	0.0005
EM CV	0.04	0.04	0.04	0.05	0.05	0.04	0.04	0.06	0.06	0.05

4.4.3 Spatiotemporal Distribution of the Land Surface Emissivity

Figure 4.8 presents the spatiotemporal distribution of LSE values for Greater Francistown City from 2014 to 2023, covering five times: 2014, 2016, 2019, 2021, and 2023. The LSE values for the whole study period were consistent, and no variations were observed (Figure 4.8; Table 4.3). The highest and lowest LSE values recorded were 0.99 and 0.986, respectively. The areas with the highest emissivity (EM) are characterised by abundant healthy vegetation found along the Tati River banks in the city.

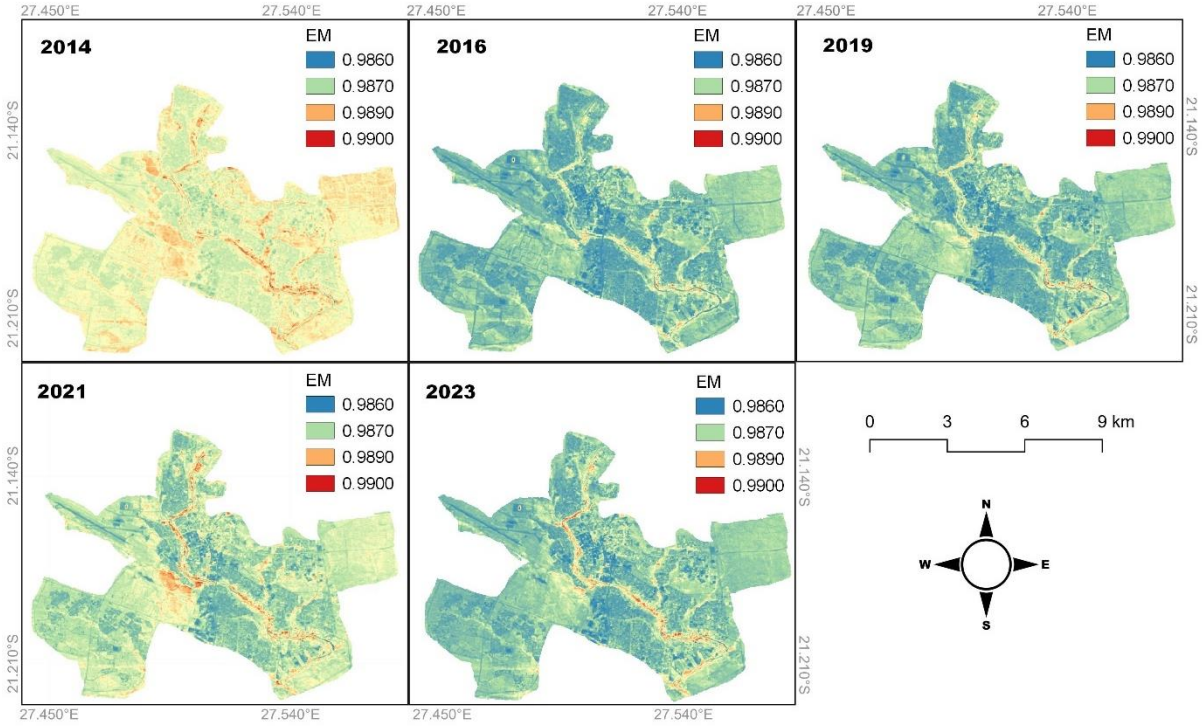


Figure 4.8. Spatiotemporal Distribution of the Land Surface Emissivity Over Francistown City

The EM remains consistently high, with slight variation over the 10 years (Table 4.3). The small standard deviation of 0.0004 from 2014-2020 and 0.0005 from 2021-2023 and coefficient of variation of 0.04-0.05% indicate a stable and uniform pattern in LSE (Table 4.3).

4.5 Spatiotemporal Distribution of LST and Air Temperature Patterns

4.5.1 Spatiotemporal Distribution of Land Surface Temperature

The LST corresponds to the level of heat that would be perceived by a person touching the Earth's "surface." It can be likened to the warmth experienced when a person's hand touches the Earth's surface (Nguyen et al., 2019). The LST is an

important reference index for analysing the state of the land's ecosystem. It impacts the area's material and energy cycles, the ecological system's stability, people's development, and human survival, among other things. Figure 4.9 presents the results of LST maps for Greater Francistown City for the study period 2014-2023, covering five time point periods: 2014, 2016, 2019, 2021, and 2023.

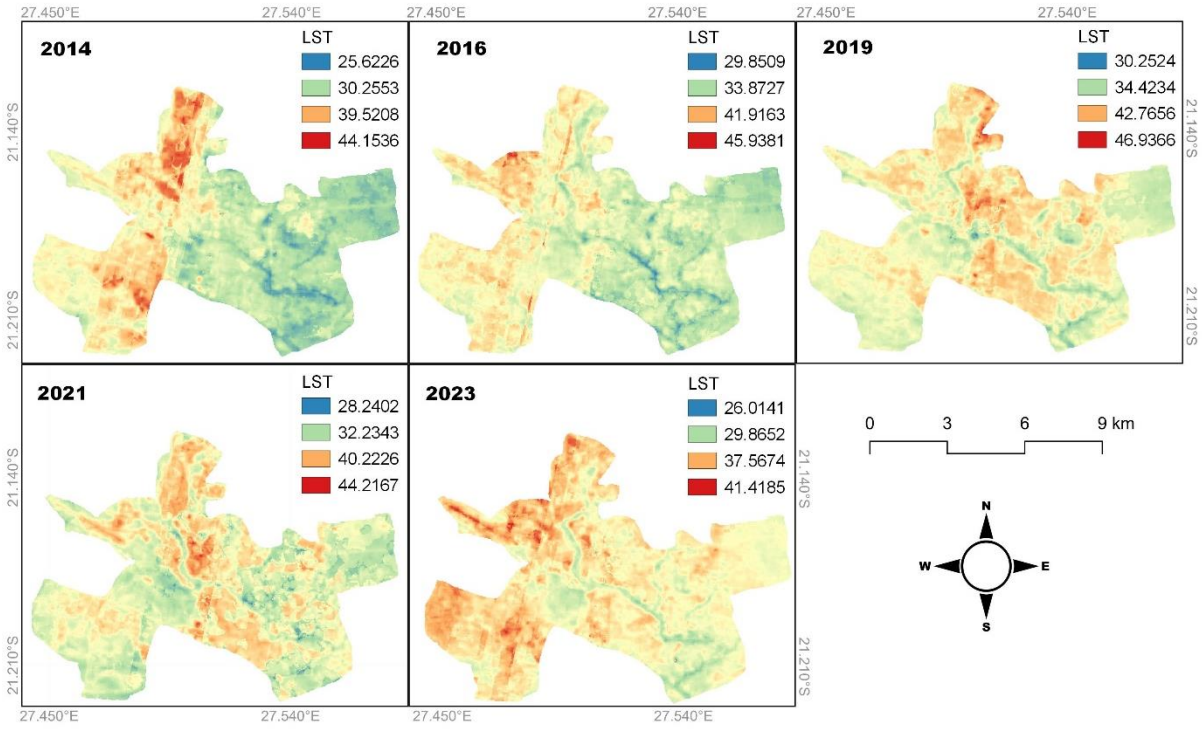


Figure 4.9. Spatiotemporal Distribution of Land Surface Temperature Over Francistown City

Throughout the study period, the LST has increased in locations near bare land and built-up structures in the city. The built-up areas are characterised by dense residential and industrial construction, increasing impervious surfaces, thereby increasing solar energy absorption and converting it into heat. Industrial and residential zones experience higher surface temperatures due to thermal energy, resulting in a higher LST than surrounding areas. The thermal energy generated by industrial endeavours within industrial regions results in higher LST in this region compared to the surrounding regions. Hence, the LST in these regions is significantly higher compared to the surrounding areas, surpassing a threshold of 25.62ºC.

In all the five time points, high LST had significantly expanded towards the northwest, aligning with the spatial distribution of LULC alterations (Figure 4.1). The LST in these areas reached a maximum of 44.2ºC (2014), 45.9ºC (2016), 46.94ºC

(2019), 44.22ºC (2021) and 41.42ºC (2023). According to Figure 4.9, in the East to South segment of the map in 2014, the region showed low LST values (blue and green colour), but by 2023, the description switched to higher LST (redder and orange). This results from more built-up areas that took place in the intervening years.

Furthermore, the spatial distribution of NDBI (Figure 4.3) is compatible with LST, whereas NDVI (Figure 4.5) is the opposite. These findings show that the city's built-up area has higher LST and NDBI values than the surrounding areas due to the decreased plant cover. The Computed standard deviation values for LST range from 1.78°C in 2023 to 3.26°C in 2014. There's variability in LST standard deviation values across the years, with a peak (2.94°C) in 2020. The increase in the LST in Greater Francistown City can be attributed to the ongoing and systematic construction of buildings and widespread deforestation.

4.5.2 Land Surface Temperature and Air Temperature Validation

Table 4.4 presents the computed LST values derived from Landsat 8 and the measured meteorological air temperature data. A comparative analysis was conducted to determine the differences between LST and the recorded air temperature. Air temperature was also used to validate LST, enhancing the reliability and applicability of Landsat 8 data and contributing to more accurate assessments of UHI and thermal comfort.

Table 4.4. The Summary of Comparison of LST and Air Temperature for 2014-2023

	Maximum Temperature			Minimum Temperature			Mean Temperature		
Time	**LST**	**AIR**	**Diff**	**LST**	**AIR**	**Diff**	**LST**	**AIR**	**Diff**
2014	44.15	38.69	5.46	25.62	22.48	3.14	33.5	21.10	12.40
2015	46.9	41.87	5.03	32.19	30.13	2.06	39.38	22.80	16.58
2016	45.94	41.26	4.68	29.85	24.89	4.96	36.78	22.55	14.23
2017	42.83	38.88	3.95	27.81	22.81	5.00	33.67	21.31	12.36
2018	43.57	39.65	3.92	30.32	25.00	5.32	36.91	22.17	14.74
2019	46.94	41.26	5.68	30.25	25.10	5.15	38.66	22.91	15.75
2020	43.76	39.5	4.26	26.45	23.55	2.90	34.39	21.69	12.70
2021	44.22	39.64	4.58	28.24	27.44	0.80	35.83	21.15	14.68
2022	45.32	38.97	6.35	27.16	23.47	3.69	34.48	21.44	13.04
2023	41.42	39.01	2.41	26.01	22.50	3.51	34.54	22.15	12.39

The maximum LST ranges from 41.42°C in 2023 to 46.94°C in 2019, and the maximum air temperatures range from 38.69°C in 2014 to 41.87°C in 2015. The

maximum temperature difference between LST and air temperature varies, with the highest difference being 6.35°C in 2022 and the lowest being 2.41°C in 2023.

The minimum LST ranged from 25.62°C in 2014 to 32.19°C in 2015, with the minimum air temperatures ranging from 0.8°C in 2021 to 5.32°C in 2018. The minimum temperature difference between LST and air temperature varies, with the highest difference being 27.44°C in 2021 and the lowest being 22.5°C in 2023.

The mean LST ranged from 33.67°C in 2017 to 39.38°C in 2015, with the mean air temperatures ranging from 21.1°C in 2014 to 22.91°C in 2019. The mean temperature difference between LST and air temperature varies, with the highest difference being 16.58°C in 2015 and the lowest being 12.36°C in 2017.

It is observed that during the study period (2014 to 2023), LSTs were consistently higher than air temperatures, as indicated by positive differences. The temperature differences fluctuate yearly, variations in local climate conditions. In 2015, temperature differences were higher than average, indicating potential climate anomalies, while in 2023, they were lower, suggesting a more balanced relationship between LST and air temperatures. Due to the discrepancies, the correlation between the LST values and the air temperature data was calculated using the linear regression analysis. The computed data in Table 4.4 was used in the analysis.

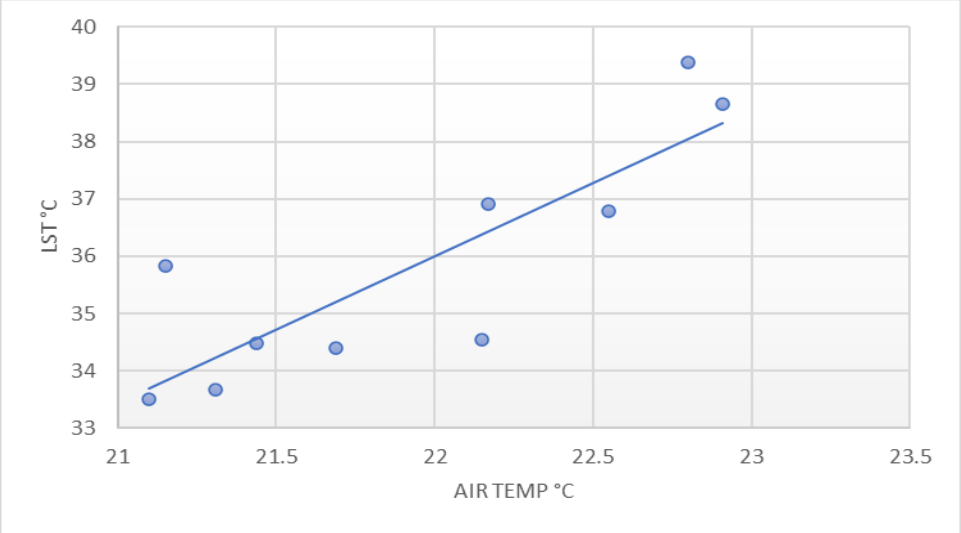


Figure 4.10. Correlation between LST and Air Temperature

The Pearson's correlation analysis implied a significant strong positive relationship (r= 0.81441; p=0.0041) between LST and air temperature at α = 0.05. The coefficient

of determination (R^2) between the mean LST and air temperature data values for 2014-2023 was 0.6633. The R^2 figures show that the LST data associates well with air temperature data. This means that the linear model explains 66.33 % of the variation in the data. The mean squared error (MSE) of 1.5305 indicates that the model is accurate. P(F) = 0.0041 at a 5% significant level and the model is significant, Figure 4.10 demonstrated a significant correlation between LST and the air temperature with the equation LST=16.68 + 2.4Air Temp, the intercept p(t)= 0.2441 and significant Air Temperature P(t) = 0.0041. The results suggest that the variables LST and air temperature are highly related, and the model fits well.

4.6 Spatiotemporal Variations of UHI, non-UHI, and Urban Hotspot Areas

4.6.1 Spatiotemporal Distribution of UHI and non-UHI

Figure 4.11 depicts the UHI and non–UHI status in Greater Francistown City at the five-time points of 2014, 2016, 2019, 2021, and 2023. Table 4.5 summarises areas and the percentages of Greater Francistown City's UHI, non-UHI, and Urban hotspot precincts. The spatial distribution of the UHI was seen mainly in the built-up and bare land precincts of the city. These areas grew from the Southwest to the Northwest from 2014 to 2016, expanded around the city's centre to the northern area in 2019-2021, and extended to the southwest in 2023 following the spatial pattern of LULC and LST changes (Figure 4.9; Figure 4.11*).*

Table 4.5. Spatiotemporal Variations of UHI, non-UHI, and Urban Hotspot Areas

	2014		2016		2019		2021		2023	
Class	**Area km²**	**%**	**Area km²**	**%**	**Area km²**	**%**	**Area km²**	**%**	**Area km²**	**%**
UHI	6.05	7.74	5.19	6.64	4.71	6.03	5.84	7.48	6.62	8.47
Non-UHI	72.07	92.26	72.93	93.36	73.41	93.97	72.28	92.54	71.49	91.53
UHS	3.02	3.87	1.59	2.04	1.88	2.41	2.02	2.59	2.44	3.12

A total area of 6.05km^2 (7.74%) was classified as UHI in 2014 and was the highest area of UHI. This area was covered by bare land (Figure 4.1). The UHI area decreased by 1.1% after 2 years, reaching 5.19km^2 (6.64%) in 2016. The total area covered by UHI slightly dropped again to 4.71km^2 in 2019. The period 2021 (7.45%) to 2023 (8.47%) experienced an increase of 0.99% in the total area that was classified as UHI (Table 4.5). The average values of LST for UHI were estimated to

be 35.13ºC (2014), 37.80ºC (2016), 39.61ºC (2019), 36.89ºC (2021), and 35.43ºC (2023). The results showed fluctuating average UHI values over the study period. Several factors, such as land-use alterations, urban development, and climate variability, influence these shifts. Modifications in land use can change the attributes of urban regions, including the quantity of impermeable surfaces and vegetation, thereby influencing UHI levels.

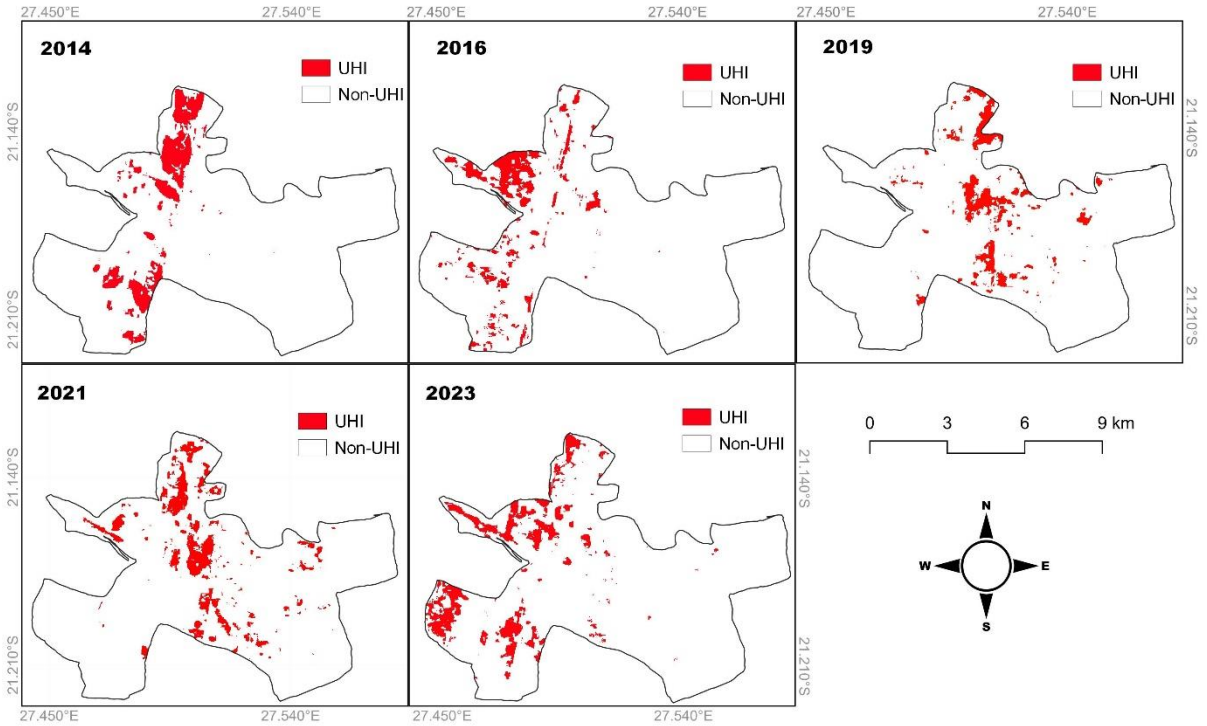


Figure 4.11. Greater Francistown City Identified UHI and Non-UHI

This increase corresponds with the city's pattern of expansion throughout this study period. Furthermore, the year 2023 confirms the growth of the UHI regions. These findings demonstrate the strong correlation between the spatial patterns of UHI and the development of LULC and LST. The spatial distribution of UHI in Greater Francistown City was prevalent in the bare lands and built-up areas. This is comparable with the spatial distribution of LST in Greater Francistown City. The occurrence of UHI in the city can give rise to climatic and environmental concerns with the capacity to affect the general welfare of individuals.

Conversely, the non–UHI areas were intense in the Northern and Southern regions of the city, covering an area of 72.07km^2 (92.26%) in 2014, 72.28% in (2019), and

91.53% in 2023, as signified by the white colour in Figure 4.11. The area of the non–UHI decreases over the study area as the area of UHI increases.

4.6.2 Spatiotemporal Distribution of Urban Hotspots

Figure 4.12 depicts the Urban Hotspot (UHS) in Greater Francistown City at the five-time points of 2014, 2016, 2019, 2021, and 2023 based on the LST analysis. The identified UHS were distributed in a few highly concentrated areas in the bare land and built-up areas. As shown in Table 4.5, the total spatial UHS precincts represented by red colour are covering an area of 1.59km^2 (2.04%) in 2016 and 2.44km^2 (3.12%) in 2023, showing an increase of 1.08% in UHS of the study area. The UHS exhibits less significance in water bodies and vegetation areas. The year 2014 had the highest area of UHS, 3.02km^2 (3.87%). On the contrary, 75.68km^2 (96.88%) of Greater Francistown City in 2023 was free from urban hotspot cases, and it is shown with white colour in Figure 4.12. The thresholds for urban hotspots were 40.02, 43.27, 40.86, 37.47, 40.06, 42.45, 40.27, 40.07, 40.07 and 38.10 for 2014-2023. These results correlate with the prominent locations for UHS: bare land, metal roofs, glass buildings, parking bays, and industrial areas. These hotspots have no water or vegetation.

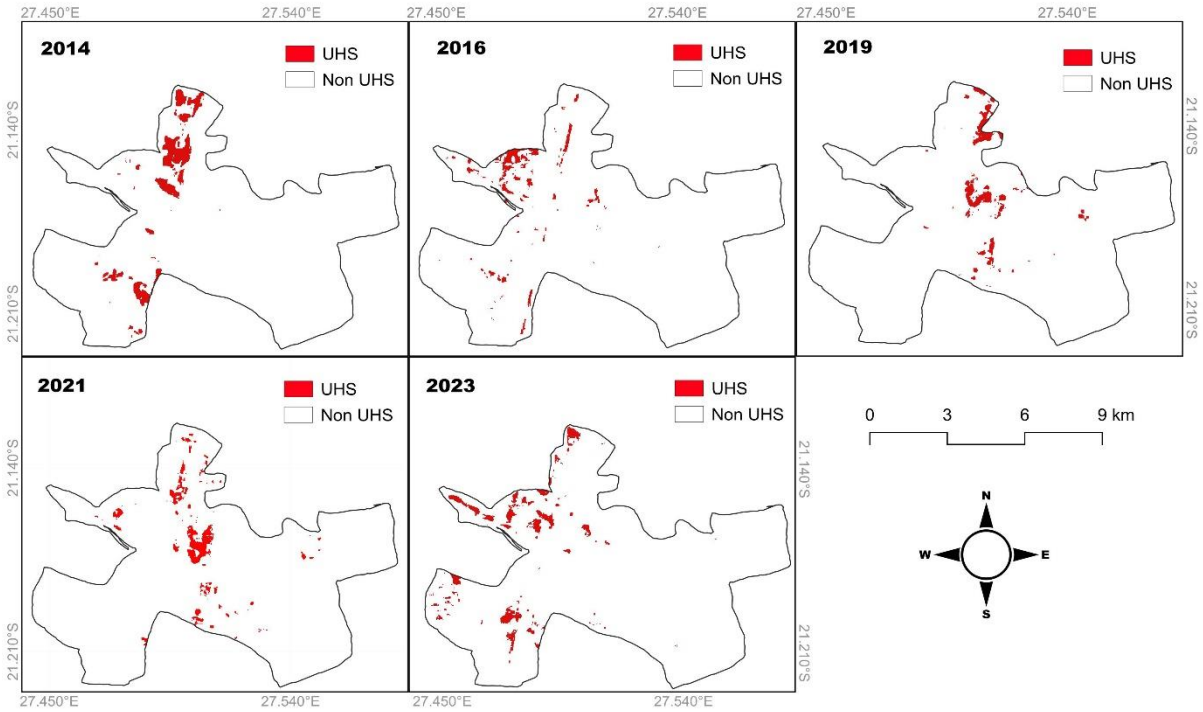


Figure 4.12. Greater Francistown City Identified Urban Hotspot

4.7 Spatiotemporal Analysis of Thermal Comfort Based on UTFVI

The study employs the use of the UTFVI to provide a quantitative analysis of the thermal and ecological comfort level concerning the existence of the UHI phenomenon effects on Greater Francistown City.

It was employed to assess the thermal comfort conditions in the city and estimate the UHI effect and varying effects of the UHI were identified throughout the study period (2013-2023). Figure 4.13 presents the spatiotemporal distribution of UTFVI across Greater Francistown City covering a five-point time: 2014, 2016, 2019, 2021, and 2023.

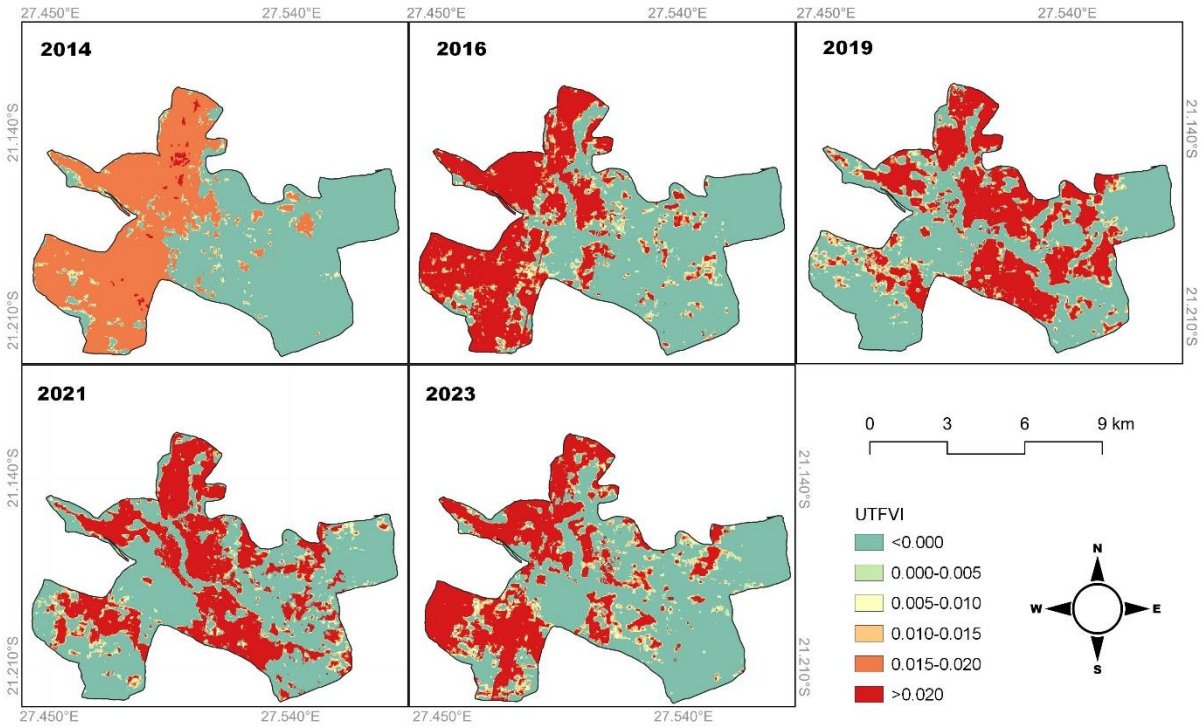


Figure 4.13. The Spatiotemporal Distribution of UTFVI Across Greater Francistown

The different effects of UHI were determined based on the level of thermal comfort related to the presence of UHI. Throughout the study period (2014-2023), Francistown City encountered six grades of thermal comfort zones ranging from excellent heat condition (UTFVI < 0) to worst heat condition (UTFVI > 0.02).

Table 4.6. Evaluations of UTFVI Thresholds and Area Covered for Each Class

Thermal Comfort measures			2014	2016	2019	2021	2023
UTFVI	**UHI**	**EEI**	Area km^2	Area km^2	Area km^2	Area km^2	Area km^2
<0.000	None	Excellent	40.95 (51.70%)	39.77 (50.21%)	40.96 (51.72%)	42.26 (53.36%)	43.12 (54.44%)
0.000-0.005	Weak	Good	1.09 (1.38%)	2.58 (3.26%)	2.8 (3.54%)	2.56 (3.23%)	3.18 (4.02%)
0.005-0.010	Middle	Normal	1.15 (1.45%)	2.54 (3.21%)	2.82 (3.56%)	2.42 (3.06%)	2.97 (3.75%)
0.010-0.015	Strong	Bad	1.21 (1.53%)	2.53 (3.19%)	2.74 (3.46%)	2.19 (2.77%)	2.72 (3.43%)
0.015-0.020	Stronger	Worse	34.23 (43.19%)	2.60 (3.28%)	2.71 (3.42%)	2.06 (2.60%)	2.51 (3.17%)
>0.020	Strongest	Worst	0.59 (0.74%)	29.18 (36.84%)	27.17 (34.31%)	27.71 (34.99%)	24.7 (31.19%)

Generally, most Greater Francistown City has favourable living conditions, particularly in areas with vegetation cover. The highest coverage of area 43.12km^2 (54.44%) in 2023, followed by 40.96km^2 (51.72%) in 2019, had an excellent EEI range UTFVI <0.000. When UTFVI <0.000, it is regarded as an indicator of a comfortable quality of life. Over the study period, the city has places with optimal microclimate with UTFVI <0.0) (Table 4.6; Figure 4.13).

The second highest coverage, which is 34.31km^2 (27.71%) in 2021 and 36.84km^2 (27.17%) in 2019, the study area exhibited the worst EEI in the threshold of UTFVI > 0.020. In 2014, the highest UTFVI was within the range 0.015 < UTFVI < 0.020, with UHI encountering Worse covering an area of 34.23km^2 (43.19%). Francistown City was under extreme heat conditions in 2016, covering an area of 29.18km^2 (Table 4.6; Figure 4.13). More significantly, the most (worse to worst) heat environments were felt in the built-up and bare land zones.

However, the areas marked by good UTFVI 0.000 < UTFVI< 0.005 to bad conditions (0.010 < UTFVI < 0.015) were relatively small, covering areas between 1.09 km^2 (1.38%) to 3.19km^2 (2.74%) over the study period. Furthermore, the ecological evaluation category with the lowest area coverage includes good, normal, bad, and worse classifications.

Table 4.7. UTFVI Calculated Descriptive Statistics for the Period 2014 to 2023

	2014	2015	2016	2017	2018	2019	2020	2021	2022	2023
UTFVI Min:	-0.307	-0.223	-0.232	-0.21	-0.217	-0.278	-0.3	-0.269	-0.269	-0.328
UTFVI Max:	0.241	0.16	0.199	0.214	0.153	0.176	0.214	0.19	0.19	0.166
UTFVI Mean:	-0.009	-0.002	-0.003	-0.003	-0.002	-0.002	-0.007	-0.004	-0.004	-0.003
UTFVI StdDev:	0.096	0.05	0.056	0.057	0.043	0.049	0.086	0.06	0.059	0.051

The UTFVI minimum values range from -0.3275 (2023) to -0.2104 (2017). These represent the minimum value of the UTFVI across the study period, indicating the existence of UHI with excellent environmental conditions. The lower values might suggest less variability in surface temperatures. The maximum UTFVI ranges from 0.1662 (2023) to 0.2413 (2014), indicating the maximum level of worse to worst environmental conditions. A higher value might suggest a stronger to strongest UHI occurrence. The UTFVI mean ranges from -0.0093 (2014) to -0.0026 (2023). A close-to-zero mean might suggest relatively stable LST temperatures, indicating an excellent environmental condition. UTFVI standard deviation ranges from 0.0428 (2018) to 0.0958 (2014), representing the spread of the UTFVI values. In context, it implies varying thermal conditions in different locations or times.

4.8 The evaluations of the LST, NDBI, NDVI, FV, and UTFVI Indices.

Table 4.8 presents the evaluations of the LST, NDBI, NDVI, FV, and UTFVI correlation matrix. The correlation between LST and NDBI is negative and moderately strong, with a correlation coefficient (r = -0.5055). This is because a significant portion of the built-up area in the city over the study period 2014 - 2023 is combined with vegetation cover, which has a cooling effect on the environment. The regression analysis between LST and NDBI shows R^2 of 0.2555 and is presented by the equation LST = 39.9 - 62.4NDBI.

Table 4.8. Pearson Correlation Coefficients for LST, NDBI, NDVI, FV UTFVI, and SUHI

	LST	**NDBI**	**NDVI**	**FV**	**UTFVI**	**SUHI**
LST	1					
NDBI	-0.50545	1				
p-value	0.1361					
NDVI	-0.30053	0.02563	1			
p-value	0.3988	0.944				
FV	-0.55723	-0.15648	0.67101	1		
p-value	0.0942	0.666	0.0337			
UTFVI	0.61137	-0.21147	0.20783	-0.44308	1	
p-value	0.0404	0.5575	0.5645	0.1997		
SUHI	1	-0.50545	-0.30053	-0.55723	0.61137	1
p-value	<.0001	0.1361	0.3988	0.0942	0.0404	

A weak negative correlation was found between LST and NDVI (r = -0.30053), and a moderate negative correlation was found between LST and PV (r= -0.55723). This negative correlation indicates that in Francistown when LST increased, NDVI decreased. The high LST values are due to limited vegetation cover, resulting in low evapotranspiration. The regression analysis results between LST and NDVI indicate an R^2 of 0.0903 for the study period 2014-2023, which depicts a 40% correlation between LST and NDVI. LST= 44.6 – 26NDVI.

A significant moderate positive correlation r = 0.61137 and P(t) = 0.0404 exists between LST and UTFVI. The positive correlation between LST and UTFVI might imply that areas with higher LST exhibit greater variability in the urban thermal field. This could be affected by several factors, such as urbanisation patterns, LULC, or local climate conditions. The computed R^2 is 0.3738, suggesting that approximately 37.38% of the variability in the dependent variable (LST) is described by the independent variable (UTFVI). The root MSE of 1.687 indicates the average magnitude of the residuals.

The correlation coefficient (r = 0.02563) between NDVI and NDBI is close to zero, indicating an extremely weak positive correlation (Table 4.8). This suggests that there is little to no linear relationship between vegetation changes and built-up areas. The p-value (P(t)) is 0.944; the results suggest no significant correlation exists between NDVI and NDBI in the study area. The regression analysis results between

NDVI and NDBI indicate a root MSE of 0.02464 and R^2 of 0.0007 with the equation NDVI = 0.33143 + 0.03658NDBI.

The results imply a highly significant perfect positive association between LST and SUHII ($r = 1$, $p < 0.0001$). These results align with expectations for the UHI effect, where higher LSTs are strongly associated with more pronounced UHI effects.

CHAPTER 5: DISCUSSIONS

5.1 Introduction

This chapter interprets and contextualises the findings presented in Chapter Four, linking them to the existing body of literature and addressing the identified research gaps. It also explores the implications of the results, assesses their significance and discusses how they align or contrast with previous studies. The discussion is structured around the key objectives of the study.

5.2 Spatiotemporal Distribution of LULC, Vegetation and Built-up Areas

The results of the LULC classification (Figure 4.1) revealed that the built-up and vegetation classes dominate Greater Francistown City, with a significant increase in built-up areas and water bodies occupying the smallest land cover (Table 4.2). The decreased water bodies were due to excessive heat and low rainfall, which increased bare land. The LULC analysis shows a significant decrease in vegetated areas and an increase in built-up land, affecting land use, LST, and UHI growth in Greater Francistown City.

The results of these studies align with the existing literature, demonstrating the significant impact of LULC changes on LST in semi-arid urban environments. Amir Siddique et al. (2023) found that in 2015 - 2020, changes in LULC significantly affected LST in Beijing City, China, with urban plantation decreasing by 3%, forest land decreasing by 5%, bare land increasing by 5%, and arable land increasing by 2%. Ouma et al. (2021) also discovered that Gaborone City in Botswana, covering an area of 190.96 km^2, experienced a 40% vegetation decrease, a 38.9% built-up increase, a 3% decrease in water bodies, and a 4.1% increase in bare land with a 30-year mean air temperature increase of 2.6^oC. The study's findings are further supported by (Rasul et al., 2017), who emphasise the effect of LULC change on SUHIs in arid and semi-arid climates. Moreover, (Bindajam et al., 2020) provide evidence of the significant influence of LULC type on LST and its spatiotemporal dynamics in semi-arid environments. Ouma et al. (2021) highlighted the need for comprehensive data on the spatiotemporal patterns of LULC changes and their impact on urban environments. This study fills this gap by providing detailed temporal and spatial analysis from 2014 to 2023, offering a clear picture of the dynamic changes in land cover and their implications.

The study indicates a significant increase in built-up area, from 20.03% in 2014 to 37.47.42% in 2023 (Figure 4.3), indicating significant urbanisation impacts on LULC. Such a dramatic alteration in land use composition indicates a rapid transformation in the urban composition. One of the critical implications of expanding built-up areas, as evidenced by the increasing built-up area over the study period, lies in its potential impact on LST and the UHI effect (Zupancic and Bulthuis, 2015). As the built-up areas have consistently grown, it is imperative to consider the potential consequences for LST and UHI. The rise in built-up surfaces can contribute to increased heat absorption, potentially leading to higher temperatures within the urban landscape. This, in turn, may have cascading effects on various aspects of the local environment, such as altering microclimates, influencing biodiversity, and impacting residents' overall quality of life.

While the effects of urbanisation on LST and UHI have been studied globally (Adulkongkaew et al., 2020; Arshad et al., 2022), there has been a lack of focused research on semi-arid regions like Greater Francistown City. This study contributes to the understanding of how rapid urbanisation influences LST and UHI in such environments, as demonstrated by the significant increase in built-up areas and corresponding temperature changes.

The NDBI means show an increasing trend over the study period, suggesting an increase in the presence of built-up structures (Figure 4.4). The NDBI, a reliable indicator of built-up areas, shows fluctuations in maximum and minimum values over the years, with a peak in 2021 and a less negative minimum in 2023. The low standard deviation values for NDBI (Figure 4.4) across the study period (2014-2023) indicate a consistent and stable pattern in the built-up index, suggesting that the NDBI is a reliable indicator for monitoring built-up areas over time. A low standard deviation implies that the NDBI values are tightly clustered around the mean. In the context of this study, where NDBI is used as an indicator of built-up areas, this suggests that the degree of built-up features remains relatively consistent over time. The small variation in NDBI values signifies a limited fluctuation in the intensity of built-up development across the study area throughout the study period.

These results were consistent with (Hishe et al., 2024) study in cities in Ethiopia, where the maximum NDBI ranges from 0.2 to 0.36 and the minimum NDBI ranges

from -0.14 to -0.24. The mean and standard deviation NDBI ranged from -0.04 to -0.07 and 0.04 to 0.05, respectively. Dilawar et al. (2021) analysed major cities in Punjab, Pakistan, and found that higher NDBI values were associated with densely built-up regions linked to maximum temperature in urban areas. Furthermore, (Adyatma et al., 2022) demonstrated a strong correlation between NDBI of built-up area density and surface temperature in Banjarmasin City, emphasising the significance of NDBI mean and density in understanding thermal patterns. Huang et al. (2022) employed NDBI to map global impervious surface area, indicating the use of NDBI mean, maximum, and standard deviation to enhance temporal information.

The study found low NDVI values in built-up areas in Greater Francistown City, with high concentrations of buildings and minimal vegetation (Figure 4.5). The highest NDVI values were primarily along the Tati River banks due to water-nourishing surrounding vegetation (Figure 4.5). High NDVI figures are associated with places with plentiful vegetation, found in the northeast to the southern part of Greater Francistown City. Hishe et al. (2023) also discovered that Mekelle City's greatest NDVI value was concentrated around riverbanks due to abundant irrigated vegetation for urban agriculture. This correlation aligns with the results of a study conducted by (Fatemi and Narangifard, 2019). The study emphasised that areas with high NDVI and low LST values are typically found in urban LULC vegetated areas, such as parks, crop fields, and urban forests. This is further corroborated (Jombo et al., 2022), who demonstrated that high NDVI values in Johannesburg correspond to suburban regions characterised by abundant green foliage, lawns, gardens, and irrigated farmland. The vegetated areas with high NDVI values have a cooling effect because they reflect more radiation than built-up surfaces, which absorb and re-emit solar energy at night (Guha et al., 2018; Fatemi and Narangifard, 2019).

The mean NDVI estimates in Greater Francistown City showed a slightly declining trend from 2014-2023, with slight variations, except in 2017 and 2021 (Figure 4.6). The standard deviation values fluctuated, with 2017 and 2021 showing higher variability (Figure 4.6). (Hishe et al. (2024) reported similar results where the NDVI values were varied across different sub-city areas, with the lowest (-0.14) and highest (0.59) values found in the Hadinet and Hawelti sub-city.

Guha et al. (2018) found that an increase in NDVI led to a gradual decrease in the UHI, with some areas exhibiting negative UHI values, known as cool islands. This demonstrates the inverse relationship between NDVI and UHI, indicating that higher vegetation density can mitigate the UHI effect. By analysing NDVI trends and their impact on UHI in Greater Francistown City, this study provides valuable insights into how urban planning and green spaces can mitigate heat effects.

5.3 LST and Its Spatiotemporal Distribution in Greater Francistown City

The results of LSE and its associated metrics reveal a notable degree of consistency and stability over the entire study period from 2014 to 2023 (Figure 4.8). The stability and uniformity observed in LSE values signify a consistent thermal behaviour of the land surface throughout the ten years. This could imply a relatively stable land cover composition or surface properties, which have remained unchanged over time. Such consistency in LSE is crucial for various applications, including urban heat island studies and LST estimation, as it ensures reliability and accuracy in thermal analysis.

The small standard deviation values of 0.0004 from 2014 to 2020 and 0.0005 from 2021 to 2023 further underscore the stability and uniformity in LSE values (Table 4.3). The minimal variation in LSE over the two distinct time periods suggests that the thermal properties of the land surface have remained remarkably consistent, with negligible temporal fluctuations. This consistency is essential for ensuring the reliability and repeatability of thermal analysis and modeling efforts.

Chen et al. (2019) and Tiangco et al. (2008) have emphasised the significance of vegetation in alleviating the UHI phenomenon. Chen et al. (2019) showed that vegetation fraction can alleviate the occurrence of surface urban heat islands, suggesting that higher FV cover can contribute to lower LSE in urban areas. Tiangco et al. (2008) also highlighted the inverse relationship between NDVI and temperature, indicating that increasing the number of plants in cities can minimise the UHI effect, thereby influencing LSE in urban settings. Chen et al. (2019). have highlighted the need for a consistent and stable measure of LSE for accurate thermal analysis. This study provides evidence of minimal variation in LSE values over the study period, ensuring reliable LST estimation and contributing to the body of knowledge on the thermal properties of urban surfaces.

Figure 4.9 presents a compelling visualisation of LST distribution, highlighting a notable trend of increasing temperatures in specific areas, particularly around bare land and built-up structures within the city. The observed pattern reveals that these regions consistently exhibit significantly higher LST values than the surrounding areas, surpassing a threshold of 25.62°C (Figure 4.9).

The concentration of higher LST around bare land and built-up structures suggests a distinct influence of LULC on local temperature dynamics (Adeyeri et al., 2024). Bare land, devoid of vegetation, tends to absorb and retain more solar radiation, contributing to elevated temperatures. Similarly, built-up structures, characterised by materials with low thermal inertia, can enhance heat absorption and contribute to the formation of UHIs. The observed temperature surpassing the 25.62°C threshold underscores the significance of this phenomenon, as it exceeds a level that may have implications for environmental comfort, human health, and urban ecosystem functioning.

The studies by (Naughton and McDonald, 2019; Fatemi and Narangifard, 2019; Asi et al., 2022; Jeyachandran, 2022; and Sanad et al., 2022) consistently reported increased LST in areas with built-up structures and reduced vegetation cover. The studies attribute the rise in LST to factors such as urbanisation, land use changes, and reduction in vegetation cover, leading to increased impervious surfaces and reduced evapotranspiration. The correlation between LST and land cover changes is apparent, as built-up and barren land consistently exhibits higher LST. In contrast, areas with greater vegetation cover and water display reduced LST.

The spatial distribution of elevated LST in Figure 4.9 is valuable for identifying areas prone to heat stress and UHI effects, which affect public health, energy consumption, and overall urban sustainability. The visual representation identifies hotspots requiring targeted interventions, such as green infrastructure implementation, urban planning strategies, and heat mitigation measures.

The maximum LST values recorded in different years (Table 4.4) reflect the peak temperatures observed, highlighting the temporal variability in LST and indicating periods of extreme heat within the study area. The computed standard deviation values for LST (Section 4.5.1) reveal variations in temperature consistency across the study period. The peak standard deviation of 3.26°C in 2014 suggests a higher

degree of variability in LST during that year, while the lower standard deviation in 2023 (1.78°C) indicates a more stable temperature pattern.

The consistently higher LSTs compared to air temperatures, as indicated by positive differences in Table 4.4, underscore the well-established UHI effect. Urban areas, characterised by impervious surfaces and human activities, tend to absorb and retain more heat, leading to higher land temperatures than the surrounding air. The positive differences observed throughout the study period emphasise the persistence of this UHI effect, with land surfaces consistently experiencing higher temperatures than the air above them (Table 4.4). The consistency of higher LSTs compared to air temperatures, coupled with temporal variability, underscores the significance of ongoing urban heat challenges and the need for informed strategies to address them.

These results align with Kasniza Jumari et al.'s (2023) study in Kuala Lumpur Metropolitan City, where the LST value attained in 2021 was higher than in 2013, with an average reading of 22.2°C. However, the measured air temperature values exceeded the LST, leading to negative discrepancies in the minimum, maximum, and mean temperatures. These temperature differences were attributed to surface roughness and atmospheric impurities obstructing radiant energy passage. More detailed temporal analyses of LST are needed to understand the variability and peak heat periods within urban areas. This study's examination of maximum LST values and standard deviation over the years provides insights into the periods of extreme heat and the overall stability of temperature patterns.

The study found a weak negative association between LST and NDVI and a moderate negative association between LST and PV (Table 4.8).

The results are in line with prior studies (Marzban et al., 2018; Guha & Govil, 2021; Alademomi et al., 2022; Değermenci, 2024) have found a negative correlation between LST and NDVI in urban areas, with LST values increasing with decreased vegetation cover and vice versa. For instance, Marzban et al. (2018) used a simple linear regression method to explore the relationship between LST and NDVI, finding a negative correlation between the two variables. Similarly, (Değermenci, 2024) identified NDVI as one of the significant indices contributing to LST, indicating a negative relationship. Conversely, other research findings have demonstrated a

positive relationship between LST and NDVI (Karnieli et al., 2010; Subzar Malik et al., 2019; Francis, 2024). Additionally, Francis (2024) found that NDVI had the closest fit with LST in the regression, suggesting a positive correlation between the two variables. The role of vegetation in mitigating the UHI effect is well-documented, yet specific regional analyses are necessary to inform local urban planning (Tiangco et al., 2008). This study confirms the inverse relationship between NDVI and LST, emphasising the importance of green spaces in urban environments to reduce surface temperatures and combat UHIs.

The association between LST and NDBI is negative and moderately strong (Figure 4.8). This is because a significant portion of the built-up area in the city over the study period 2014 - 2023 is combined with vegetation cover, which has a cooling effect on the environment. This observation is very contrary to those reported by (Guha and Govil, 2021; Sharmin Siddika et al., 2021; Çolakkadioğlu, 2023), their results consistently showed a positive association between LST and NDBI. For instance, Guha and Govil, (2021) found a strong positive correlation between LST and NDBI in Wuhan City, China, across different seasons.

Similarly, Hadibasyir et al. (2023) indicated that NDBI is directly proportional to LST. Furthermore, Colakkadioğlu (2023) emphasised the positive correlation between LST and NDBI, reinforcing the consistent findings across different studies. This implies that as more buildings are constructed, the density of NDBI and the LST increase, indicating the possibility of an increase in UHIs. The positive correlation between built-up areas and LST is a common finding in urban heat studies (Naughton & McDonald, 2019). However, due to vegetation within built-up areas, this study's observation of a negative association between LST and NDBI provides a nuanced understanding of urban heat dynamics in semi-arid environments.

5.4 Spatial Distribution and Intensity of UHI, Non-UHI, and Urban Hotspot Effect

Results (Figure 4.11) revealed that the spatial distribution of the UHI was primarily in the city's built-up and bare land precincts. In 2014, the study identified a total UHI area of 6.05 km², constituting 7.74% of the total area (Table 4.5). This marked the highest UHI extent during the study period. Identifying bare land (Figure 4.1) covering this UHI area suggests that land cover composition, specifically exposed

surfaces with low albedo, such as asphalt and concrete, could contribute to the UHI effect. Subsequent years witnessed a decrease in UHI extent (Table 4.5). These reductions might be attributed to changes in land use, urban planning interventions, or climatic conditions (Taha, 1997). However, the UHI area exhibited a slight upward trend from 2021 to 2023 (Table 4.5). The 0.99% rise suggests a potential resurgence in UHI extent during the study period. The consistently reported (Section 4.6.1) higher mean LST values for UHI areas over the years align with expectations. The elevated LST values indicate the UHI effect, where urban areas exhibit elevated temperatures compared to their surroundings due to impervious surfaces, reduced vegetation, and anthropogenic heat generation.

The UHI, prevalent in bare lands and built-up areas, can lead to climatic and environmental issues affecting individual well-being, similar to LST distribution in the study area. The consequences include increased energy consumption, changes in air and water quality, and adverse effects on human health (Lotfabadi and Hançer, 2019; Mutani and Todeschi, 2020). For instance, Peng et al. (2012) emphasised the adverse effects of the UHI on urban living conditions, such as its influence on energy usage, air and water quality, and human well-being. Similarly, Li and Bou-Zeid, (2013) underscored the augmented heat stress experienced in urban areas throughout heat waves. This circumstance may substantially influence human health more than the combined effects of the background UHI and the heat wave. Additionally, Miao et al. (2023) pointed out that the combined effect of the UHI and air pollution threatens human health and well-being in urban settings. These findings underscore the detrimental influence of the UHI on human well-being and the environment.

On the other hand, Figure 11 indicates that a significant portion of the study area exhibited characteristics associated with lower LST and a reduced UHI effect. The prevalence of non-UHI areas in the Northern and Southern regions could be influenced by vegetation cover, open spaces, and possibly less intensive urban development. The observed variations in the extent of non-UHI areas also underscore the dynamic nature of urban environments and the need for ongoing monitoring and adaptive planning. The data suggests that the city's thermal

characteristics are subject to change over time, influenced by a blend of natural and anthropogenic factors.

The year 2014 marked the highest UHS concentration in the study's initial year. In 2016, the UHS area decreased (Table 4.5), indicating a reduction in the spatial extent of urban heat hotspots. However, by 2023, the UHS area expanded to represent an increase of 1.08% compared to 2016. This upward trend suggests a resurgence or intensification of urban heat hotspots within Greater Francistown City over the study period. Most of the study area in 2023, covering 96.88%, remained free from urban hotspot cases (Figure 4.12). This indicates that most of the study area did not exhibit heightened urban heat intensity and remained relatively cooler than the identified UHS precincts. While much attention is given to UHI, understanding the characteristics of non-UHI areas is equally essential for urban planning. This study identifies cooler areas within the city, emphasising the role of vegetation and open spaces in reducing urban heat and enhancing thermal comfort.

The distribution of urban hotspots, with a high concentration in built-up and barren areas and lower occurrence in water bodies, has been a consistent finding in various studies (Nguyen et al., 2019; Amir Siddique et al., 2023; Hishe et al., 2024). These observations align with the UHI effect, where built-up areas with impervious surfaces and minimal vegetation tend to retain more heat than water bodies, which have a cooling effect. Nguyen et al. (2019) focused on limited spatial extents or specific urban areas. This study provides a comprehensive spatial analysis covering the entire city, offering a detailed understanding of the distribution and intensity of UHI and urban hotspots. The study spans a decade, providing insights into temporal dynamics and identifying increased or decreased UHI and hotspot intensity periods.

5.5 Spatiotemporal Distribution of Thermal Comfort Levels

Figure 4.13 indicates that most of the city, specifically areas with vegetation, contributes to favourable living conditions. This observation is particularly notable in areas with an excellent EEI range, specifically where the UTFVI is less than 0.000. Vegetation is crucial in mitigating urban heat, providing shade, and contributing to residents' well-being. The positive living conditions observed in areas with vegetation cover align with principles of sustainable urban development, emphasising the

importance of green infrastructure in creating aesthetically pleasing cities conducive to a high quality of life.

Table 4.6 suggests that a notable portion of the study area, particularly in 2019 and 2021, falls within a less favourable EEI range, characterised by high UTFVI values exceeding 0.020. In 2019, 27.17% of the study area and in 2021, 27.71% were identified as having a worse EEI, with UTFVI values exceeding the threshold of 0.020. This range indicates less comfortable living conditions, possibly characterised by elevated temperatures and increased heat stress. Identifying areas with unfavourable EEI underscores the spatial heterogeneity in living conditions within the city.

Table 4.6 also revealed that a significant portion of the city, covering 34.23 km² (43.19%) in 2014, experienced the highest UTFVI within the range of 0.015 < UTFVI < 0.020. This range is associated with stronger UHI effects, indicating that these areas encounter worse thermal conditions. The concentration of Stronger UHI in 2014 suggests that certain parts of Greater Francistown City were particularly prone to extreme heat conditions during the study 2014-2023 period. Furthermore, 2016 is highlighted as a period Great Francistown City was under extreme heat conditions, covering an area of 29.18km². This emphasises the temporal variability in thermal conditions, with certain years experiencing more pronounced heat stress than others.

Figure 4.13 and Table 4.6 show that the most intense heat environments (ranging from worse to worst) were predominantly felt in the built-up and bare land zones. This observation aligns with expectations, as these land cover types typically exhibit low albedo, high thermal inertia, and limited vegetation, contributing to elevated temperatures and increased vulnerability to heat stress (Taha et al., 1988; Taha, 1997). The UTFVI analysis of Greater Francistown City aligns with studies examining the UHI's spatiotemporal patterns using Landsat sensors. (Isioye and Akomolafe, 2020) found out that within the Abuja Municipal Area Council, the majority (44.18%) of the area enjoys ideal thermal conditions, a UTFVI of 0.01. However, these favourable conditions are limited to small pockets of the municipal area. Conversely, 11.25% of the study area is characterised by thermal discomfort. The overall pattern of these results aligns with the conclusions drawn by (Hishe et al., 2024) research

carried out in Ethiopian cities, where the central part of Mekelle city is characterised by excellent UTFVI conditions.

Generally, the level of UTFVI concentration is higher in urban areas, industrial areas, and bare land compared to non-urban areas due to human activities indicating the presence of UHI and ecological degradation. This could potentially subject the residents of any urban area to a significant health hazard. Likewise, (Mokhtari et al., 2021) observed that the UTFVI in Karaj, Iran, was more significant in areas with industries and barren land, and the city's central regions exhibited superior ecological conditions compared to the urban periphery. Guha et al. (2018) applied the UTFVI to establish cities' thermal and ecological comfort levels, while Kikon et al. (2023) found that the highest UTFVI zones occur in over-developed areas. Portela et al. (2020) also mapped the UTFVI using satellite images to identify the distribution and intensities of UHI, further supporting the association of high UTFVI with urbanised and industrial areas. Few studies provide a detailed temporal analysis of thermal comfort levels over an extended period (Bakhtiari et al., 2020). This study spans a decade, offering insights into the temporal variability and identifying periods of extreme thermal discomfort. Understanding the spatial heterogeneity of thermal comfort levels is crucial for effective urban planning. This study identifies areas with varying thermal comfort levels, providing valuable insights for localised urban heat mitigation strategies.

5.6 Socio-Economic Implications of UHI's Effects on Urban Residents

The study of the UHI effect in Greater Francistown City has revealed significant spatiotemporal variability in LST and thermal comfort levels. Beyond the environmental and climatic dimensions, these findings carry profound socio-economic implications for urban residents. One of the most direct socio-economic implications of the UHI effect is the increase in energy consumption (Gonzalez-Trevizo et al., 2021). The UHI effect increases energy consumption in urban areas due to higher LST, leading to higher electricity bills and economic burdens, particularly for low-income households. This results in disparities in thermal comfort and quality of life.

The UHI effect, characterised by high temperatures, poses significant health risks, including heat exhaustion, heat strokes, and exacerbation of pre-existing conditions.

Vulnerable populations, including the elderly, children, and those with chronic illnesses, are at greater risk (Qaid et al., 2016; Omonijo, 2017). The health impacts of UHI can lead to increased medical expenses, loss of productivity due to illness, and a higher burden on healthcare services. Studies have shown that urban residents in areas with higher LST are more likely to experience heat-related health issues, underscoring the need for effective mitigation strategies (Mijani et al., 2020; He et al., 2022).

High temperatures in UHI-affected areas can deter outdoor activities, reduce public spaces, and negatively impact social cohesion and physical health (Day et al., 2019). This weakens the socio-economic fabric of urban communities, affecting residents' overall well-being. The UHI effect also reduces worker efficiency, increasing fatigue and accidents (Varghese et al., 2018). Businesses may face increased operational costs due to the need for additional cooling measures, and there may be broader economic implications for the city’s economy.

The UHI effect can influence property values and urban development patterns (Tang et al., 2017). This leads to reduced property values in areas with higher LST and poor thermal comfort, exacerbated by socio-economic segregation and challenges for sustainable development (Bennet and O’Brien, 2017).

Higher temperatures and the need to cool urban environments can increase water consumption for residential use and maintaining green spaces (Coutts et al., 2013). This increased demand can strain local water resources, leading to higher water bills and potential conflicts over water usage. Ensuring an adequate water supply to meet the cooling needs of UHI-affected areas is essential for sustainable urban management. Greater Francistown City can create a more equitable, sustainable, and liveable urban environment by addressing the socio-economic impacts of UHI through a multifaceted approach.

CHAPTER 6: CONCLUSION AND RECOMMENDATIONS

6.1 Introduction

This chapter synthesises the key findings from the analysis, drawing critical conclusions about the trends and patterns observed in the UHI effect and thermal comfort across different areas of Greater Francistown City. It offers practical recommendations to mitigate UHI's adverse effects and enhance urban liveability. These recommendations guide urban planners, policymakers, and community stakeholders in developing sustainable urban development and climate adaptation strategies.

6.2 Conclusion

The study has revealed several cause-effect relationships crucial to understanding the dynamics of UHI and thermal comfort in Greater Francistown City.

Over the ten-year research period (2014-2023), there has been a significant increase in built-up areas and bare land, followed by a decrease in water bodies and vegetation cover. This expansion of built-up areas and a decrease in green spaces indicate the significant impact of urbanisation on the city's landscape. The analysis reveals a clear trend of transformation in land use, with a notable decline in vegetation cover and a substantial rise in built-up areas. The decline in vegetation suggests a loss of green spaces and potential environmental implications.

One of the primary findings is the significant impact of land cover changes on the UHI effect. Specifically, converting vegetated areas to built-up and bare land surfaces has led to increased LST values. This is because impervious surfaces such as asphalt and concrete have low albedo and high thermal inertia, causing them to absorb and retain more heat. Consequently, areas with reduced vegetation cover exhibit higher LST and intensified UHI effects.

The growth in built-up regions correlates with higher LST and the development of UHI. The expansion of urban areas leads to increased heat absorption and retention, contributing to elevated temperatures, particularly in areas with dense construction and reduced vegetation. The analysis of NDBI shows a consistent increase in built-up areas over the study period, indicating ongoing urban development. This expansion of impervious surfaces exacerbates heat retention and contributes to the

UHI effect. The NDVI analysis highlights the remarkable decline in vegetation cover in built-up areas over the years. This loss of greenery contributes to higher temperatures and reduced thermal comfort. The study indicates consistent and stable LSE values over the years, with higher emissivity associated with healthy vegetation along riverbanks, emphasising the significance of green spaces in mitigating heat.

Another critical observation is the role of vegetation in mitigating the UHI phenomenon. The analysis revealed a negative correlation between NDVI and LST, indicating that areas with higher vegetation cover tend to have lower surface temperatures. Vegetation provides shading, enhances evapotranspiration, and improves air quality, contributing to more favourable thermal conditions and higher thermal comfort levels.

The expansion of UHI areas over time, particularly in built-up and bare land precincts, underscores the influence of urbanisation on local climate conditions. Urban hotspots, concentrated in areas with dense construction, further contribute to elevated temperatures. The evaluation of UTFVI reveals varying thermal comfort levels across the city, with areas with more green spaces generally experiencing better conditions. However, the study also identifies areas with poor thermal comfort, particularly built-up areas with limited vegetation.

The spatial distribution of urban hotspots and non-UHI areas underscores the influence of land use practices and urban planning on local climate conditions. Built-up areas and bare lands consistently exhibited higher LST and more substantial UHI effects. At the same time, regions with significant vegetation cover and water bodies showed lower temperatures and better thermal comfort.

The study also identified temporal variations in the intensity of UHI and thermal comfort levels. For example, the peak UHI extent in 2014 and the resurgence in UHI from 2021 to 2023 highlight the dynamic nature of urban climate conditions, influenced by factors such as urban growth, land use changes, and climatic variations.

The study demonstrates the significant influence of urbanisation on land cover, temperature patterns, and thermal comfort in Greater Francistown City. The findings

underscore the value of sustainable urban planning and green infrastructure development to alleviate the adverse effects of UHI and enhance overall urban liveability. Addressing UHI effects aligns with broader climate change mitigation efforts, contributing to realising the Paris Agreement's goals. Policymakers and decision-makers must heed these insights and implement proactive measures to combat UHI effects, ensuring a sustainable and liveable future for Greater Francistown City and beyond.

6.3 Recommendations

Improving thermal comfort in Greater Francistown City is a multifaceted challenge that involves addressing UHIs, climate change impacts, and enhancing the liveability of city spaces. Based on the identified cause-effect relationships, the following recommendations are proposed to mitigate UHI effects and enhance thermal comfort in Greater Francistown City:

Several strategies can be employed to lessen the adverse effects of high temperatures and establish more comfortable urban environments.

Greater Francistown City's urban green infrastructure should be improved by increasing vegetation cover by planting more trees in places with bare land along all roads and pedestrian pathways, green roofs, and creating urban parks. Trees provide shade, reduce the temperature through evapotranspiration, and create a cooling effect through their canopies. Green spaces also help to mitigate the UHI effect by reducing surface temperatures, increasing natural ventilation and improving thermal comfort.

Since Greater Francistown is going through urbanisation with a lot of construction, cool roofs and pavement technologies should be incorporated into the design of new and renovated built-up structures. This involves using reflective and light-coloured materials for roofs and pavements that can reduce solar radiation absorption and lower surface temperatures. Reflective or permeable pavement materials should be used cautiously, as they can reflect solar radiation onto pedestrians' materials, absorb less heat and allow water infiltration. This helps to mitigate the UHI effect, reducing LST and improving thermal comfort. However, it is important to note that it is highly reflective and causes discomfort.

Raising awareness among the Greater Francistown city residents (public) about the importance of thermal comfort and the approaches available to enhance it can lead to behavioural changes and more sustainable practices. These strategies include developing and implementing heat action plans, public awareness campaigns, early warning systems, and guidelines for extreme heat events. The public can also be educated on the impacts of heat stress, the importance of staying hydrated, and the use of appropriate clothing during hot weather.

Greater Francistown City residents should be encouraged to support and participate in community-driven initiatives such as urban gardens, promoting local engagement and cooling through increased vegetation. The local communities should also be involved in urban planning to ensure that the solutions available are culturally sensitive and address specific neighbourhood needs.

Infrastructure should be designed and upgraded to withstand severe weather conditions linked to climate change. This includes using heat-resistant materials, stormwater management systems and adaptable urban designs. Water features like fountains and misting systems should be installed in public spaces, including all shopping malls to cool the surrounding air. Evaporative cooling from water can provide relief in hot urban areas.

The Greater Francistown City Council should invest in research and development of new technologies to address urban heat challenges. This includes innovative cooling solutions, smart city technologies, and advanced materials for sustainable urban development.

The Government should formulate and implement policies and regulations on UHI and thermal comfort. These include implementing zoning regulations encouraging green spaces, cool roofs, and energy-efficient building designs. Developers should be incentivised to adopt sustainable and heat-resilient practices. Standards and guidelines for heat-resilient infrastructure should be implemented, ensuring that new developments consider the impacts of heat on the urban environment.

Therefore, a comprehensive approach involving urban planning, technological innovation, public engagement, and policy measures is essential for improving thermal comfort in Greater Francistown City. Addressing the unique challenges of

each urban area and fostering collaboration between stakeholders can contribute to creating more liveable and sustainable urban environments.

LIST OF REFERENCES

Aburas, M. M., Ho, Y. M., Ramli, M. F., & Ash'aari, Z. H. (2016). The simulation and prediction of spatio-temporal urban growth trends using cellular automata models: A review. In *International Journal of Applied Earth Observation and Geoinformation* 52, 380–389. Elsevier B.V. https://doi.org/10.1016/j.jag.2016.07.007

Addas, A., Goldblatt, R., & Rubinyi, S. (2020). Utilizing remotely sensed observations to estimate the urban heat island effect at a local scale: Case study of a university campus. *Land*, *9*(6), 191-216. https://doi.org/10.3390/LAND9060191

Adeyeri, O. E., Folorunsho, A. H., Ayegbusi, K. I., Bobde, V., Adeliyi, T. E., Ndehedehe, C. E., & Akinsanola, A. A. (2024). Land surface dynamics and meteorological forcings modulate land surface temperature characteristics. *Sustainable Cities and Society*, *101*. 105072 https://doi.org/10.1016/j.scs.2023.105072

Adulkongkaew, T., Satapanajaru, T., Charoenhirunyingyos, S., & Singhirunnusorn, W. (2020). Effect of land cover composition and building configuration on land surface temperature in an urban-sprawl city, case study in Bangkok Metropolitan Area, Thailand. *Heliyon*, *6*(8), e04485. https://doi.org/10.1016/j.heliyon.2020.e04485

Adyatma, S., Muhaimin, M., Arisanty, D., & Hastuti, K. P. (2022). The Effect of Built-Up Area Density and Vegetation Density on Surface Temperature in Banjarmasin City. *International Journal of Forestry Research*, *2022(1), 2585719*. https://doi.org/10.1155/2022/2585719

Aghamolaei, R., Fallahpour, M., & Mirzaei, P. A. (2021). Tempo-spatial thermal comfort analysis of urban heat island with coupling of CFD and building energy simulation. *Energy and Buildings*, *251, 111317*. https://doi.org/10.1016/j.enbuild.2021.111317

Alademomi, A. S., Okolie, C. J., Daramola, O. E., Akinnusi, S. A., Adediran, E., Olanrewaju, H. O., Alabi, A. O., Salami, T. J., & Odumosu, J. (2022). The interrelationship between LST, NDVI, NDBI, and land cover change in a section of Lagos metropolis, Nigeria. *Applied Geomatics*, *14*(2), 299–314. https://doi.org/10.1007/s12518-022-00434-2

Alahmad, B., Tomasso, L. P., Al-Hemoud, A., James, P., & Koutrakis, P. (2020). Spatial distribution of land surface temperatures in Kuwait: Urban heat and cool Islands. *International Journal of Environmental Research and Public Health*, *17(9), 2993.* https://doi.org/10.3390/ijerph17092993

Amani, M., Ghorbanian, A., Ahmadi, S. A., Kakooei, M., Moghimi, A., Mirmazloumi, S. M., Moghaddam, S. H. A., Mahdavi, S., Ghahremanloo, M., Parsian, S., Wu, Q., & Brisco, B. (2020). Google Earth Engine Cloud Computing Platform for Remote Sensing Big Data Applications: A Comprehensive Review. *IEEE Journal of Selected Topics in Applied Earth Observations and Remote Sensing*, *13*, 5326–5350. https://doi.org/10.1109/JSTARS.2020.3021052

Amani-Beni, M., Zhang, B., Xie, G. Di, & Odgaard, A. J. (2021). Impacts of the microclimate of a large urban park on its surrounding built environment in the summertime. *Remote Sensing*, *13(22), 4703.* https://doi.org/10.3390/rs13224703

Amir Siddique, M., Boqing, F., & Dongyun, L. (2023). Modeling the Impact and Risk Assessment of Urbanization on Urban Heat Island and Thermal Comfort Level of Beijing City, China (2005–2020). *Sustainability (Switzerland)*, *15*(7), 6043. https://doi.org/10.3390/su15076043

Antoszewski, P., Świerk, D., & Krzyżaniak, M. (2020). Statistical review of quality parameters of blue-green infrastructure elements important in mitigating the effect of the urban heat island in the temperate climate (C) zone. In *International Journal of Environmental Research and Public Health* 17(19) 1-36. https://doi.org/10.3390/ijerph17197093

Arshad, S., Ahmad, S. R., Abbas, S., Asharf, A., Siddiqui, N. A., & Islam, Z. ul. (2022). Quantifying the contribution of diminishing green spaces and urban sprawl to urban heat island effect in a rapidly urbanizing metropolitan city of Pakistan. *Land Use Policy*, *113*. *113*, 105874. https://doi.org/10.1016/j.landusepol.2021.105874

Asi, A. N. H., Supriatna, S., & Zulkarnain, F. (2022). Spatial Study of Land Cover Changes and Land Surface Temperature in Bekasi Regency, West Java, Indonesia. *IOP Conference Series: Earth and Environmental Science*, *1111*(1), 12024. https://doi.org/10.1088/1755-1315/1111/1/012024

Aslan, N., & Koc-San, D. (2016). Analysis of relationship between urban heat island effect and Land use/cover type using Landsat 7 ETM+ and Landsat 8 OLI images. *International Archives of the Photogrammetry, Remote Sensing and Spatial Information Sciences - ISPRS Archives*, *41*, 821–828. https://doi.org/10.5194/isprsarchives-XLI-B8-821-2016

Athmani, W., Sriti, L., Dabaieh, M., & Khadraoui, M. A. (2022). An Investigation on Using Passive Cooling Roofs Techniques for Improving Climatic Performance of Residential Buildings in Hot Arid Regions based on Post-Occupancy Evaluation of Inhabitants' Thermal Comfort Appreciations. *Technium Social Sciences Journal*, *36*, 685–699. www.techniumscience.com

Azizah, V., Deffinika, I., & Arinta, D. (2022). The Effect of Land Use Changes on Land Surface Temperature in Malang City's on 2016 - 2020. *IOP Conference Series: Earth and Environmental Science*, 1066(1), 012006. https://doi.org/10.1088/1755-1315/1066/1/012006

Bakhtiari, H., Akander, J., & Cehlin, M. (2020). Evaluation of thermal comfort in a historic building refurbished to an office building with modernized HVAC systems. *Advances in Building Energy Research*, *14*(2), 218–237. https://doi.org/10.1080/17512549.2019.1604428

Balany, F., Ng, A. W. M., Muttil, N., Muthukumaran, S., & Wong, M. S. (2020). Green infrastructure as an urban heat island mitigation strategy—a review. In *Water (Switzerland) 12*(12), 3577. https://doi.org/10.3390/w12123577

Barrao, S., Serrano-Notivoli, R., Cuadrat, J. M., Tejedor, E., & Saz Sánchez, M. A. (2022). Characterization of the UHI in Zaragoza (Spain) using a quality-controlled hourly sensor-based urban climate network. *Urban Climate*, *44*. 101207 https://doi.org/10.1016/j.uclim.2022.101207

Bassoud, A., Khelafi, H., Mokhtari, A. M., & Bada, A. (2021). Evaluation of summer thermal comfort in arid desert areas. Case study: Old adobe building in Adrar (South of Algeria). *Building and Environment*, *205*, 108140. https://doi.org/10.1016/j.buildenv.2021.108140

Bennet, I. E., & O'Brien, W. (2017). Field study of thermal comfort and occupant satisfaction in Canadian condominiums. *Architectural Science Review*, *60*(1), 27-39

Betts, R. A., Alfieri, L., Bradshaw, C., Caesar, J., Feyen, L., Friedlingstein, P., Gohar, L., Koutroulis, A., Lewis, K., Morfopoulos, C., Papadimitriou, L., Richardson, K. J., Tsanis, I., & Wyser, K. (2018). Changes in climate extremes, freshwater availability and vulnerability to food insecurity projected at 1.5°C and 2°C global warming with a higher-resolution global climate model. *Philosophical Transactions of the Royal Society A: Mathematical, Physical and Engineering Sciences*, *376*(2119), 0452 https://doi.org/10.1098/rsta.2016.0452

Bibri, S. E. (2018). The IoT for smart sustainable cities of the future: An analytical framework for sensor-based big data applications for environmental sustainability. *Sustainable Cities and Society*, *38*, 230–253. https://doi.org/10.1016/j.scs.2017.12.034

Bindajam, A. A., Mallick, J., AlQadhi, S., Singh, C. K., & Hang, H. T. (2020). Impacts of vegetation and topography on land surface temperature variability over the semi-arid mountain cities of Saudi Arabia. *Atmosphere*, *11*(7).762. https://doi.org/10.3390/ATMOS11070762

Blazejczyk, K., Epstein, Y., Jendritzky, G., Staiger, H., & Tinz, B. (2012). Comparison of UTCI to selected thermal indices. *International Journal of Biometeorology*, *56*(3), 515–535. https://doi.org/10.1007/s00484-011-0453-2

Borzino, N., Chng, S., Mughal, M. O., & Schubert, R. (2020). Willingness to pay for urban heat island mitigation: A case study of Singapore. *Climate*, *8*(7), 82. https://doi.org/10.3390/CLI8070082

Botswana Climate (2011). Temperature records of the last 47 years. https://www.worlddata.info/africa/botswana/climate.php

Breiman, L. (2001). *Random Forests. Machine Learning,* 45(1) 5-32. https://link.springer.com/article/10.1023/a:1010933404324

Chandler, T. J. (1962). London's Urban Climate. In *Source: The Geographical Journal* 128(3), 279-298. https://www.jstor.org/stable/1794042

Chen, R., & You, X. yi. (2020). Reduction of urban heat islands and associated greenhouse gas emissions. *Mitigation and Adaptation Strategies for Global Change*, *25*(4), 689–711. https://doi.org/10.1007/s11027-019-09886-1

Chen, T., Sun, A., & Niu, R. (2019). Effect of land cover fractions on changes in surface urban heat islands using landsat time-series images. *International Journal of Environmental Research and Public Health*, *16*(6), 971. https://doi.org/10.3390/ijerph16060971

Chiguvi, D. (2022). Analysis of the Causes of Urban Sprawl and Dwelling Transformation in Urban Cities in Botswana.' *Journal of Legal, Ethical and Regulatory Issues 25,* 9-13. https://heinonline.org/HOL/License

Chiguvi, D., & Kgathi-Thite, D. (2022). Analysis of the Positive and Negative Effects of Urban Sprawl and Dwelling Transformation in Urban Cities: Case Study of Tati Siding Village in Botswana. *Journal. Legal of Ethical & Regulatory. Issues, 25, 1. https://heinonline.org/HOL/License*

Chun, B., & Guldmann, J. M. (2018). Impact of greening on the urban heat island: Seasonal variations and mitigation strategies. *Computers, Environment and Urban Systems*, *71*, 165–176. https://doi.org/10.1016/j.compenvurbsys.2018.05.006

Çolakkadioğlu, D. (2023). The Effects of Urbanization and Vegetation Cover on Urban Heat Island: A Case Study in Osmaniye Province. *International Journal of Environment and Geoinformatics*, *10*(1), 120–131. https://doi.org/10.30897/ijegeo.1144167

Corburn, J. (2009). Cities, climate change and urban heat island mitigation: Localising global environmental science. *Urban Studies*, *46*(2), 413–427. https://doi.org/10.1177/0042098008099361

Coutts, A. M., Tapper, N. J., Beringer, J., Loughnan, M., & Demuzere, M. (2013). Watering our cities: The capacity for Water Sensitive Urban Design to support urban cooling and improve human thermal comfort in the Australian context. *Progress in physical geography*, *37*(1), 2-28.

Cristóbal, J., Jiménez-Muñoz, J. C., Prakash, A., Mattar, C., Skoković, D., & Sobrino, J. A. (2018). An improved single-channel method to retrieve land surface temperature from the landsat-8 thermal band. *Remote Sensing*, *10*(3), 431. https://doi.org/10.3390/rs10030431

Das, A., Sarma, M. P., Sarma, K. K., & Mastorakis, N. (2018). Design of an IoT based Real Time Environment Monitoring System using Legacy Sensors. *MATEC Web of Conferences*, *210,* 3008. https://doi.org/10.1051/matecconf/201821003008

Day, E., Fankhauser, S., Kingsmill, N., Costa, H., & Mavrogianni, A. (2019). Upholding labour productivity under climate change: an assessment of adaptation options. *Climate policy*, *19*(3), 367-385.

de Almeida, C. R., Teodoro, A. C., & Gonçalves, A. (2021). Study of the urban heat island (UHI) using remote sensing data/techniques: A systematic review. *Environments*, *8*(10), 105. https://doi.org/10.3390/environments8100105

Değermenci, A. S. (2024). Estimation of land surface temperature from Landsat-8 OLI: comparative analysis of two periods for Duzce in Turkey. *International Journal of Environmental Science and Technology, 21(8), 6389-6404*. https://doi.org/10.1007/s13762-023-05416-4

Dilawar, A., Chen, B., Trisurat, Y., Tuankrua, V., Arshad, A., Hussain, Y., Measho, S., Guo, L., Kayiranga, A., Zhang, H., Wang, F., & Sun, S. (2021). Spatiotemporal shifts in thermal climate in responses to urban cover changes: a-case analysis of major cities in Punjab, Pakistan. *Geomatics, Natural Hazards and Risk*, *12*(1), 763–793. https://doi.org/10.1080/19475705.2021.1890235

Duffy, J. P., Anderson, K., Fawcett, D., Curtis, R. J., & Maclean, I. M. D. (2021). Drones provide spatial and volumetric data to deliver new insights into microclimate modeling. In *Landscape Ecology* 36(3),685–702. https://doi.org/10.1007/s10980-020-01180-9

Duhita Puspita, B., Wibisono, B. H., & Saleh, M. (2022). Exploring Technical Policy Solution to Reduce Urban Heat Island in the City of Yogyakarta Corresponding Author. *BEST: Journal of Built Environment Studies*, *3*(2), 46–52. https://journal.ugm.ac.id/v3/BEST

Dutta, D., Rahman, A., Paul, S. K., & Kundu, A. (2021). Impervious surface growth and its inter-relationship with vegetation cover and land surface temperature in peri-urban areas of Delhi. *Urban Climate*, *37, 100799*. https://doi.org/10.1016/j.uclim.2021.100799

Francis, E, O. (2024). Investigating the Spatio-Temporal Relationship between NDVI and LST in Abakaliki LGA, Ebonyi State Nigeria, Using Landsat, and Correlation Analysis: Implications for Landscape Management. *Global Academic Journal of Linguistics and Literature*, *6*(01), 1–14. https://doi.org/10.36348/gajll.2024.v06i01.001

Fanger, P. O., & Toftum, J. (2002Extension of the PMV model to non-air-conditioned buildings in warm climates. *Energy and buildings*, *34*(6), 533-536. https://doi.org/10.1016/S0378-7788(02)00003-8

Faragallah, R. N., & Ragheb, R. A. (2022). Evaluation of thermal comfort and urban heat island through cool paving materials using ENVI-Met. *Ain Shams Engineering Journal*, *13*(3),4. https://doi.org/10.1016/j.asej.2021.10.004

Fatemi, M., & Narangifard, M. (2019). Monitoring LULC changes and its impact on the LST and NDVI in District 1 of Shiraz City. *Arabian Journal of Geosciences*, *12*(4).6. https://doi.org/10.1007/s12517-019-4259-6

Feng, L., Zhao, M., Zhou, Y., Zhu, L., & Tian, H. (2020). The seasonal and annual impacts of landscape patterns on the urban thermal comfort using Landsat. *Ecological Indicators*, *110, 105798.*. https://doi.org/10.1016/j.ecolind.2019.105798

Ferrini, F., Fini, A., Mori, J., & Gori, A. (2020). Role of vegetation as a mitigating factor in the urban context. In *Sustainability (Switzerland)* 12(10), 4247. https://doi.org/10.3390/su12104247

Fiorillo, E., Brilli, L., Carotenuto, F., Cremonini, L., Gioli, B., Giordano, T., & Nardino, M. (2023). Diurnal Outdoor Thermal Comfort Mapping through Envi-Met Simulations, Remotely Sensed and In Situ Measurements. *Atmosphere*, *14*(4).641. https://doi.org/10.3390/atmos14040641

Gagge, A. P., Fobelets, A. P., & Berglund, L. (1986). *A Standard Predictive Index of Human Response to the Thermal Environment*. AVIC 1, 709 -731.

García-Santos, V., Cuxart, J., Martínez-Villagrasa, D., Jiménez, M. A., & Simó, G. (2018). Comparison of three methods for estimating land surface temperature from Landsat 8-TIRS Sensor data. In *Remote Sensing* 10(9), 1450. https://doi.org/10.3390/rs10091450

Garuma, G. F. (2023). Tropical surface urban heat islands in East Africa. *Scientific Reports*, *13*(1), 6. https://doi.org/10.1038/s41598-023-31678-6

Gatto, E., Buccolieri, R., Aarrevaara, E., Ippolito, F., Emmanuel, R., Perronace, L., & Santiago, J. L. (2020). Impact of Urban vegetation on outdoor thermal comfort: Comparison between a Mediterranean city (Lecce, Italy) and a northern European city (Lahti, Finland). *Forests*, *11*(2). 228. https://doi.org/10.3390/f11020228

Goldblatt, R., Addas, A., Crull, D., Maghrabi, A., Levin, G. G., & Rubinyi, S. (2021). Remotely sensed derived land surface temperature (LST) as a proxy for air temperature and thermal comfort at a small geographical scale. *Land*, *10*(4), 410. https://doi.org/10.3390/land10040410

Gómez, F., Gil, L., & Jabaloyes, J. (2004). Experimental investigation on the thermal comfort in the city: Relationship with the green areas, interaction with the urban microclimate. *Building and Environment*, *39*(9), 1077–1086. https://doi.org/10.1016/j.buildenv.2004.02.001

Gonzalez-Trevizo, M. E., Martinez-Torres, K. E., Armendariz-Lopez, J. F., Santamouris, M., Bojorquez-Morales, G., & Luna-Leon, A. (2021). Research trends on environmental, energy and vulnerability impacts of Urban Heat Islands: An overview. In *Energy and Buildings 246*, 111051.https://doi.org/10.1016/j.enbuild.2021.111051

Guha, S., & Govil, H. (2021). An assessment on the relationship between land surface temperature and normalized difference vegetation index. *Environment, Development and Sustainability*, *23*(2), 1944–1963. https://doi.org/10.1007/s10668-020-00657-6

Guha, S., Govil, H., Dey, A., & Gill, N. (2018). Analytical study of land surface temperature with NDVI and NDBI using Landsat 8 OLI and TIRS data in Florence and Naples city, Italy. *European Journal of Remote Sensing*, *51*(1), 667–678. https://doi.org/10.1080/22797254.2018.1474494

Guha, S., Govil, H., Gill, N., & Dey, A. (2020). Analytical study on the relationship between land surface temperature and land use/land cover indices. *Annals of GIS*, *26*(2), 201–216. https://doi.org/10.1080/19475683.2020.1754291

Gwak, J., Shino, M., Ueda, K., & Kamata, M. (2019). An investigation of the effects of changes in the indoor ambient temperature on arousal level, thermal comfort, and physiological indices. *Applied Sciences, 9(5), 899.* https://doi.org/10.3390/app9050899

Gwebu, T. D. (2012). Botswana's mining path to urbanisation and poverty alleviation. *Journal of Contemporary African Studies*, *30*(4), 611–630. https://doi.org/10.1080/02589001.2012.724868

Hadibasyir, H. Z., Firdaus, N. S., Fikriyah, V. N., & Sari, D. N. (2023). Assessing Performance of Modified Spectral Indices as Land Surface Temperature Indicators in Tropical Urban Areas. *IOP Conference Series: Earth and Environmental Science*, *1190*(1), 012005. https://doi.org/10.1088/1755-1315/1190/1/012005

Haghshenas, M., Hadianpour, M., Matzarakis, A., Mahdavinejad, M., & Ansari, M. (2021). Improving the suitability of selected thermal indices for predicting outdoor thermal sensation in Tehran. *Sustainable Cities and Society*, *74,* 103205 https://doi.org/10.1016/j.scs.2021.103205

Hashim, B. M., Al Maliki, A., Sultan, M. A., Shahid, S., & Yaseen, Z. M. (2022). Effect of land use land cover changes on land surface temperature during 1984–2020: a case study of Baghdad city using Landsat image. *Natural Hazards*, *112*(2), 1223–1246. https://doi.org/10.1007/s11069-022-05224-y

He, B. J. (2019). Towards the next generation of green building for urban heat island mitigation: Zero UHI impact building. *Sustainable Cities and Society*, *50, 101647*. https://doi.org/10.1016/j.scs.2019.101647

He, Y., Wong, N. H., Kvan, T., Liu, M., & Tong, S. (2022). How green building rating systems affect indoor thermal comfort environments design. *Building and Environment*, *224, 109514*. https://doi.org/10.1016/j.buildenv.2022.109514

Heaviside, C., Vardoulakis, S., & Cai, X. M. (2016). Attribution of mortality to the urban heat island during heatwaves in the West Midlands, UK. *Environmental Health: A Global Access Science Source*, *15,9* . https://doi.org/10.1186/s12940-016-0100-9

Hishe, S., Gidey, E., Zenebe, A., Girma, A., Dikinya, O., Sebego, R., & Lyimo, J. (2024). Urban heat island and ecological condition modeling using thermal remote sensing in Tigray–Northern Ethiopia. *Modeling Earth Systems and Environment*, *10*(1), 735-749. https://doi.org/10.1007/s40808-023-01804-4

Hoan, N. T., Liou, Y. A., Nguyen, K. A., Sharma, R. C., Tran, D. P., Liou, C. L., & Cham, D. D. (2018). Assessing the effects of land-use types in surface urban heat islands for developing comfortable living in Hanoi City. *Remote Sensing*, *10(12), 1965.* https://doi.org/10.3390/rs10121965

Huang, C., & Ye, X. (2015). Spatial modeling of urban vegetation and land surface temperature: A case study of Beijing. *Sustainability (Switzerland)*, *7*(7), 9479–9504. https://doi.org/10.3390/su7079478

Huang, X., Liu, W., Han, Y., Wang, C., Wang, H., & Hu, S. (2019). Performance evaluation and comparison of modified spectral mixture analysis method for different images of Landsat series satellites. *Sustainability*, *11(22), 6227.* https://doi.org/10.3390/su11226227

Huang, X., Yang, J., Wang, W., & Liu, Z. (2022). Mapping 10 m global impervious surface area (GISA-10m) using multi-source geospatial data. *Earth System Science Data*, *14*(8), 3649–3672. https://doi.org/10.5194/essd-14-3649-2022

Huo, H., Chen, F., Geng, X., Tao, J., Liu, Z., Zhang, W., & Leng, P. (2021). Simulation of the urban space thermal environment based on computational fluid dynamics: A comprehensive review. In *Sensors 21*(20), 6898. https://doi.org/10.3390/s21206898

Ibrahim, S. H., Ibrahim, N. I. A., Wahid, J., Goh, N. A., Koesmeri, D. R. A., & Nawi, M. N. M. (2018). The impact of road pavement on urban heat island (UHI) phenomenon. *International Journal of Technology*, *9*(8), 1597–1608. https://doi.org/10.14716/ijtech.v9i8.2755

Imamura, I. R. (1993). *Role of soil moisture in the determination of urban heat island intensity in different climate regimes. WIT Transactions on Ecology and the Environment 1*, 1-8.

Imran, H. M., Hossain, A., Islam, A. K. M. S., Rahman, A., Bhuiyan, M. A. E., Paul, S., & Alam, A. (2021). Impact of Land Cover Changes on Land Surface Temperature and Human Thermal Comfort in Dhaka City of Bangladesh. *Earth Systems and Environment*, *5*(3), 667–693. https://doi.org/10.1007/s41748-021-00243-4

Imran, H. M., Hossain, A., Shammas, M. I., Das, M. K., Islam, M. R., Rahman, K., & Almazroui, M. (2022). Land surface temperature and human thermal comfort responses to land use dynamics in Chittagong city of Bangladesh. *Geomatics, Natural Hazards and Risk*, *13*(1), 2283–2312. https://doi.org/10.1080/19475705.2022.2114384

Isioye, O. A., Ikwueze, H. U., & Akomolafe, E. A. (2020). Urban heat island effects and thermal comfort in Abuja Municipal Area Council of Nigeria. *FUTY Journal of the Environment*, *14*(2), 19-34.

Jeyachandran, I. (2022). ANALYZING IMPACTS of LAND COVER CHANGES on LAND SURFACE TEMPERATURE in BAY AREA, CALIFORNIA. *International Archives of the Photogrammetry, Remote Sensing and Spatial Information Sciences - ISPRS Archives*, *46*(M-2–2022), 127–129. https://doi.org/10.5194/isprs-Archives-XLVI-M-2-2022-127-2022

Jia, C., Zhao, S., Gao, S., Tong, Y., & Zhai, Y. (2022). Field Study of thermal comfort of indoor fitness places in cold region. *E3S Web of Conferences*, *356, 3010*. https://doi.org/10.1051/e3sconf/202235603010

Jombo, S., Adam, E., Byrne, M. J., & Newete, S. W. (2022). Assessing the intraurban differences in vegetation coverage and surface climate in a heterogeneous area. *Transactions of the Royal Society of South Africa*, *77*(1), 1–10. https://doi.org/10.1080/0035919X.2021.2004470

Jonsson, P. (2004). Vegetation as an urban climate control in the subtropical city of Gaborone, Botswana. *International Journal of Climatology*, *24*(10), 1307–1322. https://doi.org/10.1002/joc.1064

Kabano, P., Lindley, S., & Harris, A. (2021). Evidence of urban heat island impacts on the vegetation growing season length in a tropical city. *Landscape and Urban Planning*, *206*. 3989. https://doi.org/10.1016/j.landurbplan.2020.103989

Kalogeropoulos, G., Dimoudi, A., Toumboulidis, P., & Zoras, S. (2022). Urban Heat Island and Thermal Comfort Assessment in a Medium-Sized Mediterranean City. *Atmosphere*, *13*(7), 1102. https://doi.org/10.3390/atmos13071102

Karimi, A., Mohammad, P., García-Martínez, A., Moreno-Rangel, D., Gachkar, D., & Gachkar, S. (2023). New developments and future challenges in reducing and controlling heat island effect in urban areas. In *Environment, Development and Sustainability* 25(10), 10485–10531. https://doi.org/10.1007/s10668-022-02530-0

Karnieli, A., Agam, N., Pinker, R. T., Anderson, M., Imhoff, M. L., Gutman, G. G., Panov, N., & Goldberg, A. (2010). Use of NDVI and land surface temperature for drought assessment: Merits and limitations. *Journal of Climate*, *23*(3), 618–633. https://doi.org/10.1175/2009JCLI2900.

Kasniza Jumari, N. A. S., Ahmed, A. N., Huang, Y. F., Ng, J. L., Koo, C. H., Chong, K. L., Sherif, M., & Elshafie, A. (2023). Analysis of urban heat islands with Landsat satellite images and GIS in Kuala Lumpur Metropolitan City. *Heliyon*, *9*(8), e18424. https://doi.org/10.1016/j.heliyon.2023.e18424

Kaushal, A. A., Anand, P., Aithal, B. H., & Sen, J. (2024). Thermal comfort in Indian naturally ventilated buildings: A comprehensive review. *Energy and Buildings*, *306*, 113923 https://doi.org/10.1016/j.enbuild.2024.113923

Khallef, B., Biskri, Y., Mouchara, N., & Brahamia, K. (2020). Analysis of Urban Heat Islands Using Landsat 8 OLI / TIR Data: Case of the City of Guelma (Algeria). *Asian Journal of Environment & Ecology*, 42–51. https://doi.org/10.9734/ajee/2020/v12i430167

Khalvandi, R., & Karimimoshaver, M. (2023). The optimal ratio in the street canyons: Comparison of two methods of satellite images and simulation. *Building and Environment*, *229,109927* https://doi.org/10.1016/j.buildenv.2022.109927

Khamchiangta, D., & Dhakal, S. (2020). Time series analysis of land use and land cover changes related to urban heat island intensity: Case of Bangkok Metropolitan Area in Thailand. *Journal of Urban Management*, *9*(4), 383–395. https://doi.org/10.1016/j.jum.2020.09.001

Khatoon, S., & Kim, M. H. (2020). Thermal comfort in the passenger compartment using a 3-D numerical analysis and comparison with Fanger's comfort models. *Energies*, *13*(3),690. https://doi.org/10.3390/en13030690

Kikon, N., Kumar, D., & Ahmed, S. A. (2023). Quantitative assessment of land surface temperature and vegetation indices on a kilometer grid scale. *Environmental Science and Pollution Research*, *30*(49), 107236–107258. https://doi.org/10.1007/s11356-023-27418-y

Kumar, P., & Sharma, A. (2020). Study on importance, procedure, and scope of outdoor thermal comfort –A review. In *Sustainable Cities and Society* 61, 102297. https://doi.org/10.1016/j.scs.2020.102297

Lai, D., Liu, W., Gan, T., Liu, K., & Chen, Q. (2019). A review of mitigating strategies to improve the thermal environment and thermal comfort in urban outdoor spaces. In *Science of the Total Environment* 661, 337–353. https://doi.org/10.1016/j.scitotenv.2019.01.062

Landsberg, H. E. (1970). Climatic Consequences of Urbanization. In *Source: Journal of the Washington Academy of Sciences* 60, 3-9.

Lanza, K., Jones, J., Acuña, F., Coudert, M., Bixler, R. P., Kamath, H., & Niyogi, D. (2023). Heat vulnerability of Latino and Black residents in a low-income community and their recommended adaptation strategies: A qualitative study. *Urban Climate*, *51,* 101656 https://doi.org/10.1016/j.uclim.2023.101656

Leal Filho, W., Echevarria Icaza, L., Neht, A., Klavins, M., & Morgan, E. A. (2018). Coping with the impacts of urban heat islands. A literature-based study on understanding urban heat vulnerability and the need for resilience in cities in a global climate change context. *Journal of Cleaner Production*, *171*, 1140–1149. https://doi.org/10.1016/j.jclepro.2017.10.086

Leatherdale, S. T. (2019). Natural experiment methodology for research: a review of how different methods can support real-world research. *International Journal of Social Research Methodology*, *22*(1), 19–35. https://doi.org/10.1080/13645579.2018.1488449

Lee, I., Voogt, J. A., & Gillespie, T. J. (2018). Analysis and comparison of shading strategies to increase human thermal comfort in urban areas. *Atmosphere*, *9*(3), 91. https://doi.org/10.3390/atmos9030091

Lee, Y. Y., Md Din, M. F., Ponraj, M., Noor, Z. Z., Iwao, K., & Chelliapan, S. (2017). Overview of Urban Heat Island (UHI) phenomenon towards human thermal comfort. *Environmental Engineering and Management Journal*, *16*(9), 2097–2112. https://doi.org/10.30638/eemj.2017.217

Li, B., Liu, Z., Nan, Y., Li, S., & Yang, Y. (2018). Comparative analysis of urban heat island intensities in Chinese, Russian, and DPRK regions across the transnational urban agglomeration of the Tumen River in Northeast Asia. *Sustainability*, *10*(8), 2637. https://doi.org/10.3390/su10082637

Li, D., & Bou-Zeid, E. (2013). Synergistic interactions between urban heat islands and heat waves: The impact in cities is larger than the sum of its parts. *Journal of applied Meteorology and Climatology*, *52*(9), 2051-2064.

Li, D., Bou-Zeid, E., & Oppenheimer, M. (2014). The effectiveness of cool and green roofs as urban heat island mitigation strategies. *Environmental Research Letters*, *9*(5), 055002. https://doi.org/10.1088/1748-9326/9/5/055002

Li, J., Sun, R., Liu, T., Xie, W., & Chen, L. (2021). Prediction models of urban heat island based on landscape patterns and anthropogenic heat dynamics. *Landscape Ecology*, *36*(6), 1801–1815. https://doi.org/10.1007/s10980-021-01246-2

Li, M., & Stein, A. (2020). Mapping land use from high-resolution satellite images by exploiting the spatial arrangement of land cover objects. *Remote Sensing*, *12*(24), 1–21. https://doi.org/10.3390/rs12244158

Li, X., Stringer, L. C., & Dallimer, M. (2022). The Impacts of Urbanisation and Climate Change on the Urban Thermal Environment in Africa. *Climate* 10(11),106. https://doi.org/10.3390/cli10110164

Li, Y., Wang, J., Gao, T., Sun, Q., Zhang, L., & Tang, M. (2020). Adoption of Machine Learning in Intelligent Terrain Classification of Hyperspectral Remote Sensing Images. *Computational Intelligence and Neuroscience*, 2020(1), 8886932. https://doi.org/10.1155/2020/8886932

Liu, H., Li, J., Du, J., Zhao, B., Hu, Y., Li, D., & Yu, W. (2022). Identification of Smoke from Straw Burning in Remote Sensing Images with the Improved YOLOv5s Algorithm. *Atmosphere*, 13(6), 925. https://doi.org/10.3390/atmos13060925

Loola Bokonda, P., Sidibe, M., Souissi, N., & Ouazzani-Touhami, K. (2023). Machine Learning Model for Predicting Epidemics. *Computers*, *12*(3),54. https://doi.org/10.3390/computers12030054

Lotfabadi, P., & Hançer, P. (2019). A comparative study of traditional and contemporary building envelope construction techniques in terms of thermal comfort and energy efficiency in hot and humid climates. *Sustainability 11(13), 3582.* https://doi.org/10.3390/su11133582

Ma, H., Zhao, W., Li, F., Yan, H., & Liu, Y. (2023). Study on Remote Sensing Image Classification of Oasis Area Based on ENVI Deep Learning. *Polish Journal of Environmental Studies*, *32*(3), 2231–2242. https://doi.org/10.15244/pjoes/160190

Martin-Vide, J., Sarricolea, P., & Moreno-García, M. C. (2015). On the definition of urban heat island intensity: The "rural" reference. *Frontiers in Earth Science*, *3*, 24 https://doi.org/10.3389/feart.2015.00024

Marzban, F., Sodoudi, S., & Preusker, R. (2018). The influence of land-cover type on the relationship between NDVI–LST and LST-Tair. *International Journal of Remote Sensing*, *39*(5), 1377–1398. https://doi.org/10.1080/01431161.2017.1402386

Matenge, R. G., Parida, B. P., Letshwenyo, M. W., & Ditalelo, G. (2023). Impact of Climate Variability on Rainfall Characteristics in the Semi-Arid Shashe Catchment (Botswana) from 1981–2050. *Earth (Switzerland)*, *4*(2), 398–441. https://doi.org/10.3390/earth4020022

Matzarakis, A., & Mayer, H. (2000). Atmospheric conditions and human thermal comfort in urban areas. In *11th Seminar on Environmental Protection "Environment and Health* 18, 20-23.

McElroy, J. L. (1973). A numerical study of the nocturnal heat island over a medium-sized mid-latitude city (Columbus, Ohio). *Boundary-Layer Meteorology*, *3*(4), 442-453.

Memon, R. A., Leung, D. Y. C., & Liu, C. H. (2009). An investigation of urban heat island intensity (UHII) as an indicator of urban heating. *Atmospheric Research*, *94*(3), 491–500. https://doi.org/10.1016/j.atmosres.2009.07.006

Miao, C., Li, P., Huang, Y., Sun, Y., Chen, W., & Yu, S. (2023). Coupling outdoor air quality with thermal comfort in the presence of street trees: a pilot investigation in Shenyang, Northeast China. *Journal of Forestry Research*, *34*(3), 831–839. https://doi.org/10.1007/s11676-022-01497-y

Mijani, N., Alavipanah, S. K., Firozjaei, M. K., Arsanjani, J. J., Hamzeh, S., & Weng, Q. (2020). Modeling outdoor thermal comfort using satellite imagery: A principal component analysis-based approach. *Ecological Indicators*, *117*. https://doi.org/10.1016/j.ecolind.2020.106555

Moghaddam, S. A., Mattsson, M., Ameen, A., Akander, J., Gameiro Da Silva, M., & Simões, N. (2021). Low-emissivity window films as an energy retrofit option for a historical stone building in cold climate. *Energies*, *14*(22), 7584. https://doi.org/10.3390/en14227584

Mohammad Harmay, N. S., & Choi, M. (2022). Effects of heat waves on urban warming across different urban morphologies and climate zones. *Building and Environment*, *209, 108677*. https://doi.org/10.1016/j.buildenv.2021.108677

Mokhtari, Z., Barghjelveh, S., & Sayahnia, R. (2021). Heterogeneity of the Thermal Environment and its Ecological Evaluation in the Urban Region of Karaj. *Geography and Sustainability of Environment*, *11*(4), 37–58. https://doi.org/10.22126/GES.2021.6654.2418

Morabito, M., Crisci, A., Messeri, A., Orlandini, S., Raschi, A., Maracchi, G., & Munafò, M. (2016). The impact of built-up surfaces on land surface temperatures in Italian urban areas. *Science of the Total Environment*, *551–552*, 317–326. https://doi.org/10.1016/j.scitotenv.2016.02.029

Moses, O. (2017). Special Issue on Environment, Tourism and Contemporary Socio-economic Issues in the Okavango Delta and other. *Ecosystems*, *49*, 13–25. https://doi.org/10.2307/90024331

Mushore, T. D., Odindi, J., Dube, T., & Mutanga, O. (2018). Outdoor thermal discomfort analysis in Harare, Zimbabwe in Southern Africa. *South African Geographical Journal*, *100*(2), 162–179. https://doi.org/10.1080/03736245.2017.1339630

Mustapa, M. S., Zaki, S. A., Rijal, H. B., Hagishima, A., & Ali, M. S. M. (2016). Thermal comfort and occupant adaptive behaviour in Japanese university buildings with free running and cooling mode offices during summer. *Building and Environment*, *105*, 332–342. https://doi.org/10.1016/j.buildenv.2016.06.014

Mustapha, T. D., Hassan, A. S., Nasir, M. H. A., & Onubi, H. O. (2022). An Investigation of Thermal Comfort in Classrooms in the Tropical Savanna Climate. *Journal of Advanced Research in Applied Sciences and Engineering Technology*, *29*(1), 62–75. https://doi.org/10.37934/araset.29.1.6275

Mutani, G., & Beltramino, S. (2022). Geospatial Assessment and Modeling of Outdoor Thermal Comfort at Urban Scale. *International Journal of Heat and Technology*, *40*(4), 871–878. https://doi.org/10.18280/ijht.400402

Mutani, G., & Todeschi, V. (2020). The effects of green roofs on outdoor thermal comfort, urban heat island mitigation and energy savings. *Atmosphere*, *11*(2),123. https://doi.org/10.3390/atmos11020123

Natarajan, S., Rodriguez, J., & Vellei, M. (2015). A field study of indoor thermal comfort in the subtropical highland climate of Bogota, Colombia. *Journal of Building Engineering*, *4*, 237–246. https://doi.org/10.1016/j.jobe.2015.10.003

Naughton, J., & McDonald, W. (2019). Evaluating the variability of urban land surface temperatures using drone observations. *Remote Sensing*, *11*(14). https://doi.org/10.3390/rs11141722

New, M., & Bosworth, B. (2018). What global warming of 1.5 C and higher means for Botswana and Namibia. *Climate and Knowledge Development Network*. 6(2),17-35 https://policycommons.net/artifacts/1443722/

Ngcamu, B. S. (2023). Climate change effects on vulnerable populations in the Global South: a systematic review. In *Natural Hazards* 118(2), 977–991. https://doi.org/10.1007/s11069-023-06070-2

Ngie, A. (2020). Thermal Remote Sensing of Urban Climates in South Africa Through the Mono-Window Algorithm. *International Archives of the Photogrammetry, Remote Sensing and*

Spatial Information Sciences - ISPRS Archives, *42*(3/W11), 117–123. https://doi.org/10.5194/isprs-archives-XLII-3-W11-117-2020

Nguyen, T. M., Lin, T. H., & Chan, H. P. (2019). The environmental effects of urban development in Hanoi, Vietnam from satellite and meteorological observations from 1999-2016. *Sustainability 11(6), 1768.* https://doi.org/10.3390/su11061768

Nkemelang, T., New, M., & Zaroug, M. (2018). Temperature and precipitation extremes under current, 1.5 °c and 2.0 °c global warming above pre-industrial levels over Botswana, and implications for climate change vulnerability. *Environmental Research Letters*, *13*(6). https://doi.org/10.1088/1748-9326/aac2f8

Oke, T. R. (1969). Towards a more rational understanding of the urban heat island. *McGill Climatological Bulletin*, *3*, 1-21.

Oke, T. R. (1973). City size and the urban heat island. *Atmospheric Environment*, *7*(8), 769-779.

Oliveira, A. M., & Corvacho, H. (2021). Application of thermal comfort assessment models to indoor areas near glazed walls - experimental evaluation. *Revista de La Construccion*, *20*(1), 106–127. https://doi.org/10.7764/RDLC.20.1.106

Omonijo, A. G. (2017). Assessing seasonal variations in urban thermal comfort and potential health risks using Physiologically Equivalent Temperature: A case of Ibadan, Nigeria. *Urban Climate*, *21*, 87–105. https://doi.org/10.1016/j.uclim.2017.05.006

Onačillová, K., Gallay, M., Paluba, D., Péliová, A., Tokarčík, O., & Laubertová, D. (2022). Combining Landsat 8 and Sentinel-2 Data in Google Earth Engine to Derive Higher Resolution Land Surface Temperature Maps in Urban Environment. *Remote Sensing*, *14*(16,4076. https://doi.org/10.3390/rs14164076

Ouma, Y. O., Tjitemisa, T., Segobye, M., Moreri, K., Nkwae, B., Maphale, L., & Manisa, B. (2021). *Urban land surface temperature variations with LULC, NDVI and NDBI in semi-arid urban environments: case study of Gaborone City, Botswana (1989–2019)*. *VI*(11864), 28-40. https://doi.org/10.1117/12.2595031

Peng, S., Piao, S., Ciais, P., Friedlingstein, P., Ottle, C., Bréon, F. M., Nan, H., Zhou, L., & Myneni, R. B. (2012). Surface urban heat island across 419 global big cities. *Environmental Science and Technology*, *46*(2), 696–703. https://doi.org/10.1021/es2030438

Petralli, M., Massetti, L., Brandani, G., & Orlandini, S. (2014). Urban planning indicators: Useful tools to measure the effect of urbanization and vegetation on summer air temperatures. *International Journal of Climatology*, *34*(4), 1236–1244. https://doi.org/10.1002/joc.3760

Piasecki, M., Radziszewska-Zielina, E., Czerski, P., Fedorczak-Cisak, M., Zielina, M., Krzyściak, P., Kwaśniewska-Sip, P., & Grześkowiak, W. (2020). Implementation of the indoor environmental quality (Ieq) model for the assessment of a retrofitted historical masonry building. *Energies*, *13*(22,51). https://doi.org/10.3390/en13226051

Population and Housing Census (2022). Population of Cities, Towns, and villages. www.statsbots.org.bw accessed 20 May 2023.

Portela, C. I., Massi, K. G., Rodrigues, T., & Alcântara, E. (2020). Impact of urban and industrial features on land surface temperature: Evidence from satellite thermal indices. *Sustainable Cities and Society*, *56, 102100*. https://doi.org/10.1016/j.scs.2020.102100

Prasad, H. P. S., & Satyanarayana, A. N. V. (2023). Assessment of Outdoor Thermal Comfort Using Landsat 8 Imageries with Machine Learning Tools over a Metropolitan City of India. *Pure and Applied Geophysics*, *180*(10), 3621–3637. https://doi.org/10.1007/s00024-023-03328-5

Qaid, A., Bin Lamit, H., Ossen, D. R., & Raja Shahminan, R. N. (2016). Urban heat island and thermal comfort conditions at micro-climate scale in a tropical planned city. *Energy and Buildings*, *133*, 577–595. https://doi.org/10.1016/j.enbuild.2016.10.006

Qureshi, A. M., & Rachid, A. (2021). Review and comparative study of decision support tools for the mitigation of urban heat stress. *Climate*, *9*(6). https://doi.org/10.3390/cli9060102

Ranagalage, M., Estoque, R. C., Zhang, X., & Murayama, Y. (2018). Spatial changes of urban heat island formation in the Colombo District, Sri Lanka: Implications for sustainability planning. *Sustainability (Switzerland)*, *10*(5). https://doi.org/10.3390/su10051367

Rasul, A., Balzter, H., Smith, C., Remedios, J., Adamu, B., Sobrino, J., Srivanit, M., & Weng, Q. (2017). A Review on Remote Sensing of Urban Heat and Cool Islands. *Land*, *6*(2), 38. https://doi.org/10.3390/land6020038

Ratajczak, K., Amanowicz, Ł., Pałaszyńska, K., Pawlak, F., & Sinacka, J. (2023). Recent Achievements in Research on Thermal Comfort and Ventilation in the Aspect of Providing People with Appropriate Conditions in Different Types of Buildings—Semi-Systematic Review. In *Energies*, *16*(17), 6254.https://doi.org/10.3390/en16176254

Ravnikar, Ž., Bahillo, A., & Goličnik Marušić, B. (2023). A Protocol for Microclimate-Related Street Assessment and the Potential of Detailed Environmental Data for Better Consideration of Microclimatology in Urban Planning. *Sustainability*, *15*(10),8236. https://doi.org/10.3390/su15108236

Ren, J., Shi, K., Li, Z., Kong, X., & Zhou, H. (2023). A Review on the Impacts of Urban Heat Islands on Outdoor Thermal Comfort. *Buildings*, *13*(6), 1368. https://doi.org/10.3390/buildings13061368

Richard, Y., Pohl, B., Rega, M., Pergaud, J., Thevenin, T., Emery, J., Dudek, J., Vairet, T., Zito, S., & Chateau-Smith, C. (2021). Is Urban Heat Island intensity higher during hot spells and heat waves (Dijon, France, 2014–2019)? *Urban Climate*, *35*.,747 https://doi.org/10.1016/j.uclim.2020.100747

Ruiz-Aviles, V., Brazel, A., Davis, J. M., & Pijawka, D. (2020). Mitigation of Urban Heat Island Effects through “Green Infrastructure”: Integrated Design of Constructed Wetlands and Neighborhood Development. *Urban Science*, *4*(4),78. https://doi.org/10.3390/urbansci4040078

Sanad, A., Kusratmoko, E., & Wibowo, A. (2022). Urban heat island phenomenon in Majalengka Regency. *IOP Conference Series: Earth and Environmental Science*, *1089*(1),012024. https://doi.org/10.1088/1755-1315/1089/1/012024

Sari, D. P. (2021). A Review of How Building Mitigates the Urban Heat Island in Indonesia and Tropical Cities. In *Earth (Switzerland)* 2(3), 653–666. https://doi.org/10.3390/earth2030038

Schweiker, M., André, M., Al-Atrash, F., Al-Khatri, H., Alprianti, R. R., Alsaad, H., Amin, R., Ampatzi, E., Arsano, A. Y., Azar, E., Bannazadeh, B., Batagarawa, A., Becker, S., Buonocore, C., Cao, B., Choi, J. H., Chun, C., Daanen, H., Damiati, S. A., … Zomorodian, Z. S. (2020). Evaluating assumptions of scales for subjective assessment of thermal environments – Do laypersons perceive them the way, we researchers believe? *Energy and Buildings*, *211,*109761, https://doi.org/10.1016/j.enbuild.2020.109761

Scott, A. A., Waugh, D. W., & Zaitchik, B. F. (2018). Reduced Urban Heat Island intensity under warmer conditions. *Environmental Research Letters*, *13*(6), 064003. https://doi.org/10.1088/1748-9326/aabd6c

Setaih, K., Hamza, N., Mohammed, M. A., Dudek, S., & Townshend, T. (2014). This work is licensed under a Creative Commons Attribution 3.0 Unported License CFD Modeling as a Tool for Assessing Outdoor Thermal Comfort Conditions in Urban Settings in Hot Arid Climates Guest editors: Bhzad Sidawi and Neveen Hamza. In *www.itcon.org-Journal of Information Technology in Construction 19*, 248-269.

Sharma, R., Pradhan, L., Kumari, M., & Bhattacharya, P. (2021). Assessing urban heat islands and thermal comfort in Noida City using geospatial technology. *Urban Climate*, *35,100751*. https://doi.org/10.1016/j.uclim.2020.100751

Sharmin Siddika, Haque, Md. N., & Mizbah Ahmed Sresto. (2021). Assessing the Relationship among the Land Surface Features: A Geographic Information System (GIS) and Remote Sensing (RS) Based Approach for City Area. *Journal of Applied Science & Process Engineering*, *8*(2), 935–952. https://doi.org/10.33736/jaspe.3616.2021

Sidiqui, P., Roös, P. B., Herron, M., Jones, D. S., Duncan, E., Jalali, A., Allam, Z., Roberts, B. J., Schmidt, A., Tariq, M. A. U. R., Shah, A. A., Khan, N. A., & Irshad, M. (2022). Urban Heat Island vulnerability mapping using advanced GIS data and tools. *Journal of Earth System Science*, *131*(4), 266. https://doi.org/10.1007/s12040-022-02005-w

Stewart, I. D. (2011). *Redefining the urban heat island (Doctoral dissertation, University of British Columbia). https://open.library.ubc.ca/soa/cIRcle/collections/ubctheses/24/items/1.0072360 accessed 20 October 2023.*

Subzar Malik, M., Prakash Shukla, J., & Mishra, S. (2019). Relationship of LST, NDBI and NDVI using Landsat-8 data in Kandaihimmat Watershed, Hoshangabad, India. In *Indian Journal of Geo Marine Sciences* 48(01), 25-31.

Sufrianto, W., & Candra, O. (2022). The Effect Of Electrical Installation Trainer Media On Undergraduate Students Learning Outcomes Of Domestic Electrical Installation Practice

Course. *JTEV (Jurnal Teknik Elektro Dan Vokasional*, *8*(1), 128-136. https://doi.org/10.24036/jtev.v8i1.116682

Taha, H. (1997). Urban climates and heat islands: albedo, evapotranspiration, and anthropogenic heat. *Energy and buildings*, *25*(2), 99-103.

Taha, H., Akbari, H., Rosenfeld, A., & Huang, J. (1988). Residential Cooling Loads and the Urban Heat Island the Effects of Albedo. In *Building and Environment* 23(4), 271-283.

Taleghani, M. (2018). Outdoor thermal comfort by different heat mitigation strategies- A review. In *Renewable and Sustainable Energy Reviews* 81, 2011–2018. https://doi.org/10.1016/j.rser.2017.06.010

Tan, J., Zheng, Y., Tang, X., Guo, C., Li, L., Song, G., Zhen, X., Yuan, D., Kalkstein, A. J., Li, F., & Chen, H. (2010). The urban heat island and its impact on heat waves and human health in Shanghai. *International Journal of Biometeorology*, *54*(1), 75–84. https://doi.org/10.1007/s00484-009-0256-x

Tang, C. F. (2022). A study of the urban heat island effect in Guangzhou. *IOP Conference Series: Earth and Environmental Science*, *1087*(1),012015. https://doi.org/10.1088/1755-1315/1087/1/012015

Tang, J., Di, L., Xiao, J., Lu, D., & Zhou, Y. (2017). Impacts of land use and socioeconomic patterns on urban heat Island. *International Journal of Remote Sensing*, *38*(11), 3445-3465.

Tariq, A., Shu, H., Gagnon, A. S., Li, Q., Mumtaz, F., Hysa, A., Siddique, M. A., & Munir, I. (2021). Assessing burned areas in wildfires and prescribed fires with spectral indices and sar images in the Margalla hills of Pakistan. *Forests*, *12(10), 1371.* https://doi.org/10.3390/f12101371

Thapa, S. (2019). Insights into the thermal comfort of different naturally ventilated buildings of Darjeeling, India – Effect of gender, age and BMI. *Energy and Buildings*, *193*, 267–288. https://doi.org/10.1016/j.enbuild.2019.04.003

Thapa, S. (2020). Thermal comfort in high altitude Himalayan residential houses in Darjeeling, India – An adaptive approach. *Indoor and Built Environment*, *29*(1), 84–100. https://doi.org/10.1177/1420326X19853877

Tiangco, M., Lagmay, A. M. F., & Argete, J. (2008). ASTER-based study of the night-time urban heat island effect in Metro Manila. *International Journal of Remote Sensing*, *29*(10), 2799–2818. https://doi.org/10.1080/01431160701408360

Tiwari, A., Kumar, P., Kalaiarasan, G., & Ottosen, T. B. (2021). The impacts of existing and hypothetical green infrastructure scenarios on urban heat island formation. *Environmental Pollution*, *274, 115898*. https://doi.org/10.1016/j.envpol.2020.115898

Tyson, P. D., Du Toit, F., & Fuggle, R. F. (1972). Temperature structure above cities: review and preliminary findings from the Johannesburg urban heat island project. *Atmospheric Environment (1967)*, *6*(8), 533-54,

Uddin, A. S. M. S., Khan, N., Islam, A. R. M. T., Kamruzzaman, M., & Shahid, S. (2022). Changes in urbanization and urban heat island effect in Dhaka city. *Theoretical and Applied Climatology*, *147*(3–4), 891–907. https://doi.org/10.1007/s00704-021-03872-x

Ullah, N., Siddique, M. A., Ding, M., Grigoryan, S., Khan, I. A., Kang, Z., Tsou, S., Zhang, T., Hu, Y., & Zhang, Y. (2023). The Impact of Urbanization on Urban Heat Island: Predictive Approach Using Google Earth Engine and CA-Markov Modelling (2005–2050) of Tianjin City, China. *International Journal of Environmental Research and Public Health*, *20(3), 2642.* https://doi.org/10.3390/ijerph20032642

Ullah, N., Siddique, M. A., Ding, M., Grigoryan, S., Zhang, T., & Hu, Y. (2022). Spatiotemporal Impact of Urbanization on Urban Heat Island and Urban Thermal Field Variance Index of Tianjin City, China. *Buildings*, *12*(4),399. https://doi.org/10.3390/buildings12040399

van der Linden, N., Longden, T., Richards, J. R., Khursheed, M., Goddijn, W. M. T., van Veelen, M. J., Khan, U. R., & Christien van der Linden, M. (2019). The use of an 'acclimatisation' heatwave measure to compare temperature-related demand for emergency services in Australia, Botswana, Netherlands, Pakistan, and USA. *PLoS ONE*, *14*(3), *14*(3), e0214242.. https://doi.org/10.1371/journal.pone.0214242

Varghese, B. M., Hansen, A., Bi, P., & Pisaniello, D. (2018). Are workers at risk of occupational injuries due to heat exposure? A comprehensive literature review. *Safety science*, *110*, 380-392

Vergara, D. C. D. M., Blanco, A. C., Marciano, J. J. S., Meneses, S. F., Borlongan, N. J. B., & Sabuito, A. J. C. (2023). Assessing and modelling Urban Heat Island in Baguio City using Landsat imagery and machine learning. *International Archives of the Photogrammetry, Remote Sensing and Spatial Information Sciences - ISPRS Archives*, *48*(4), 457–464. https://doi.org/10.5194/isprs-archives-XLVIII-4-W6-2022-457-2023

Waleed, M., & Sajjad, M. (2022). Leveraging cloud-based computing and spatial modeling approaches for land surface temperature disparities in response to land cover change: Evidence from Pakistan. *Remote Sensing Applications: Society and Environment*, *25,665*. https://doi.org/10.1016/j.rsase.2021.100665

Waleed, M., Sajjad, M., Acheampong, A. O., & Alam, Md. T. (2023). Towards Sustainable and Livable Cities: Leveraging Remote Sensing, Machine Learning, and Geo-Information Modelling to Explore and Predict Thermal Field Variance in Response to Urban Growth. *Sustainability*, *15*(2), 1416. https://doi.org/10.3390/su15021416

Wang, F., Qin, Z., Song, C., Tu, L., Karnieli, A., & Zhao, S. (2015). An improved mono-window algorithm for land surface temperature retrieval from Landsat 8 thermal infrared sensor data. *Remote Sensing*, *7*(4), 4268–4289. https://doi.org/10.3390/rs70404268

Wang, H., & Liu, L. (2020). Experimental investigation about effect of emotion state on people's thermal comfort. *Energy and Buildings*, *211*, 109789 https://doi.org/10.1016/j.enbuild.2020.109789

Wang, M., Zhang, Z., Hu, T., & Liu, X. (2019). A Practical Single-Channel Algorithm for Land Surface Temperature Retrieval: Application to Landsat Series Data. *Journal of Geophysical Research: Atmospheres*, *124*(1), 299–316. https://doi.org/10.1029/2018JD029330

Wong, N. H., Kwang Tan, A. Y., Chen, Y., Sekar, K., Tan, P. Y., Chan, D., Chiang, K., & Wong, N. C. (2010). Thermal evaluation of vertical greenery systems for building walls. *Building and Environment*, *45*(3), 663–672. https://doi.org/10.1016/j.buildenv.2009.08.005

Wu, W., Ren, H., Yu, M., & Wang, Z. (2018). Distinct influences of urban villages on urban heat islands: A case study in the Pearl River Delta, China. *International Journal of Environmental Research and Public Health*, *5(8), 1666.* https://doi.org/10.3390/ijerph15081666

Wu, Z., Li, N., Cui, H., Peng, J., Chen, H., & Liu, P. (2017). Using upper extremity skin temperatures to assess thermal comfort in office buildings in Changsha, China. *International Journal of Environmental Research and Public Health*, *14*(10),1096. https://doi.org/10.3390/ijerph14101092

Wulder, M. A., White, J. C., Loveland, T. R., Woodcock, C. E., Belward, A. S., Cohen, W. B., Fosnight, E. A., Shaw, J., Masek, J. G., & Roy, D. P. (2016). The global Landsat archive: Status, consolidation, and direction. *Remote Sensing of Environment*, *185*, 271–283. https://doi.org/10.1016/j.rse.2015.11.032

Xia, B., Kong, F., Zhou, J., Wu, X., & Xie, Q. (2022). Land Resource Use Classification Using Deep Learning in Ecological Remote Sensing Images. *Computational Intelligence and Neuroscience*, *2022(1), 7179477*. https://doi.org/10.1155/2022/7179477

Xiong, L., Li, S., Zou, B., Peng, F., Fang, X., & Xue, Y. (2022). Long Time-Series Urban Heat Island Monitoring and Driving Factors Analysis Using Remote Sensing and Geodetector. *Frontiers in Environmental Science*, *9, 828230*. https://doi.org/10.3389/fenvs.2021.828230

Xu, H., Hu, X., Guan, H., & He, G. (2017). Development of a fine-scale discomfort index map and its application in measuring living environments using remotely sensed thermal infrared imagery. *Energy and Buildings*, *150*, 598–607. https://doi.org/10.1016/j.enbuild.2017.06.003

Xu, Y., Qin, Z., & Wan, H. (2010). Spatial and Temporal Dynamics of Urban Heat Island and Their Relationship with Land Cover Changes in Urbanization Process: A Case Study in Suzhou, China. *Journal of the Indian Society of Remote Sensing*, *38*(4), 654–663. https://doi.org/10.1007/s12524-011-0073-7

Yang, C., He, X., Yan, F., Yu, L., Bu, K., Yang, J., Chang, L., & Zhang, S. (2017). Mapping the influence of land use/land cover changes on the urban heat island effect-A case study of Changchun, China. *Sustainability*, *9(2), 312.* https://doi.org/10.3390/su9020312

Yang, Y., Song, F., Ma, J., Wei, Z., Song, L., & Cao, W. (2022). Spatial and temporal variation of heat islands in the main urban area of Zhengzhou under the two-way influence of urbanization and urban forestry. *PLoS ONE*, *17*(8), *17*(8), e0272626. https://doi.org/10.1371/journal.pone.0272626

Yin, J. F., Zheng, Y. F., Wu, R. J., Tan, J. G., Ye, D. X., & Wang, W. (2012). An analysis of influential factors on outdoor thermal comfort in summer. *International Journal of Biometeorology*, *56*(5), 941–948. https://doi.org/10.1007/s00484-011-0503-9

Yu, W., Li, B., Yao, R., Wang, D., & Li, K. (2017). A study of thermal comfort in residential buildings on the Tibetan Plateau, China. *Building and Environment*, *119*, 71–86. https://doi.org/10.1016/j.buildenv.2017.04.009

Zhang, H., Qi, Z. Fang, Ye, X. Yue, Cai, Y. Bin, Ma, W. Chun, & Chen, M. nan. (2013). Analysis of land use/land cover change, population shift, and their effects on spatiotemporal patterns of urban heat islands in metropolitan Shanghai, China. *Applied Geography*, *44*, 121–133. https://doi.org/10.1016/j.apgeog.2013.07.021

Zhang, J., Li, Z., Wei, Y., & Hu, D. (2022). The impact of the building morphology on microclimate and thermal comfort-a case study in Beijing. *Building and Environment*, *223, 109469*. https://doi.org/10.1016/j.buildenv.2022.109469

Zhang, M., Dong, S., Cheng, H., & Li, F. (2021). Spatio-temporal evolution of urban thermal environment and its driving factors: Case study of Nanjing, China. *PLoS ONE*, *16(5), e0246011.* https://doi.org/10.1371/journal.pone.0246011

Zhang, M., Zhang, C., Kafy, A. Al, & Tan, S. (2022). Simulating the relationship between land use/cover change and urban thermal environment using machine learning algorithms in Wuhan city, China. *Land*, *11*(1),14. https://doi.org/10.3390/land11010014

Zhang, Y., Jiang, P., Zhang, H., & Cheng, P. (2018). Study on urban heat island intensity level identification based on an improved restricted Boltzmann machine. *International Journal of Environmental Research and Public Health*, *15*(2). https://doi.org/10.3390/ijerph15020186

Zhao, J., Zhao, X., Liang, S., Zhou, T., Du, X., Xu, P., & Wu, D. (2020). Assessing the thermal contributions of urban land cover types. *Landscape and Urban Planning*, *204,* 103927 https://doi.org/10.1016/j.landurbplan.2020.103927

Zhao, Q., Lian, Z., & Lai, D. (2021). Thermal comfort models and their developments: A review. In *Energy and Built Environment* 2(1), 21–33. https://doi.org/10.1016/j.enbenv.2020.05.007

Zhao, Q., Yu, L., Li, X., Peng, D., Zhang, Y., & Gong, P. (2021). Progress and trends in the application of google earth and google earth engine. In *Remote Sensing 13*(18), 3778. https://doi.org/10.3390/rs13183778

Zhao, Z., Ye, R., Wang, Y., & Tao, Y. (2023). How Plot Spatial Morphology Drives Surface Thermal Environment: A Spatial and Temporal Analysis of Nanjing Main City. *Sustainability*, *15(1), 383.* https://doi.org/10.3390/su15010383

Zhou, B., Rybski, D., & Kropp, J. P. (2017). The role of city size and urban form in the surface urban heat island. *Scientific Reports*, *7(1), 4791.* https://doi.org/10.1038/s41598-017-04242-2

Zhou, D., Xiao, J., Bonafoni, S., Berger, C., Deilami, K., Zhou, Y., Frolking, S., Yao, R., Qiao, Z., & Sobrino, J. A. (2019). Satellite remote sensing of surface urban heat islands: Progress,

challenges, and perspectives. In *Remote Sensing* 11(1),48. https://doi.org/10.3390/rs11010048

Zhou, W., Yu, W., Zhang, Z., Cao, W., & Wu, T. (2023). How can urban green spaces be planned to mitigate urban heat island effect under different climatic backgrounds? A threshold-based perspective. *Science of the Total Environment*, *890, 164422*. https://doi.org/10.1016/j.scitotenv.2023.164422

Zou, M., & Zhang, H. (n.d.). *Cooling strategies for thermal comfort in cities: a review of key methods in landscape design*. https://doi.org/10.1007/s11356-021-15172-y/Published

Zullo, F., Fazio, G., Romano, B., Marucci, A., & Fiorini, L. (2019). Effects of urban growth spatial pattern (UGSP) on the land surface temperature (LST): A study in the Po Valley (Italy). *Science of the Total Environment*, *650*, 1740–1751. https://doi.org/10.1016/j.scitotenv.2018.09.331

Zupancic, T., Bulthuis, M., & Westmacott, C. (2015). The impact of green space on heat and air pollution in urban communities. *A Meta-narrative Systematic Review*. *Policy commons*. 2,1-68 https://policycommons.net/artifacts/1202600